

Presented Before the Division of Fuel Chemistry  
American Chemical Society  
Chicago, Ill., August 1964

The Production of Nonagglomerating Char from Caking Coal  
in a Continuous Fluid-Bed Reactor

A. J. Forney, R. F. Kenny, S. J. Gasior, and J. H. Field

U. S. Bureau of Mines, 4800 Forbes Avenue,  
Pittsburgh, Pennsylvania 15213

### INTRODUCTION

The goal of this investigation is to develop a method of producing a nonagglomerating fuel from strongly caking coals. This fuel then could be used in a fluidized-bed gasifier or hydrogenator to make methane. The strongly caking coals, found mainly in Eastern United States where the large market for gas exists, become plastic and cake when heated to gasification temperatures.

An earlier paper described a method of operating with a batch charge of coal in a fluid-bed system.<sup>1</sup> The caking properties of Pittsburgh seam coal and other highly caking coals were destroyed at 400° to 425° C by fluidizing fine coal (18-100 mesh) with steam or nitrogen which contain at least 0.2 percent oxygen. In the batch system a thoroughly nonagglomerating char could be produced in about 5 minutes. The surface of the char was made noncaking in about 1 minute. It was found that the coal must be heated by the fluidizing gas and not through the reactor wall to avoid agglomerating in the pretreating vessel.

The criteria adopted to indicate that the pretreatment was successful in these continuous tests are:

1. Good fluidization must be maintained in the pretreating reactor at the temperature employed.
2. The free-swelling index (FSI) of the resulting char must be less than 2.
3. The char must be noncaking when subjected to a hydrogen treatment at 600° C.

All three conditions must be satisfied before the char is considered noncaking. The free-swelling index, while not a direct measurement of agglomeration properties, does indicate the change in this property. For example, the FSI of Pittsburgh seam coal, a high-volatile A bituminous coal, is about 8, and after successful pretreatment, less than 2.

To optimize the pretreatment, the following information was to be derived from the experiments with continuous feed of coal and discharge of char:

1. The minimum residence time of the coal.
2. The minimum temperature.
3. The minimum oxygen-to-coal feed ratio.
4. The minimum weight loss.
5. The optimum mesh size of coal.
6. The effect of pressure.
7. The quality of the offgas.

#### APPARATUS AND EXPERIMENTATION

The flowsheet of the continuous unit is shown in figure 1. Nitrogen or steam plus air was used as the fluidizing medium. Coal feed is semicontinuous in that the feeder delivers batches at the rate of about 8 to 20 per minute, producing a feed rate of 120 to 900 grams per hour. This coal is conveyed to the bottom of the reactor by the feed gas. The char is discharged from the lower side arm while the gases, tars, and dusts are discharged from the upper one. The reactor is a stainless steel tube of 1-inch diameter, with the expanded section at the top 2 inches in diameter. The 29-inch section containing the bed of coal is heated electrically. A manometer indicates the pressure drop developed over the coal bed. Because the height of the bed is fixed, the residence time of the coal depends on the rate of coal feed.

#### DISCUSSION OF RESULTS

More drastic pretreatment was required to destroy the caking properties of coal in the unit with continuous feed and discharge of solids than in comparable batch operations reported previously. Due to the back-mixing of fresh and treated material, some particles remain in the reaction zone a relatively short time and others for a much longer time. Thus the treatment must be severe enough to convert those particles which are in the reactor for a very short time.

Figure 2 shows the results of tests in which the temperature of the bed was varied from 410° to 450° C and the oxygen content of the inert gas used for pretreating was 1.4 and 2.3 percent during pretreatment. Nonagglomerating char was produced in only two of these tests. These employed an oxygen content of 2.3 percent and temperatures of 440° to 450° C, whereas only 0.2 percent oxygen in the fluidizing gas was needed in the batch tests. With a lower oxygen content of 1.4 percent, the chars produced at 440° C caked in the reactor. The higher oxygen content is necessary in the continuous tests because there is a constant feed of raw coal and a greater inventory of coal in the bed tests.

The reason the chars cake during pretreatment at the higher temperatures but not at the lower ones, as demonstrated in figure 2 by the 1.4-percent oxygen parameter, may be explained with the photographs of chars shown in figure 3. At 410° C the particles are discrete, but at 435° C the smaller particles stick to the larger ones. It is believed that more of the viscous,

tarry material exudes from the inside of the large particles at the higher temperature. Once the limited amount of oxygen in the gas has been consumed, there is none to oxidize this additional viscous material and the particles stick together. The smaller particles are rendered noncaking more rapidly than the larger particles, so they did not stick to each other, but only to the large particles.

Figure 4 shows the effect on the FSI of varying the residence time from 9 to 34 minutes while holding the oxygen-to-coal ratio constant at about 0.2 cubic foot per pound of coal. Temperature parameters were 420°, 430°, 440°, and 450° C. At this oxygen content, a minimum of about 25 minutes is needed to make noncaking char at 440° C. The time could not be decreased at this oxygen-to-coal ratio by increasing the temperature because at 450° C the char caked in the reactor during treatment. Figure 5 shows the same type plot using an oxygen-to-coal ratio of about 0.3. A residence time of only 7 minutes was adequate to render the coal noncaking at 440° C, and less than 7 minutes at 450° C.

As shown in figure 5, the percentage of volatile matter in the char decreases with increasing pretreatment temperature and residence time. At 14 minutes the volatile matter content of the char is 29 percent at 420° C, and is 23 percent at 450° C. After 34 minutes the volatile matter is 26 percent at 420° C and 21 percent at 450° C.

Since the char from Pittsburgh seam coal is noncaking when its FSI is decreased to 1-1/2, all the data yielding this FSI at 420°, 430°, and 440° C obtained at various residence times and oxygen-to-coal ratios were cross-plotted as shown in figure 6. If a residence time of 5 minutes is desired, the required oxygen-to-coal ratio is about 0.40 when operating at 430° C. Lower temperatures resulted in a much higher oxygen-to-coal ratio or a longer residence time.

Figure 7 shows the effect of temperature on the FSI and volatile matter of char from Pittsburgh seam coal for four different particle sizes at a constant residence time of 14 minutes. The oxygen-to-coal feed ratio was constant at 0.3 cubic foot oxygen per pound of coal. For the 18-48 mesh size the FSI decreased rapidly from 6-1/2 at 410° to 1 at 440° C. Lower free-swelling values were obtained with decreasing sizes of particles treated at similar temperatures; for example, for the 150-200 mesh the indices were 1 at 410° C and noncaking (NC) at 450° C. These results show how much more readily the finer coal sizes can be pretreated.

Loss of volatile matter is more rapid for the small particles than the coarser sizes. Also, as anticipated, the loss of volatiles increases with increasing temperatures. The loss of volatile matter of 18-48 and 48-100 mesh sizes for satisfactory decaking of coal is about 10 percent. This is roughly equivalent to the weight loss and to the loss in heating value of the coal.

Since the finer size particles require less drastic treatment, an attempt was made to show that the oxygen needed for pretreatment varied with the particle diameter. As shown in figure 8, the oxygen-to-coal ratio varied from 0.42 for the 18-48 mesh to 0.06 for the 150-200 mesh. This theory was partially successful, but the finer mesh sizes caked in the reactor when the bed temperature was raised above 430° C. The mesh sizes finer than 100 mesh were more difficult to fluidize.

Figure 9 shows the effect of temperature on the quality of offgas made during pretreatment with steam plus air. The oxygen-to-coal feed ratio was 0.4 cubic foot per pound. The quantity of methane and higher hydrocarbons increased with increasing temperatures. The yields of carbon oxides increased slightly, but the hydrogen yield remained constant at about 0.2 cc/gram. Similar results were obtained in the batch tests except that the yield of hydrogen (about 66 cc/gram in the batch tests) is lower in the continuous operation, probably because the oxygen needed to treat the coal reacted with the hydrogen.

Table 1 shows analysis of coal and chars used in the above tests. As in the batch tests, the oxygen content is greater in the raw coal than in the chars.

**TABLE 1.- Analysis of coal and chars from the tests to study the effect of temperature on the offgas made during steam-air treatment of Pittsburgh seam coal of 48-100 mesh size**

Analysis (as received)	Coal	Chars				
		410° C	420° C	430° C	440° C	450° C
<b>Proximate, percent</b>						
Moisture	1.5	0.1	0.1	0.3	0.0	0.3
Volatile matter	36.0	27.2	26.9	25.9	23.4	22.7
Fixed carbon	54.4	64.4	64.6	66.9	68.6	67.9
Ash	8.1	8.3	8.4	6.9	8.0	9.1
<b>Ultimate, percent</b>						
Hydrogen	5.2	4.5	4.4	4.4	4.2	4.1
Carbon	75.2	77.3	76.9	78.0	77.0	76.1
Nitrogen	1.5	1.6	1.3	1.6	1.6	1.6
Oxygen	7.9	6.4	7.1	7.4	7.4	7.2
Sulfur	2.1	1.9	1.9	1.7	1.8	1.9
Ash	8.1	8.3	8.4	6.9	8.0	9.1
<b>Heating value,</b>						
Btu/lb	13,410	--	13,240	13,470	--	13,130

The effect of pressure was studied at 1, 5, 10, and 20 atmospheres using steam plus air as the fluidizing gas. A mesh size of 150-200 was used so that a lower fluidization gas velocity could be employed. Generally there was no great change due to pressure. Using a fluidizing gas mixture of steam plus air with an oxygen-to-coal ratio of 0.3 cubic foot per pound at 430° C, as the pressure was increased the yield of carbon oxide gases decreased, but the hydrocarbon yield increased. The amount of coal throughput increased as the pressure was increased, but at a rate less than linearly. Again, as in the batch tests, the particles seemed to explode when the pressure was released, probably because trapped gas in the particles escaped on depressurization.

#### CONCLUSION

The tests have demonstrated the operability of a small-scale continuous unit designed to pretreat highly caking coal to remove its caking quality. The principal difference between results of continuous and batch operation is the need for a higher oxygen content of the feed gas in continuous flow. The minimum residence time required for the coal to be in the reactor is about 5 minutes at 430° C. About 0.4 cubic foot of oxygen is needed in the treating gas for each pound of coal to destroy the caking quality of Pittsburgh seam coal. Although the optimum mesh size is 18-100, finer mesh sizes permit less drastic treatment. However, finer mesh sizes are more difficult to fluidize. Minimum weight loss was 10 percent, which is equivalent to 10 percent loss of heating value of the original coal. The effect of pressure is negligible compared to atmospheric pressure. However, higher throughputs can be achieved at higher pressures.

Steam plus oxygen is the desired fluidizing medium if both the char and the offgas are to be utilized in a gasifier. This results in an advantage over other methods of treatment because the volatile matter evolved during the pretreatment is not removed from the system.

#### Reference Cited

1. Forney, A. J., R. F. Kenny, S. J. Gasior, and J. H. Field. The Destruction of the Caking Properties of Coal by Pretreatment in a Fluidized Bed. Ind. and Eng. Chem. Product Research and Development, v. 3, No. 1, March 1964, pp. 48-53.

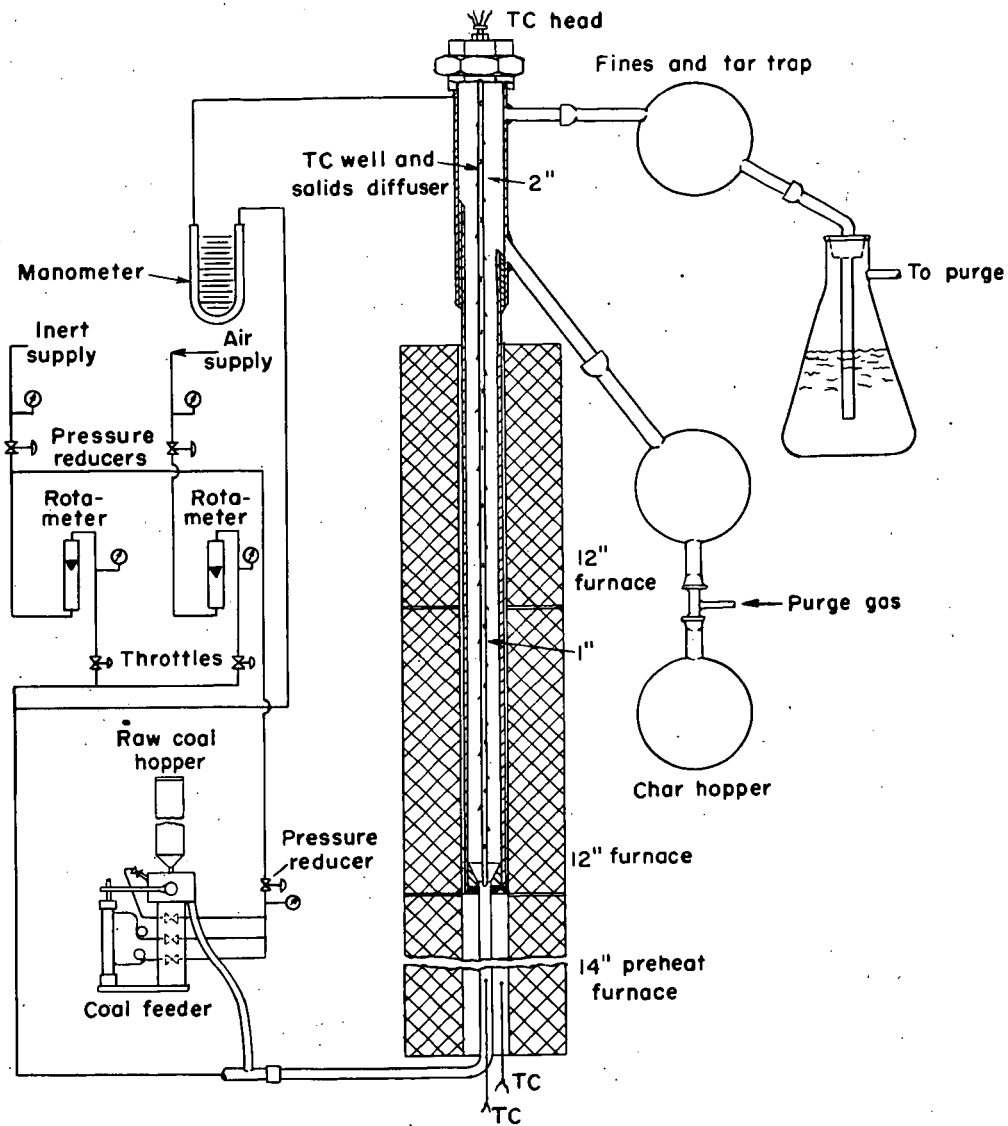


Figure 1. Continuous fluidized-bed coal pretreater.

3-16-64

L-8422

(1) ▲                      ▲                      ▲                      ■                      ■  
 (2) ▲                      ▲                      ▲                      ▲

Char subject to hydrogen atmosphere at 600° C for 10 minutes  
 ( ▲ Caking                      ■ Non-caking )

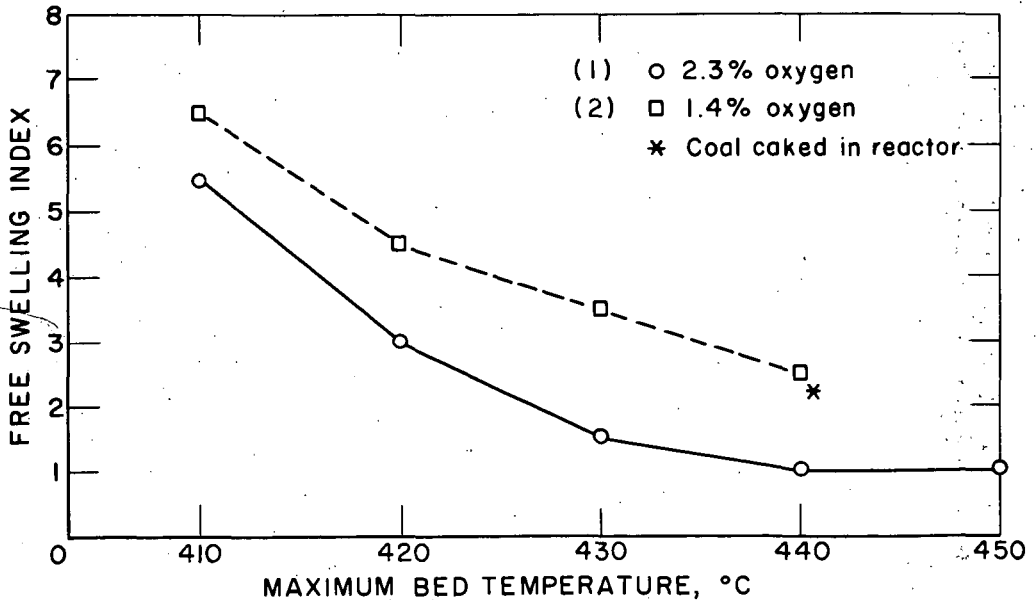
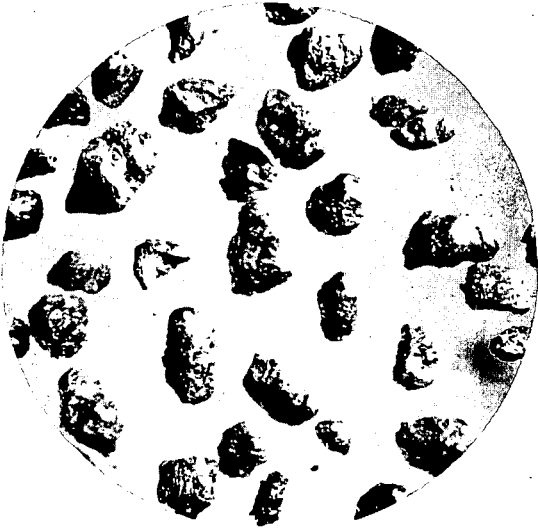
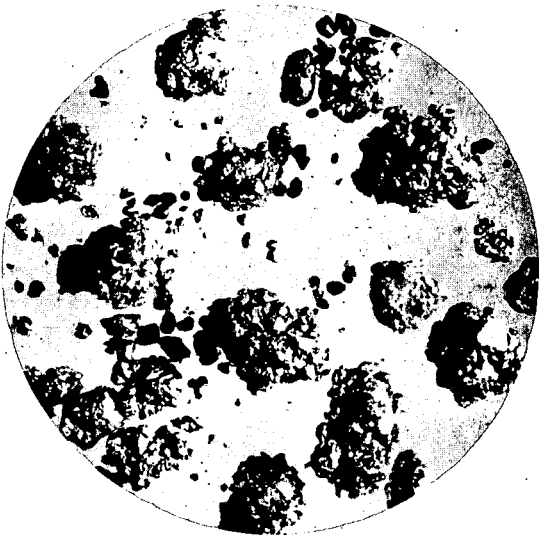


Figure 2. The effect of oxygen content of the fluidizing gas and of temperature on the caking properties of Pittsburgh seam coal (18-100 mesh). The fluidizing gas is inert gas with oxygen content as noted. The average residence time of the char in the reactor is 19 minutes.



410° C



435° C

Figure 3. The effect of increased temperature on the caking property of char made from Pittsburgh seam coal (18-100 mesh), 1.4 percent oxygen in the feed gas.

H-91086-P

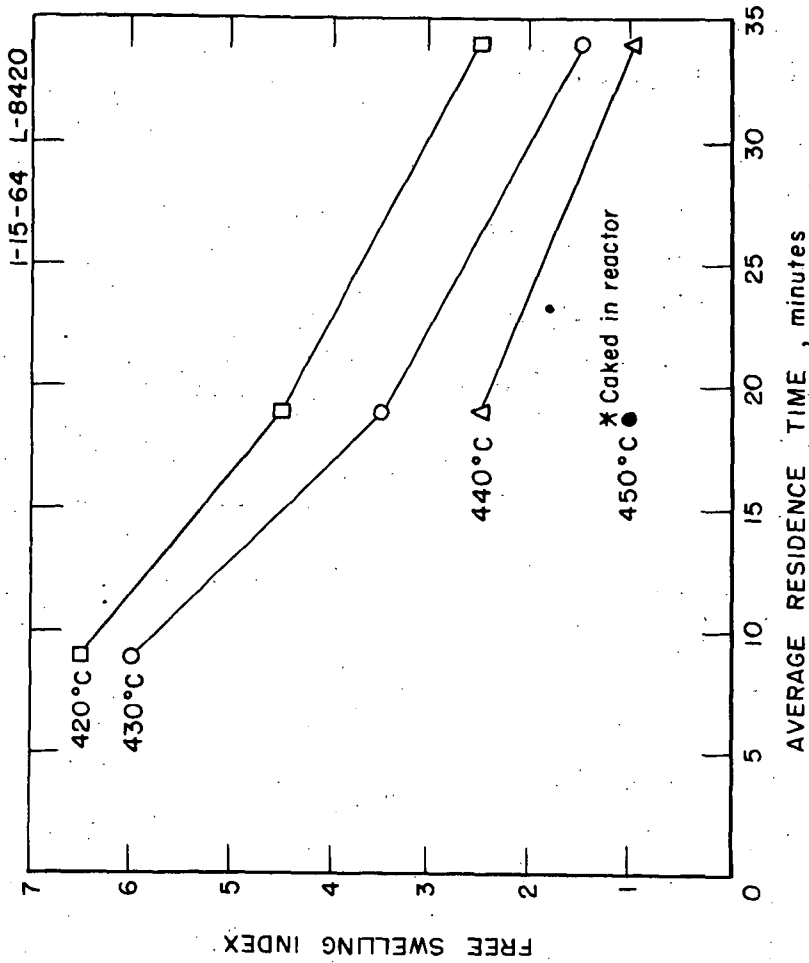


Figure 4. The effect of residence time and of temperature of pretreatment on the free-swelling index of char from Pittsburgh seam coal (18-100 mesh) 0.18-0.20 ft.<sup>3</sup> oxygen/lb coal feed.

3-17-64 L-8421

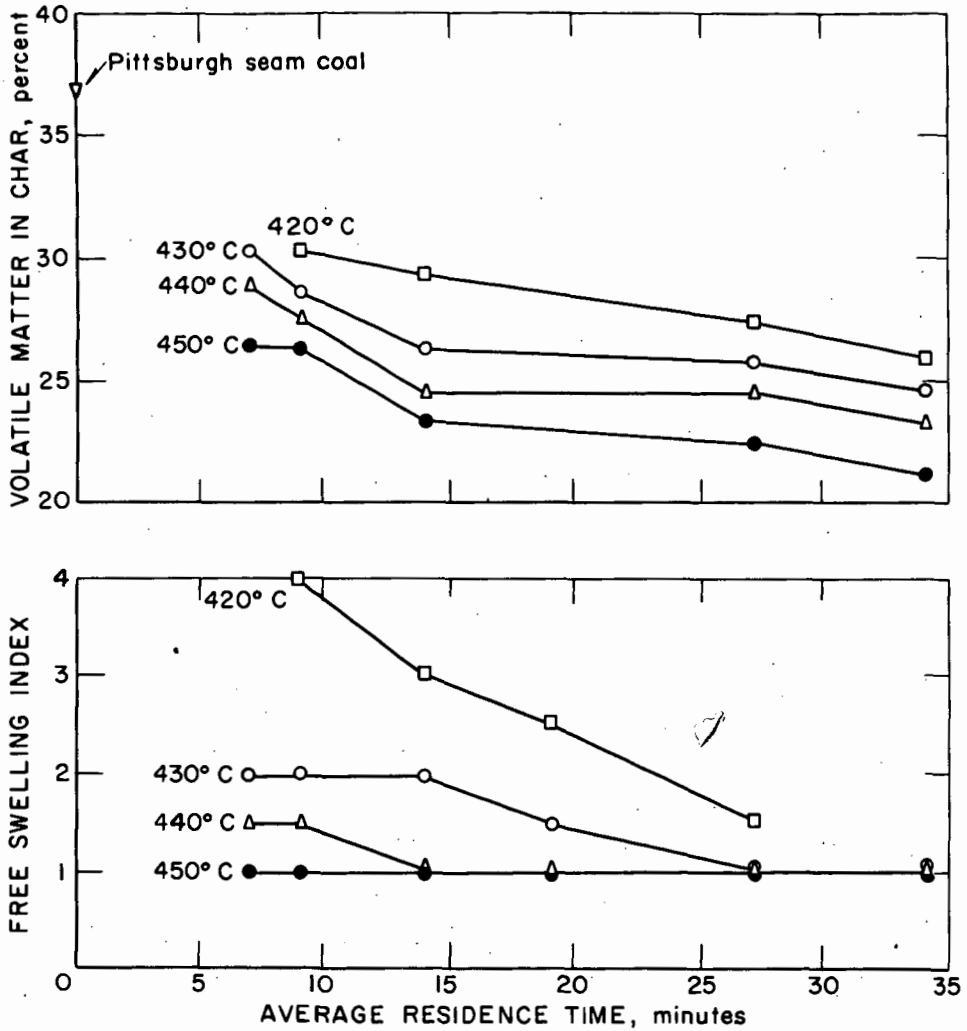


Figure 5. The effect of residence time and of temperature of pretreatment on the free-swelling index and the volatile matter of the char from Pittsburgh seam coal (18-100 mesh; 0.28-0.33 cu ft oxygen/lb coal feed).

3-17-64 L-8522

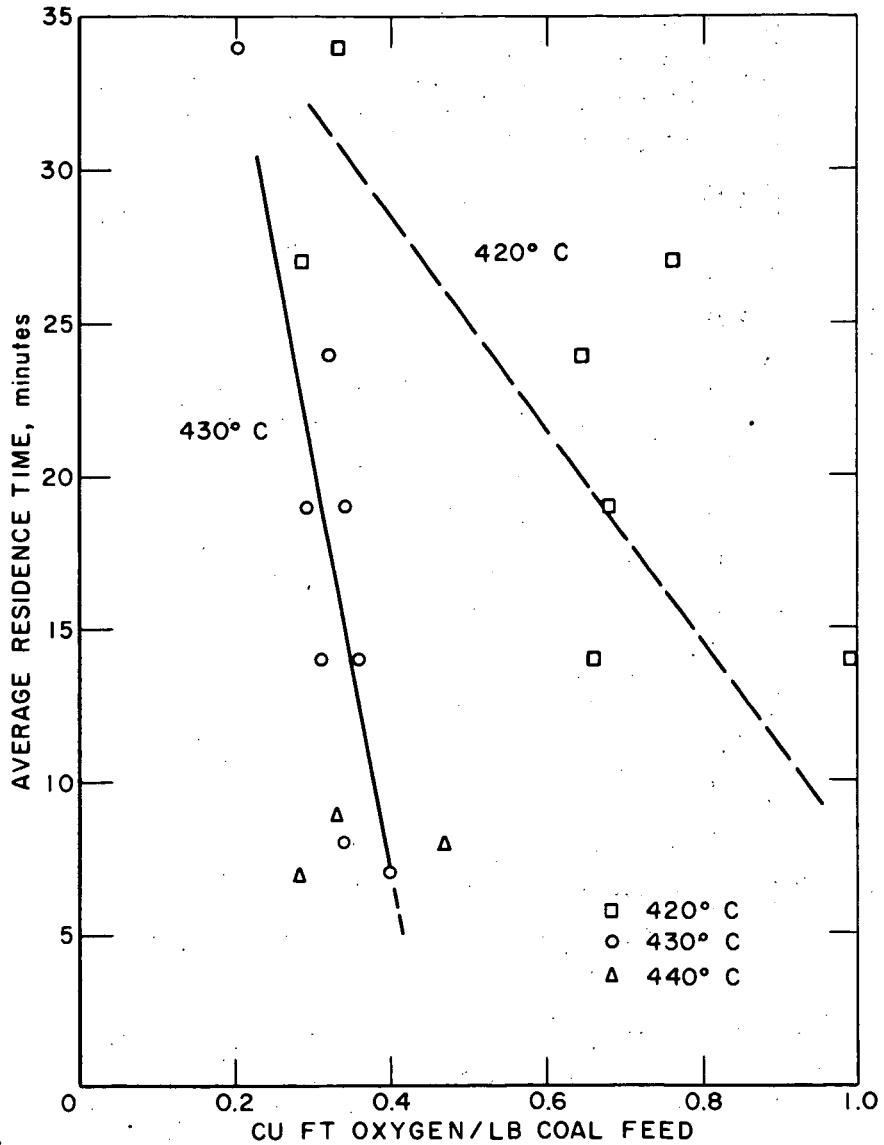


Figure 6. The effect of temperature and oxygen-coal ratio on the residence time of Pittsburgh seam coal of 18-100 mesh (FSI = 1-1/2).

3-17-64 L-8525

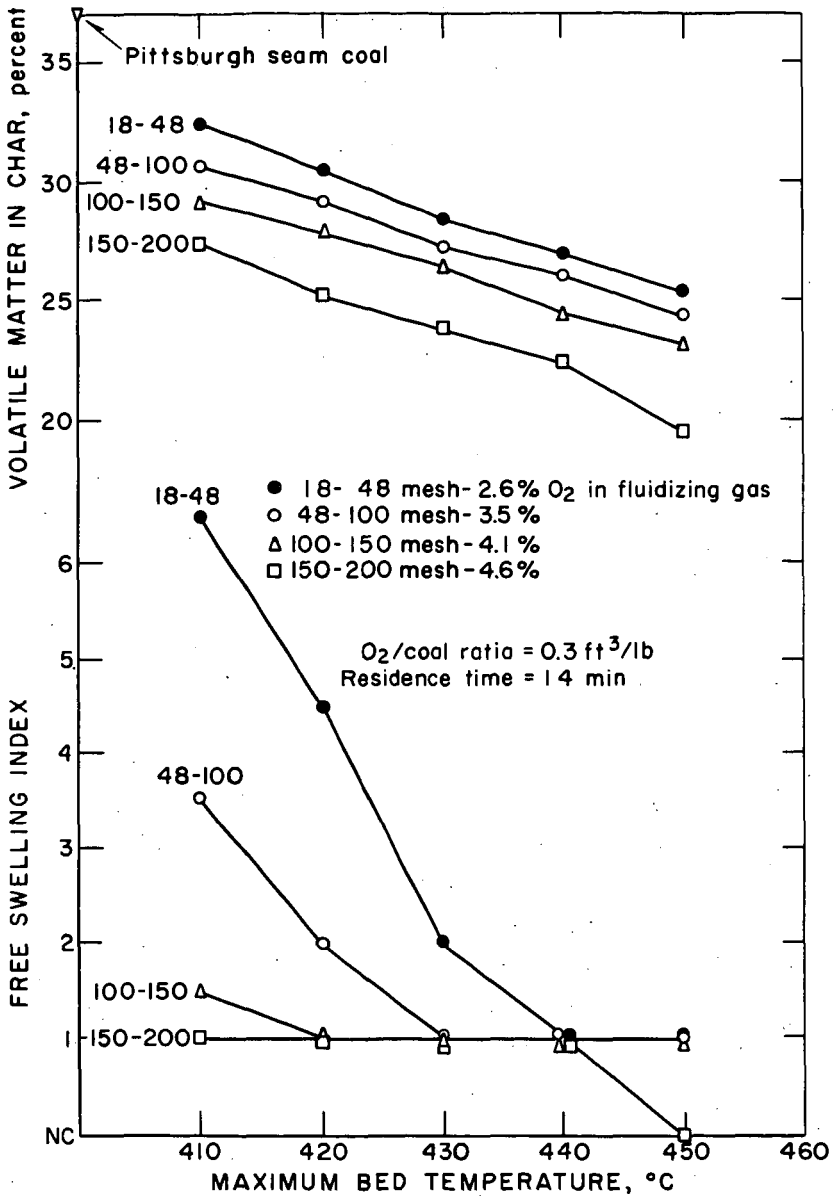


Figure 7. The effect of mesh-size and temperature on the free-swelling index and volatile matter content of the char made from Pittsburgh seam coal.

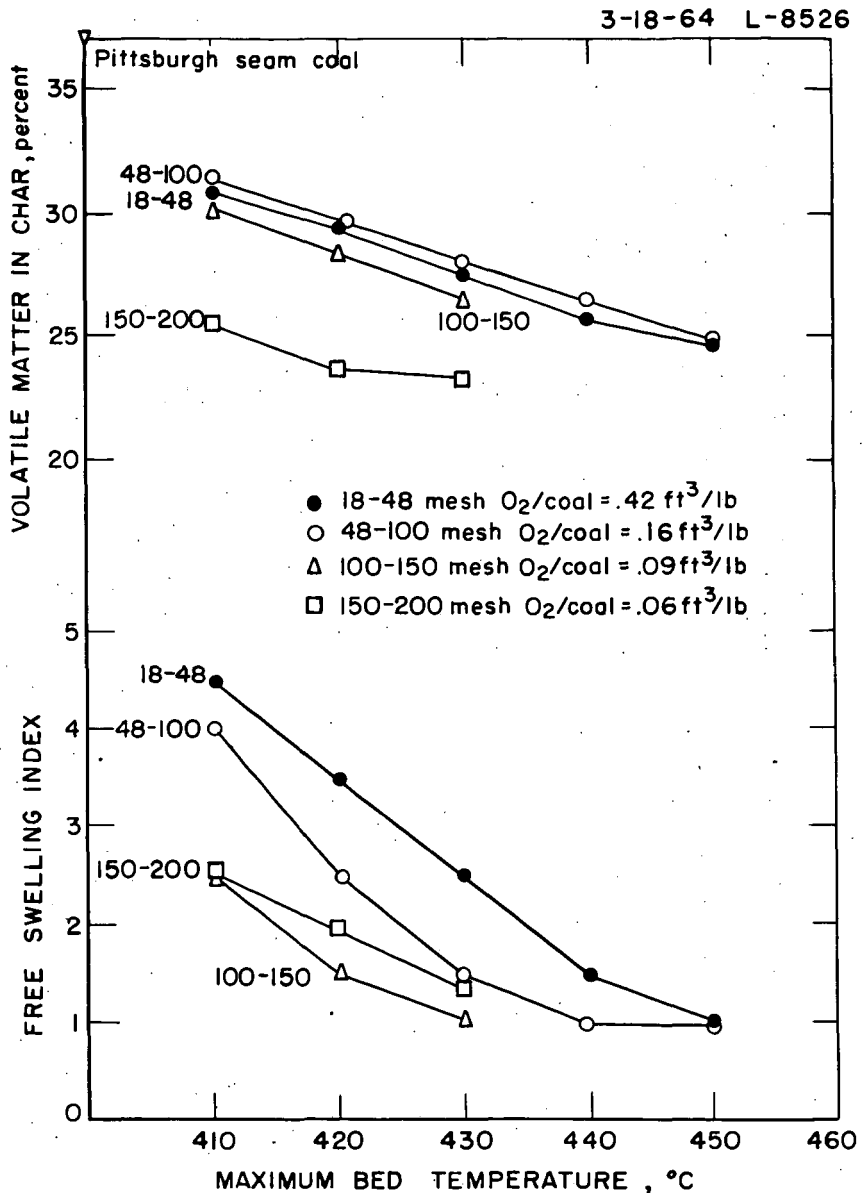


Figure 8. The effect of mesh size and temperature on the free-swelling index of char made from Pittsburgh seam coal. (The oxygen/coal feed ratio varied as noted; residence time is 14 minutes.)

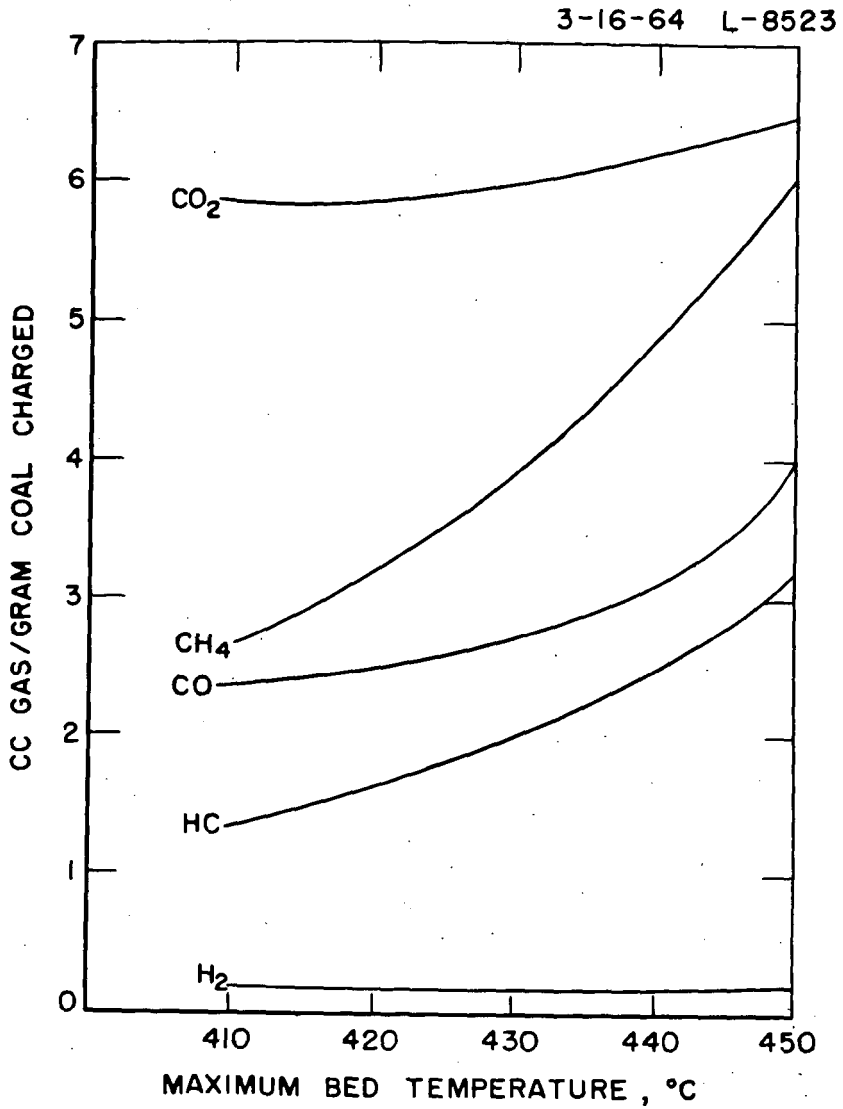


Figure 9. The effect of temperature on off gas made during steam-air treatment of Pittsburgh seam coal of 48-100 mesh ( $O_2$ -coal ratio = 0.4 cu ft/lb; residence time is 14 minutes).

Presented Before the Division of Fuel Chemistry  
American Chemical Society  
Chicago, Ill., August 30 - September 4, 1964

LABORATORY SCALE CARBONIZATION OF NORTH DAKOTA LIGNITE:  
INFLUENCE OF TEMPERATURE AND ATMOSPHERE ON PRODUCT  
DISTRIBUTION AND ACTIVITY

Robert B. Porter and Robert C. Ellman

U. S. Department of the Interior, Bureau of Mines  
Grand Forks Lignite Research Laboratory  
Grand Forks, N. Dak.

INTRODUCTION

The purpose of this investigation has been to study the effect of temperature and atmosphere on carbonization characteristics of lignite. An objective has been to produce a char with minimum sulfur and maximum reactivity toward air, with minimum loss of heating value. Research in carbonization has been extensive on higher rank solid fuels, including efforts to reduce sulfur and control reactivity of chars and cokes (1, 2). For North Dakota lignite, previous attention has been focused upon yield and composition of byproducts.

The considerable influence of atmosphere and temperature on the proportion of sulfur volatilized during carbonization of coal from Illinois and Indiana has been reported by Snow (3) and Mangelsdorf and Broughton (4). Significant differences in sulfur removal were found, depending upon atmosphere during carbonization. More recently, Draycott (5), of the University of Sydney, Australia, reported studies of desulfurization of metallurgical coke in a variety of atmospheres. Best desulfurization occurred at 1,000°C in oil gas with intermittent blasts of steam. Ninety-two percent of the sulfur was removed with a coke loss of about forty percent.

CARBONIZATION EQUIPMENT

The test apparatus was essentially a tube furnace with three separately controlled electric heaters to provide a reproducible and uniform temperature distribution within the unit during carbonization. The carbonization tube was constructed of 1-1/2-inch, schedule 40, stainless steel pipe. Three thermocouples were mounted in the 14-1/2-inch length which held the sample, a fourth in an end heater section, and a fifth was imbedded in the sample; these provided for temperature measurement and control. The tube was charged externally and then placed in the furnace.

The arrangement of the carbonization equipment, including the modifications for various atmospheres, is shown in figure 1. A collection train was provided for the byproduct tar, water, hydrogen sulfide, ammonia, light hydrocarbons, and gas.

PROCEDURE

Each charge consisted of 200 grams (0.441 lb) of lignite, sized 4 x 8 mesh, from the Kincaid mine, Burke County, North Dakota. Nitrogen was passed through the carbonization tube at the rate of 0.6 cubic feet per hour. In the tests in which

carbonization gas was recycled, its flow was regulated to give a superficial space velocity of one-half foot per second, and in the tests in which carbonization was done in a steam atmosphere, steam was injected at the rate of about 500 grams (1.102 lb) per hour. The average heating rate was 400°F per hour, and the sample was held at temperature for 2 hours.

All products except gas were weighed. Gas volume was measured, the gas analyzed, and the weight of the nitrogen-free gas calculated. The condensate contained most of the tar and water and part of the ammonia and hydrogen sulfide product. These components were separated, and their weights were added to those collected in the remainder of the product collection train.

In nitrogen and carbonization gas atmospheres, the test temperatures were 500°, 800°, 900°, 1,000°, 1,300°, and 1,700°F. Three individual tests were performed at each temperature for material balance plus one test to produce char for reactivity measurements.

For carbonization in steam, similar tests were performed at a lower range of temperatures, 500° to 1,100°F, at 100°F intervals because of the significant gasification that occurred at higher temperatures. Char for reactivity measurements was made at 1,200° and 1,300°F in steam, and for comparison purposes, in nitrogen atmosphere at 800°, 900°, and 1,000°F, using the same lignite feed sample.

#### LIGNITE FEED SAMPLES

Three different batches of lignite from the Kincaid mine were used in these tests. Feed number 1 was used for the nitrogen atmosphere material balance tests. Feed number 2 was used for the nitrogen atmosphere char production tests, and all of the tests in recycled carbonization gas atmosphere. Feed number 3 was used for steam atmosphere tests, and the three comparison tests that were made in nitrogen atmosphere. Analyses of these feeds are shown in table 1. The much higher sulfur content of feed number 3 is of special interest.

TABLE 1. - Analyses of lignite feed for carbonization experiments<sup>1/</sup>

Feed number	1	2	3
Proximate analysis, percent:			
Moisture.....	31.9	26.9	32.3
Volatile matter.....	26.6	29.5	29.6
Fixed carbon.....	32.2	34.7	30.6
Ash.....	9.3	8.9	7.5
Ultimate analysis, percent:			
Hydrogen.....	6.5	5.9	6.7
Carbon.....	42.7	46.7	44.2
Nitrogen.....	.4	.8	.7
Oxygen.....	40.7	37.3	38.8
Sulfur.....	.4	.4	2.1
Ash.....	9.3	8.9	7.5
Heating value, Btu/lb.....	7,200	7,780	7,660

<sup>1/</sup> Kincaid lignite "as-charged."

## PRODUCT YIELDS

The product yields obtained by carbonizing in nitrogen and carbonization gas atmospheres were very similar. As carbonization temperature increased, yields of gas, tar, and water product increased at the expense of the char; the rate of increase became less as temperature advanced. Product yields as a function of carbonization temperature are shown in figures 2 and 3.

The product yields obtained from steam carbonization, as shown in figure 4, were similar to the others below 900°F. Above this temperature the yield of char product continued to decline steeply with advancing temperature, and the yield of gas product increased very rapidly. Figure 5 compares the char yields obtained from nitrogen and steam carbonization to illustrate the effect of gasification.

## TESTS OF CHARs

### Crossing-Point Temperature

The reactivity of each char in air was determined in a crossing-point-temperature apparatus. The apparatus was constructed of a length of 1/2-inch stainless steel pipe placed in a small vertical tube furnace. A 1-1/2-inch deep charge sized 40 x 60 mesh was supported on a screen in the middle of the tube. The wall temperature and the temperature at the center of the charge were recorded. The wall temperature was increased at a rate of 27°F per minute, while air was diffused through the sample at the rate of 0.45 cubic feet per hour. The crossing-point temperature was defined as the temperature at which the inside temperature overtook the wall temperature which means the lower the crossing-point temperature the more reactive the char towards air.

The crossing-point temperatures for chars are shown in figure 6. The lowest crossing-point temperatures were found for the chars carbonized in the 800° to 1,000°F region. Both recycled carbonization gas and steam decrease char activity toward air. Char produced from feed number 3 gave higher crossing points than char produced from feed number 2 under similar conditions.

### Acetic Acid Adsorption

The chars produced in steam atmosphere were tested for their ability to adsorb acetic acid. After evidence of soluble alkali in the chars was found, each char was treated in a Soxhlet extractor with water for 60 hours and then dried. The acetic acid adsorption test procedure was to mix a half gram of 40 x 60-mesh soluble-alkali-free char with 50 milliliters of 5 millinormal acetic acid in a closed container and shake mechanically for 2 hours. The final acid strength was determined, and an adsorption constant calculated. This constant was the ratio of acid concentration in the char to that in the liquid at equilibrium.

Figure 7 shows the acetic acid adsorption constants of the chars tested as functions of the carbonization temperatures. Activity shows a rapid increase as the carbonization temperature increases from 1,000°F.

Low crossing-point temperatures and low acetic acid adsorption constants occur in the same carbonization temperature region. These two types of activity seem to

be quite distinct. The opposite trends of the two char activities with carbonization temperature were confirmed by a statistical rank test.

### Sulfur Removal Relationships

The criteria used for a well desulfurized char was low sulfur and high heating value. The sulfur content of the chars was therefore compared in this report on the basis of pounds of sulfur per million Btu. Figure 8 shows the sulfur contents of the various chars on this basis as a function of carbonization atmosphere and temperature.

The chars carbonized in nitrogen show the lowest sulfur content at 900°F carbonization temperature. The chars carbonized in recycled carbonization gas were similar except that the 900°F char was higher in sulfur than the 800° or 1,000°F chars.

The sulfur contents of the chars carbonized in steam were different: increasing from 500° to 700°F, dropping to 1,000°F, holding fairly constant to 1,200°F, and rising rapidly to 1,300°F. The higher sulfur in feed number 3 is reflected in the chars produced from it.

The criterion used for a good desulfurization process was a high ratio of sulfur loss to heating value loss. This function, the loss ratio, was obtained by dividing the percentage sulfur lost by the percentage Btu lost, and it depends upon the sulfur content and heating value of the feed, the char yield, and the sulfur content and heating value of the char produced.

The loss ratios as functions of carbonization atmosphere and temperature are shown in figure 9. The highest loss ratios were at 900°F for chars produced in nitrogen atmospheres and best at 800°F for chars produced in recycled carbonization gas. For chars produced in steam, two peaks were found, the highest loss ratio was at 500°F, and the second highest was at 1,000°F.

### SUMMATION

The highest reactivities of chars toward air were found in chars produced by carbonizing in the region of 800° to 1,000°F. Carbonization in either recycled carbonization gas or steam produced chars less reactive than those carbonized in nitrogen.

The reactivity measured by acetic acid adsorption was not the same reactivity as that measured by crossing-point temperature. The acetic acid adsorption value varies with carbonization temperature in the opposite manner as compared to crossing-point values for the chars that were produced by carbonization in steam.

The lowest char sulfur content and highest loss ratio occurred at 900°F when carbonizing in a nitrogen atmosphere. For carbonization in recycled carbonization gas, the lowest sulfur content occurred at 1,000°F and the highest loss ratio at 800°F. The desulfurization by carbonizing in steam was quite different. The lowest sulfur content occurred at 1,200°F, the highest loss ratio was found at 500°F, and the next best at 1,000°F. Differences in lignite feed were reflected in the char produced, both in reactivity toward air and in sulfur removal.

## REFERENCES

- (1) Thiessen, Gilbert, Forms of Sulfur in Coal, Ch. in Chemistry of Coal Utilization, ed. by H. H. Lowry, John Wiley & Sons, New York, N. Y., 1, 425-449 (1945).
- (2) Wilson, Philip J., Jr., and Clendenin, J. D., Low-Temperature Carbonization, Ch. in Chemistry of Coal Utilization, ed. by H. H. Lowry, John Wiley & Sons, New York, N. Y., Supp. v., 395-460 (1963).
- (3) Snow, R. D., Conversion of Coal Sulfur to Volatile Sulfur Compounds During Carbonization in Streams of Gases, Ind. and Eng. Chem., 24 903-909 (1932).
- (4) Mangelsdorf, A., and Broughton, F. B., Effect of Atmosphere on Desulfurization of Coal During Carbonization, Ind. and Eng. Chem., 24, 1136-1137 (1932).
- (5) Draycott A., Production of Low Sulphur Coke from High Sulphur Coals. Chem. Ind. & Eng. 3, No. 7, 17-30 (1954).

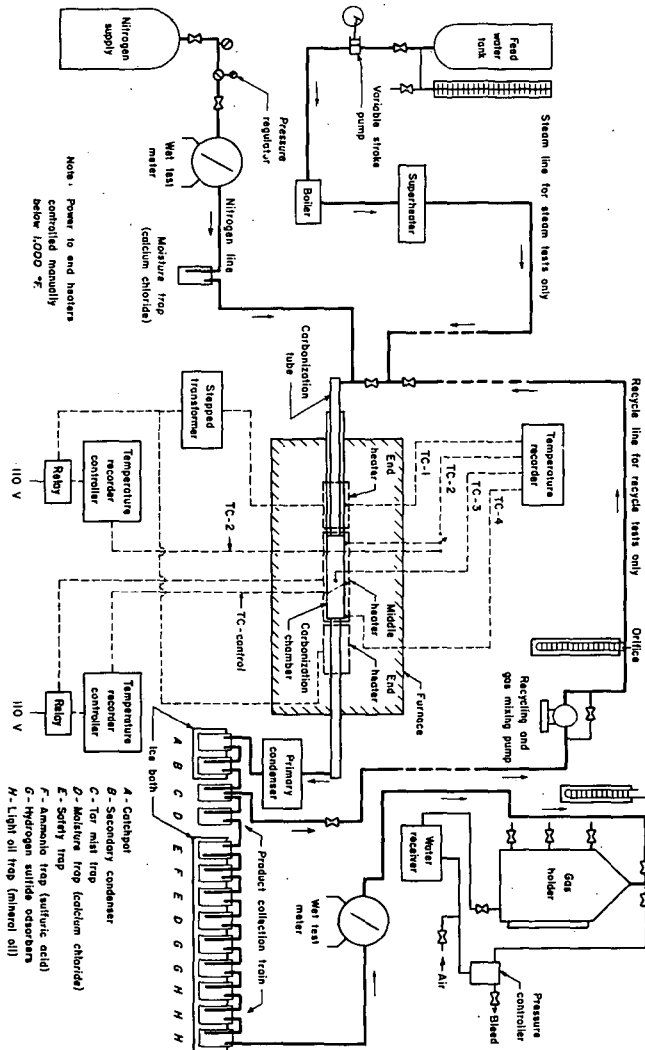


Fig 1 Flow sheet, carbonizer and auxiliary equipment.

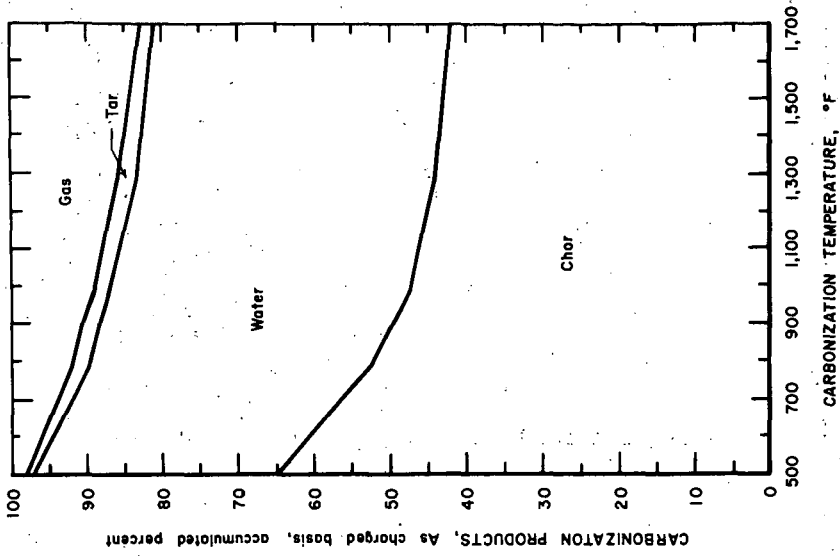


Fig 3 Product yields, carbonization in recycled carbonization gas atmosphere.

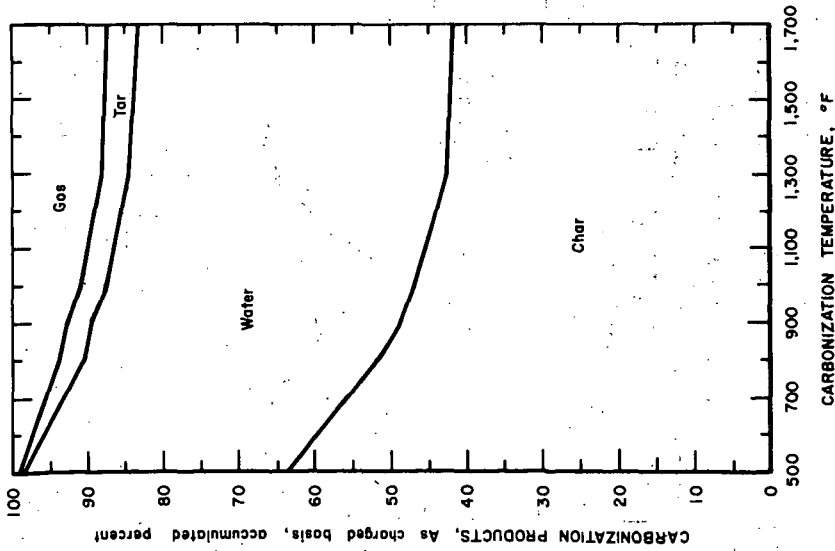


Fig 2 Product yields, carbonization in nitrogen atmosphere.

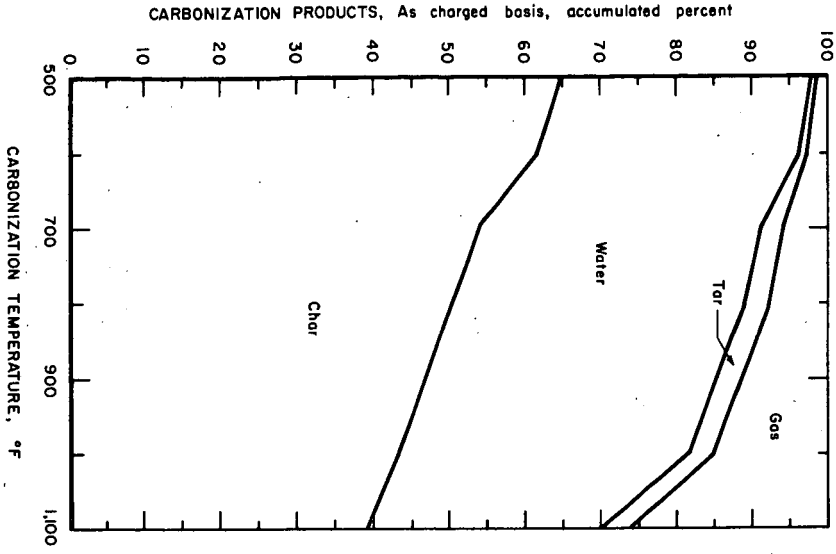


Fig. 4 Product yields, carbonization in steam atmosphere.

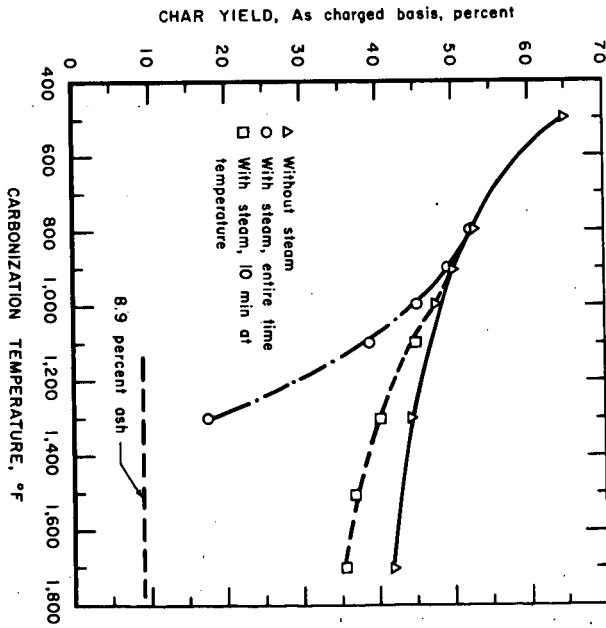


Fig. 5 Effect of steam on char yield.

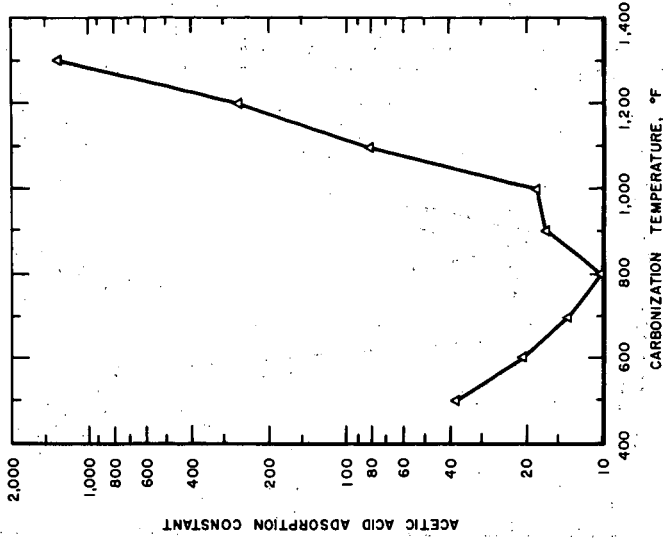


Fig 7 Acetic acid adsorption of chars as a function of carbonization temperature in steam atmosphere.

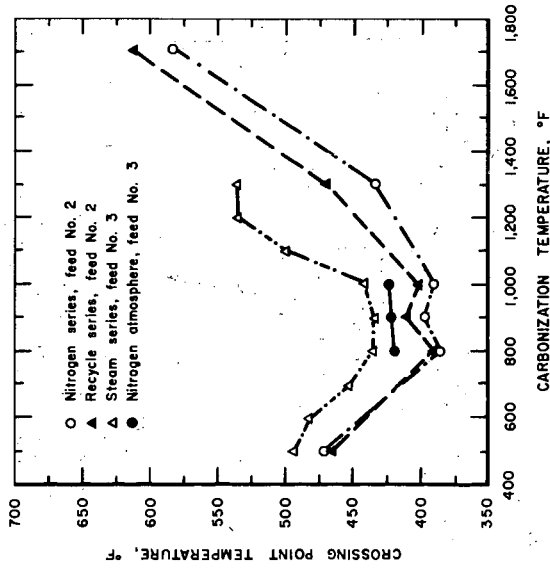


Fig 6 Crossing-point temperatures of chars as a function of carbonization temperature and atmosphere.

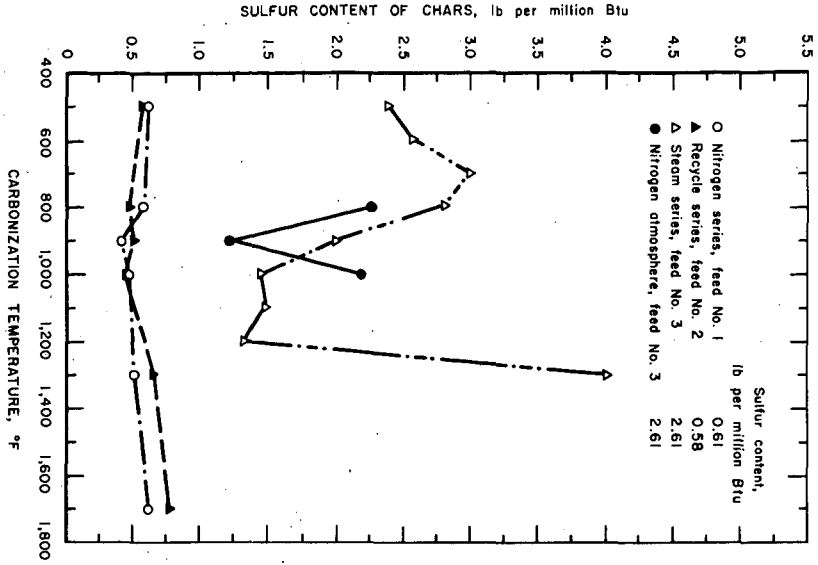


Fig 8 Sulfur contents of chars as a function of carbonization temperature and atmosphere.

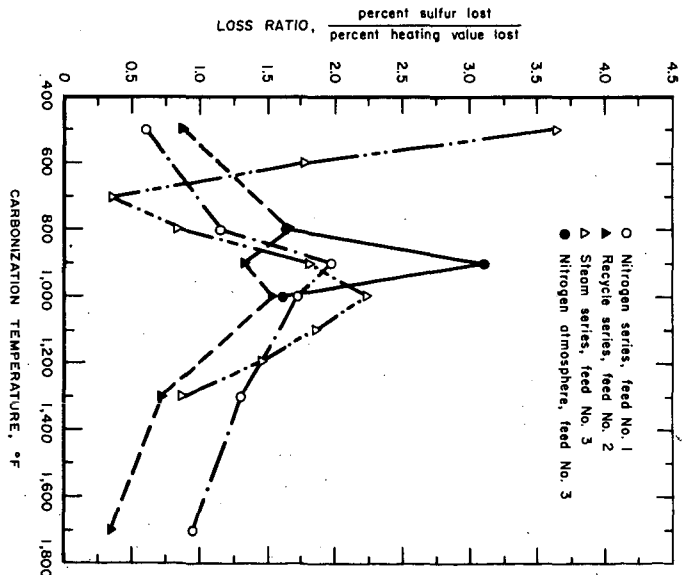


Fig 9 Sulfur-heating value loss ratio as a function of carbonization temperature and atmosphere.

Presented Before the Division of Fuel Chemistry  
American Chemical Society  
Chicago, Ill., August 30 - September 4, 1964

## ETHYLENE AND AROMATICS BY CARBONIZATION OF CANNEL COAL

R. S. Montgomery and D. L. Decker

The Dow Chemical Company, Midland, Michigan

The low-temperature carbonization of coal is a possible alternative to the cracking of crude oil for the production of ethylene and aromatics. The previous investigations reported by this laboratory were concerned with the carbonization of lignites.<sup>1</sup> It was found that if lignites were carbonized at a low temperature in order to obtain the maximum yield of tar and this tar cracked without being allowed to condense, acceptable yields of ethylene, propylene and aromatics could be obtained. Once the low temperature tar is allowed to condense, however, large amounts of char and heavy residue are formed in the cracker and the yields of the desired products are small. It was concluded from this work that this process could be commercially important if the cost of crude oil increases enough to offset the high initial capital cost.

The present investigation was concerned with the use of West Virginia and Kentucky cannel coals in this process. Cannel coal is a high volatile, non-coking coal and occurs in lenticular pockets in bituminous coal beds. It was hoped that the higher yields which would certainly be obtained with these coals, and therefore the lower capital investment required for the same production, would more than offset the increased cost of the coal.

### EXPERIMENTAL

#### Equipment

The equipment used in this work is very similar to that used in the earlier work. The evolved volatile matter passed from a batch carbonizer through the cracker into the collection train, which consisted of a water-jacketed receiver, condenser, and two low-temperature absorbers. These absorbers consisted of jacketed pyrex columns packed with steel wool. The noncondensable gas passed through a cotton trap and then through a wet-test gas meter, which measured the volume of the evolved gas. After leaving the wet-test gas meter, the gas passed into a solenoid-actuated valve which allowed a fraction of the gas to be collected in a gas holder. The remainder was vented to the atmosphere.

The carbonizer used in these experiments was similar to that used in the lignite experiments, except that it was modified so that superheated steam could be blown through the coal during carbonization. It was made from a two inch stainless steel pipe, 24 inches in length. Near the top of the retort, a one-half inch pipe was provided as a take-off for the volatile matter. A one inch plug fitted with a thermocouple well was used at the top of the carbonizer for the introduction of the coal. A removable steel sparger was provided at the bottom of the carbonizer for the introduction of the superheated steam and the removal of the char. Heat for the carbonizer was provided by electric furnaces controlled by means of Variacs.

The cracking reactors were 36 inches long and were fabricated of Vycor tubing of 31 mm outside diameter. A concentric 9 mm Vycor tube, through the entire length of the cracking tube, allowed a thermocouple to be placed inside the tube and the cracking temperature to be measured for any point in the tube. The cracking temperature was controlled by the temperature near the exit of the reactor. The cracker was heated with resistance tape wound directly on the tubing and the electric current controlled by a Variac. Different average retention times were obtained by using two, three or four of these reactors in series.

### Coals Used

Samples of four different cannel coals were used in this work. Three were from West Virginia - Gay Mine, Logan County; Stollings Mine, Madison County; and Dorothy Mine, Boone County; one was from the Big Chief Mine, Letcher County, Kentucky. The samples which were received as 6 to 8 inch lumps were crushed, and the fraction which passed through a 3-1/2 mesh and remained on a 10 mesh screen was used in the experiments.

Table 1

<u>Proximate Analysis</u>	Gay	Stollings	Dorothy	Big Chief
Moisture	0.31%	0.56%	0.63%	0.46%
Net Volatile	48.46	54.86	61.05	53.07
Fixed Carbon	37.42	34.26	32.52	41.49
Ash	13.81	10.32	5.80	4.98
<u>Ultimate Analysis</u>				
Hydrogen	6.56	7.04	7.71	7.29
Carbon	74.52	74.79	78.84	80.96
Nitrogen	0.67	1.22	0.88	1.23
Sulfur	0.52	1.24	0.86	0.77
Oxygen	3.92	5.39	5.91	4.77
<u>Fisher Assay</u>				
Oil, gal/ton	85.8	90.6	104.2	86.5
Water, gal/ton	2.4	3.6	3.8	3.4
Gas and loss, %	9.1	9.2	10.9	6.7
Sp. Gr. oil 60/60°F	0.9056	0.9106	0.9079	0.9022

### PROCEDURE

Cannel Coal (500 grams) was charged into the carbonizer and the cracker temperature brought up to the predetermined level. Then the temperature of the carbonizer was slowly and uniformly raised from room temperature to a maximum of 550°C. When the carbonizer reached 300°, superheated steam at 500° was introduced into it. After the experiment, the carbonizer was allowed to cool to room temperature and the train disassembled, and the contents of the receiver and two absorbers steam distilled. The steam-distilled oil was then fractionated, and the fractions examined by mass spectrometry. The residual oil and tar in the distillation pot plus any increase in weight of the absorbers was designated as

heavy oil. The volume of gas produced was measured with the wet-test gas meter and samples of the gas examined by mass spectrometry.

Exploratory experiments indicated that the primary process variables were cracking temperature, retention time and the steam-coal ratio. Therefore the effect of these three process variables at three different levels were investigated on the cannel coal from the Gay Mine, using nine experiments in a "Latin Square" arrangement. With this arrangement, the effect of a single variable can be determined with the effects, first order at least, of the other variables confounded or cancelled out. The levels of the process variables that were chosen were:

Cracking temperature - 800°, 850°, and 900°.

Average retention time - 0.5, 0.7, and 0.9 seconds.

Steam-to-coal ratio - 1.0, 1.25, and 1.5.

The "average retention time" deserves some comment. Since a batch carbonizer was used in these experiments, the rate of volatile generation in the carbonizer varied within rather wide limits as the carbonizer temperature was raised from 300° to 550°. Because of this, the gas velocity through the crackers, and therefore the retention time in the cracker also, varied within rather wide limits. "The average retention time" was calculated on the basis of the total volume of volatiles generated and volume of the crackers used in the experiment. These "average retention times" can only be used as guides; all that can be said for certain is that the retention times are in the ratios two, three and four.

Another problem which arises with regard to the interpretation of the effects of retention time is that the actual retention time is affected by the steam-coal ratio used. When more steam is passed through the carbonizer, the space velocity is increased, and therefore the retention time in the cracker correspondingly decreased. Because of this, the effects of average retention time and steam-coal ratio are interrelated despite the Latin Square arrangement of the data. This must be taken into account when interpreting the retention time data.

## RESULTS

Analysis of the products obtained in these experiments makes it possible to evaluate the effects of the process variables on the yields of the various products. Since all of the volatile matter passed through the cracker, the volume and composition of the evolved gases and oils was affected by all the process variables, that is, cracking temperature, retention time, and steam-coal ratio. The character of the char produced, however, could only be affected by the steam-coal ratio.

### Effect of Process Variables on Gas Produced

The composition of the gas evolved from the coal varies as different levels of the process variables are employed. Some constituents of the gas are affected greatly by the process variables, others, very little.

The chief components of the gas are ethylene, ethane, acetylene, propylene, butadiene, methane, hydrogen, and carbon monoxide and dioxide. These comprise at least 98% of the total gas produced.

The process variables have little or no effect on the total yield of gas, at least at the levels investigated. It might be expected that

the higher cracking temperatures and longer retention times would produce more gas, but this is not the case.

The yield of ethylene, too, is not particularly affected by the process variables. However, the best yield was produced at a cracking temperature of 850°, an average retention time of 0.5 seconds, and a steam-coal ratio of 1.25.

The lowest cracking temperature and the shortest retention time investigated result in the production of the largest amount of ethane. Apparently more of the ethane is converted to ethylene at the more rigorous cracking conditions. At a cracking temperature of 800°, 24.8 pounds/ton is obtained, while at 900°, only 9.9 pounds/ton is obtained. The steam-coal ratio, however, does not seem to have any significant effect.

As might be expected, the highest yield of acetylene is obtained at the highest cracking temperature. At a cracking temperature of 800°, only 8.1 pounds/ton is obtained, but this is raised to 22.3 pounds/ton by increasing the cracking temperature to 900°. The steam-coal ratio is not nearly so important, but the production of acetylene is favored by the higher ratio. Perhaps surprisingly, the retention time has only little effect.

There is a substantial decrease in the yield of propylene when the higher cracking temperatures and longer retention times are employed. At a cracking temperature of 800°, 64.6 pounds/ton is obtained, but this falls to only 23.8 pounds/ton at 900°. Similarly, increasing the average retention time from 0.5 to 0.9 seconds resulted in a decrease in the yield of propylene from 59.8 to 32.1 pounds/ton. The steam-coal ratio, however, had comparatively little effect.

The yield of butadiene decreases rapidly as the cracking temperature and retention time are increased. At a cracking temperature of 800°, 22.0 pounds/ton is obtained, but at 900° only 11.2 pounds/ton is obtained. Similarly, increasing the retention time from 0.5 to 0.9 seconds decreases the yield of butadiene from 20.9 to 12.7 pounds/ton. The best steam-coal ratio for the production of butadiene is 1.25.

The process variables do not greatly affect the yield of methane. On the average, the methane yield is about 150 pounds/ton.

As might be expected, greater quantities of hydrogen are produced at the more rigorous cracking conditions. At a cracking temperature of 800°, a ton yields 12 pounds of hydrogen, at 900°, 19.4 pounds. Increasing the retention time from 0.5 to 0.9 seconds, similarly raises the yield of hydrogen from 13.5 to 17.1 pounds/ton. An increase in the steam-coal ratio from 1.0 to 1.5 decreases the amount of hydrogen obtained from a yield of 17 pounds/ton to 14 pounds/ton, probably because of its effect on the retention time.

The yield of carbon dioxide is quite constant at 15 pounds/ton at all levels of the process variables studied, and only cracking temperature has much effect on the yield of carbon monoxide. When the cracking temperature is raised from 800° to 900°, the yield of carbon monoxide increases from 40.9 to 72.2 pounds/ton.

#### Effect of Process Variables on Light Oil Produced

The process variables at the levels studied have no significant effect on the total yield of light oil. It might be expected that higher

temperatures and longer retention times would favor the production of light oil owing to the conversion of heavy oil to light oil at the more rigorous conditions, but this is not true. Evidently, if more light oil is produced, more light oil is also converted into gaseous hydrocarbons. At all the conditions studied, the yield of light oil was about 115 pounds/ton.

The light oil contains a large number of compounds. The more easily identifiable components of the mixture are benzene, toluene, styrene, C<sub>2</sub> benzenes, indene, indan, and/or methylstyrene, naphthalene, and methyl naphthalene. These components comprise 58 to 73% of the total. The remainder is made up of more highly substituted benzenes, styrenes, and naphthalenes. Only the effects of the process variables on the production of benzene, toluene, styrene, and naphthalene will be discussed, since these are the most commercially important components.

The yield of benzene as a function of retention time shows a definite maximum at 0.7 seconds; and as a function of steam-coal ratio, a definite minimum at a ratio of 1.25. However, the levels of cracking temperature employed seem to have no significant effect.

The yield of toluene as a function of steam-coal ratio shows, like the yield of benzene, a definite minimum at a ratio of 1.25, although in this case neither the cracking temperature nor the retention time seem to be important.

The process variables have very little effect on the yield of styrene. It is relatively constant at about 6.0 pounds/ton.

The highest cracking temperatures and the longest retention times investigated favored the production of naphthalene. At a cracking temperature of 800°, the yield was 9.3 pounds/ton, while at 900° it increased to 13.9 pounds/ton. In the same way, increasing the retention time from 0.5 to 0.9 seconds increased the yield from 9.0 to 13.6 pounds/ton. The steam-coal ratio, on the other hand, seemed to have little effect.

#### Effect of Process Variables on Heavy Oil Produced

As expected, the higher cracking temperatures favored the conversion of the heavy oil to light oil and volatile gases. Surprisingly, however, there was a definite maximum in the yield at the intermediate retention time and the intermediate steam-coal ratio, that is, 0.7 seconds and a ratio of 1.25.

Some analytical work was done on the heavy oil, but due to its complex nature, no individual components were determined. The heavy oil is mainly aromatic in character and is composed of polynuclear aromatic hydrocarbons of high molecular weight. An ultimate analysis was made on the heavy oil from each run, but there was little difference. The average analysis is:

Carbon	90.35%
Hydrogen	5.03
Nitrogen	1.46
Sulfur	0.67
Ash	1.36
Oxygen (by diff.)	1.13

### Comparison of the Different Cannel Coals

In view of the fact that the yields of the commercially important products are, in general, not particularly sensitive to the process conditions in the ranges investigated, the four different cannel coals were compared at only a single set of conditions. A cracking temperature of 850°, an average retention time of 0.9 seconds, and a steam-coal ratio of 1.0 was chosen. While these conditions are not optimum, it seems unlikely that the comparison would be drastically different at any other generally-similar conditions. The results of these experiments are given in Tables 2, 3, 4, 5 and 6.

There is a good correlation between the yields of total gas, ethylene, total light oil, benzene, toluene, etc., and the gas and oil yield in the Fisher assay. When more gas and oil is obtained in the Fisher assay, a similar increase is noticed in the yields of the more valuable products. This is not, however, true with the yields of heavy oil. There is probably a tendency for the high assaying coals to produce more heavy oil, but the correlation is not nearly as high as it is for the light oils and gases.

### DISCUSSION

The low-temperature carbonization of cannel coal immediately followed by a thermal cracking of the volatile products produces excellent yields of ethylene, benzene, and other aromatic hydrocarbons. As expected, the yields of these products are much higher than could be obtained from lignite; over five times as much ethylene and benzene can be obtained. This did indeed result in a lower capital investment for a commercial plant producing the same amount of ethylene and aromatics as the lignite plant, and undoubtedly more than offset the increased cost of the cannel coal. A preliminary economic analysis, however, indicated that this process is still probably not competitive with the conventional crude oil cracking process. If the cost of crude oil should increase significantly, or if significant engineering improvements could be made to lower the capital cost, the commercial use of this process would be a possibility.

### REFERENCE

- <sup>1</sup> R. S. Montgomery, D. L. Decker and J. C. Mackey, *Ind. Eng. Chem.*, 51, p. 1293 (1959).

TABLE 2

Cracking Temperature: 850°C                      Average retention time: 0.9 sec.  
 Steam-coal ratio: 1.0

Charge: 500 gms. of 3-1/2 - 10 mesh "Gay" cannel coal

Yield of Gas:	107.9 gms.	431.0 lbs/ton	502.6 lbs/ton(MAF)
Ethylene	42.3	169.0	197.0
Acetylene	2.2	8.8	10.2
Propylene	4.3	17.2	20.0
Butadiene	1.7	6.8	7.9
Butene-2	0.5	2.0	2.3
Methane	35.6	142.0	166.0
Ethane	3.1	12.4	14.4
Hydrogen	3.7	14.8	17.2
Carbon monoxide	11.2	44.8	52.2
Carbon dioxide	3.3	13.2	15.4

Yield of Light Oil:	23.7	94.8	110.3
Benzene		18.2	21.2
Toluene		10.4	12.1
Styrene		5.7	6.6
C <sub>2</sub> Benzenes		2.5	2.9
Indene		4.9	5.7
Indan/or methylstyrene		1.7	2.0
Naphthalene		9.7	11.3
Methyl naphthalenes		3.4	4.0

Yield of Heavy Oil:            53.0                      212.0                      247.0

Yield of Char                    290.1                      1160.0

Heat Content of Gas: 747 BTU/cu.ft. (ethylene-free)

TABLE 3

Cracking Temperature: 850°C                      Average retention time: 0.9 sec.  
 Steam-coal ratio: 1.0

Charge: 500 gms. of 3-1/2 - 10 mesh "Big Chief" cannel coal

Yield of Gas:	121.1 gms.	484.0 lbs/ton	509.4 lbs/ton(MAF)
Ethylene	45.3	181.4	191.0
Acetylene	1.6	6.4	6.7
Propylene	6.6	26.4	27.8
Butadiene	2.7	10.8	11.4
Butene-2	0.5	2.0	2.1
Methane	35.7	143.0	150.5
Ethane	2.9	11.6	12.2
Hydrogen	4.2	16.8	17.7
Carbon monoxide	16.7	66.0	69.4
Carbon dioxide	4.9	19.6	20.6
Yield of Light Oil:	26.6	106.2	111.5
Benzene		29.9	31.4
Toluene		11.9	12.5
Styrene		4.5	4.7
C <sub>2</sub> Benzenes		3.1	3.3
Indene		6.0	6.3
Indan/or methylstyrene		2.0	2.1
Naphthalene		7.3	7.7
Methyl naphthalene		3.0	3.2
Yield of Heavy Oil:	60.7	242.8	254.0
Yield of Char:	272.2	1088.0	
Heat Content of Gas:	728 BTU/cu.ft. (ethylene-free)		

TABLE 4

Cracking Temperature: 850°C      Average retention time: 0.9 sec.  
 Steam-coal ratio: 1.0

Charge 500 gms. of 3-1/2 - 10 mesh "Stollings" cannel coal.

Yield of Gas:	123.0 gms.	491.8 lbs/ton	549.7 lbs/ton(MAF)
Ethylene	46.5	186.0	208.8
Acetylene	2.7	10.8	12.1
Propylene	8.6	34.4	38.6
Butadiene	2.9	11.6	13.0
Butene-2	0.5	2.0	2.2
Methane	33.9	135.6	152.3
Ethane	3.9	15.6	17.5
Hydrogen	3.7	14.8	16.6
Carbon monoxide	14.1	56.2	63.0
Carbon dioxide	5.7	22.8	25.6

Yield of Light Oil:

	28.0	112.0	126.0
Benzene		35.8	40.2
Toluene		14.1	15.8
Styrene		5.4	6.1
C <sub>2</sub> Benzenes		4.3	4.8
Indan/or methylstyrene		2.6	2.9
Naphthalene		8.1	9.1
Methyl naphthalene		3.6	4.0

Yield of Heavy Oil:

	71.4	284.0	309.0
--	------	-------	-------

Yield of Char: 265.8      1063.0

Heat Content of Gas: 784 BTU/cu.ft. (ethylene-free)

TABLE 5

Cracking Temperature: 850°C                      Average retention time: 0.9 sec.  
 Steam-coal ratio: 1.0

Charge: 500 gms. of 3-1/2 - 10 mesh "Dorothy" cannel coal

Yield of Gas:	138.0 gms.	552.2 lbs/ton	587.9 lbs/ton(MAF)
Ethylene	57.5	230.0	245.0
Acetylene	4.1	16.4	17.5
Propylene	9.6	38.4	40.8
Butadiene	3.4	13.6	14.5
Butene-2	0.5	2.0	2.1
Methane	37.6	150.6	160.2
Ethane	5.0	20.0	21.3
Hydrogen	4.6	18.4	19.6
Carbon monoxide	9.2	36.8	39.2
Carbon dioxide	6.5	26.0	27.7
Yield of Light Oil:	33.5	133.8	142.3
Benzene		43.8	46.6
Toluene		16.7	17.8
Styrene		6.3	6.7
C <sub>2</sub> Benzenes		3.9	4.2
Indene		7.7	8.2
Indan/or methylstyrene		11.1	11.8
Methyl naphthalenes		4.5	4.8
Yield of Heavy Oil:	65.1	260.2	277.0
Yield of Char:	236.1	944.0	
Heat Content of Gas:	794 BTU/cu.ft. (ethylene-free)		

TABLE 6

Ultimate Analysis of Heavy Oil:

	"Gay"	"Stollings"	"Big Chief"	"Dorothy"
Carbon	90.26%	89.58%	87.42%	88.40%
Hydrogen	5.00	4.94	5.51	4.98
Nitrogen	1.35	1.57	1.38	1.74
Sulfur	.62	.74	.74	.84
Ash	2.01	1.60	1.30	.66
Oxygen (by diff.)	.76	1.57	3.65	3.38

Proximate Analysis of Char:

Moisture	0.67%	0.75%	0.63%	0.76%
Net volatile	8.69	9.90	9.43	11.06
Fixed carbon	66.95	70.56	80.84	76.89
Ash	23.70	18.79	9.10	11.29

Ultimate Analysis of Char:

Hydrogen	2.82	2.91	3.09	3.05
Carbon	68.70	71.73	81.63	79.59
Nitrogen	0.69	1.46	1.46	1.53
Sulfur	0.37	1.12	0.62	0.83
Oxygen (by diff.)	3.72	4.29	4.00	3.71

<u>BTU/lb. of Char (MAF)</u>	14,350	14,680	14,865	14,900
------------------------------	--------	--------	--------	--------

Presented Before the Division of Fuel Chemistry  
American Chemical Society  
Chicago, Ill., August 30 - September 4, 1964

#### CHANGES IN THE ULTRAFINE STRUCTURE OF ANTHRACITE UPON HEAT TREATMENT

S. P. Nandi, V. Ramadass, and P. L. Walker, Jr.

Department of Fuel Technology, Pennsylvania State University, University  
Park, Pennsylvania

It is well known that the ultrafine structure of anthracite exhibits molecular-sieve properties (1-6). It has further been shown that upon using appropriate activation procedures (during the reaction of anthracite with carbon dioxide at elevated temperatures), a large increase in adsorption capacity and rate of adsorption can be obtained in the ultrafine structure while still retaining its molecular-sieve behavior (6). Little quantitative data are available, however, on the changes produced in the ultrafine structure of anthracite upon thermal treatment to elevated temperatures in the absence of oxidizing gases. In this paper, the change in the ultrafine structure of three anthracites upon heat treatment has been followed using conventional techniques (gas adsorption and density measurements) and the newer technique (unsteady-state diffusion of gases from the ultrafine structure).

#### EXPERIMENTAL

##### Anthracites Used

Three Pennsylvania anthracites of 200x325 Tyler mesh were used in this study. The analyses of the anthracites used are given in Table I.

##### Heat Treatment

Heat treatment up to 1000°C was carried out in a tubular furnace, with the power input to the furnace controlled by a Leeds-Northrup duration-adjusting type program controller. A desired linear heating rate of  $5.0 \pm 0.1^\circ\text{C}/\text{min}$  and maximum temperatures during soaking within  $2^\circ\text{C}$  could be maintained. Nitrogen of 99.96% purity was passed over the sample (ca. 25g held in a quartz boat) throughout the heating and cooling cycle, after it was first circulated over copper turnings at 550°C to remove traces of oxygen.

In selected cases, heat treatments at temperatures in the range 1200-1700°C were performed in an induction furnace under an atmosphere of helium of 99.98% purity. Desired heating rates and maximum temperatures were obtained by manually adjusting the power input.

##### Apparatus to Measure Properties of Anthracites

The apparatus and procedures used to measure the properties of anthracite have been completely described previously: gas adsorption (7,8), mercury density (9), helium density (8), crystallite height measurements (10,11), and unsteady-state diffusion (12). Considering the unsteady-state diffusion measurements briefly, a differential experimental system was used to avoid errors caused by small temperature fluctuations. In principle, the procedure consisted of charging the particle sample under investigation with the selected gas up to some pressure in excess of atmospheric (by exposure to the gas at the diffusion temperature for

24 hr) and then measuring the unsteady-state release of the gas after sudden reduction of the pressure outside the particles back to atmospheric. The charging pressure never exceeded 2 atm. and usually was ca. 1.7 atm. Prior to charging the samples with gas, they were outgassed at 450°C for 24 hr.\* It was essential that the outgassing temperature be higher than the maximum temperature of diffusion measurement, since removal of water and/or occluded gases during the measurement would invalidate the experiment.

Detailed studies have been made on the kinetics of VM release from anthracites (13, 14). The volume and analysis of the VM release, as a function of temperature, have been measured. Where appropriate, these results will be presented in this paper. The experimental apparatus and procedure have been fully described (13).

## RESULTS AND DISCUSSION

### Volatile Matter Release From Anthracites

Prior to examining the change in ultrafine structure of the anthracites upon heat treatment, results on the liberation of VM and the accompanying weight loss during heat treatment should be examined. Samples were heated to maximum temperature at 5°C/min and soaked for 24 hr. Table II summarizes the results. Three separate heating runs were made on St. Nicholas and Dorrance anthracites to 800 and 900°C. Weight losses agreed to within ±2%.

For the St. Nicholas and Dorrance anthracites, relatively small decreases in weight occurred upon heating to 500°C. In fact, the VM release remained small up to 650°C for the St. Nicholas anthracite, as seen in Figure 1. Figure 2 shows that a sharp increase in VM release from the St. Nicholas anthracite coincided with the occurrence of substantial amounts of hydrogen and methane in the recovered gas. At heat treatment temperatures (HTT) up to 650°C, the VM primarily consisted of carbon dioxide and carbon monoxide. For the Treverton anthracite, a substantial weight loss occurred upon heating to 500°C. This is believed to be a result of release of much greater quantities of the oxides of carbon from this anthracite relative to St. Nicholas and Dorrance.

It is of interest that the weight losses for St. Nicholas and Dorrance anthracites were higher for maximum HTT of 700 and 800°C than for a HTT of 900°C, for the particular heating cycle selected. This is thought to be a result of the sharp increase in the H<sub>2</sub>-CH<sub>4</sub> ratio in the product gas with increasing temperatures above ca. 750°C, as seen in Figure 2. The equilibrium H<sub>2</sub>-CH<sub>4</sub> ratio for the reaction,  $C + 2H_2 \rightleftharpoons CH_4$ , is ca. 10 at 1000°K and 1 atm. total pressure (15). It is seen from Figure 2 that the H<sub>2</sub>-CH<sub>4</sub> ratio in the VM at this liberation temperature is ca. 0.3. This indicates either that a sizeable amount of methane is being produced as a primary product by desorption of functional groups on the coal and then slowly decomposing to produce hydrogen or that the gas pressure within the ultrafine structure of the anthracite is very high. For example; at 1000°K and a total pressure of 100 atm., the H<sub>2</sub>-CH<sub>4</sub> equilibrium ratio is ca. 0.3. Heat treatment runs were made on St. Nicholas anthracite up to 800 and 900°C, but with no soak-time at maximum temperature. In this case, the weight losses were 2.7 and 3.1% respectively. With increasing soak time (and at a value of less than 2 hr.), the weight loss for the

\* Outgassing at 450°C is thought to have produced a negligible change in the ultrafine structure of the St. Nicholas and Dorrance anthracites, as will be seen later from the surface area results. In the case of the higher volatile matter Treverton anthracite, this outgassing temperature apparently produced a significant change in the raw coal.

900°C HTT eventually falls below that for the 800°C HTT, since the difference in average molecular weight of the total VM produced for these HTT will more than compensate for the larger volume of VM released in the 900°C heat treatment run.

It is noteworthy that the weight loss for the Treverton anthracite did not go through a maximum with increasing HTT. This could be a result of the oxides and carbon making a greater contribution to the total VM for this anthracite and thus reducing the effect of an increase in the  $H_2-CH_4$  ratio on the average molecular weight of the VM. Confirming results are not available on this point.

### Surface Areas

Table III summarizes the surface area results obtained from nitrogen and carbon dioxide adsorption. As suggested by Walker and Geller (2) and later supported by Anderson, Hofer, and Bayer (16), areas calculated from carbon dioxide adsorption at 195°K represent closely the total surface area of coal. On the other hand, nitrogen at 77°K diffuses slowly into pores less than ca. 4.5A in diameter and thus is not adsorbed by most of the ultrafine structure in coals. For heat treatment temperatures up to 800°C, the anthracites retained their large surface areas. In fact, for the Dorrance and Treverton samples (and probably St. Nicholas) the surface areas went through a maximum with increasing HTT. The increase in surface area upon heat treatment at the lower temperatures can be attributed to the release of gaseous oxides of carbon, resulting in the opening up of pores which were closed to carbon dioxide adsorption in the raw anthracites. As expected, the Treverton anthracite, which showed the greatest VM release at lower temperatures, also showed the greatest increase in surface area. At HTT above 800°C, the total surface area of the anthracites decreased sharply as the ultrafine pores decreased in size and ultimately became inaccessible to carbon dioxide. This model will be further clarified by the unsteady-state diffusion results. A sizeable activation energy can be attributed to the process which decreased the size of the ultrafine pores. That is, for the 900°C heat treatment run on St. Nicholas anthracite, with no soak time, the area was still 206  $m^2/g$ .

It is seen, from the nitrogen adsorption results, that the amount of area in pores greater than ca. 4.5A varied widely. These areas also went through a maximum with increasing HTT. For a HTT of 900°C the areas were particularly low for the Dorrance and Treverton anthracites.

### Densities and Pore Volumes

Table IV presents the helium and mercury density values on a m.m.f.b. The helium and mercury density of the mineral matter in all samples was taken as 2.7 g/cc (17). The helium densities increased with increasing HTT. At low HTT, the helium density would be expected to increase because the release of the gaseous oxides of carbon would open up closed pores. In the intermediate range up to ca. 800°C, the release of methane would remove carbon atoms and unblock pores. Further, the release of the low density species, hydrogen, would increase the helium density. At HTT above 800°C, it is suggested that most of the increase in helium density is attributed to a decrease in average size of the closed pores and their ultimate elimination.

As expected from the helium density results, the mercury densities also increased with increasing HTT as seen in Table IV. From the helium and mercury densities, the total open pore volume and porosity of the samples can be calculated. The results are summarized in Table V. In spite of the large increases in densities with increasing HTT, the total open pore volumes and porosities

showed erratic and relatively little change. This indicates that most of the pore volume which was eliminated upon heat treatment was located in pores already closed to helium.

### Crystallite Heights

As shown by transmission electron microscopy studies, pore volume in carbons can be produced by the irregular packing of crystallites (17). Therefore, it is of interest to compare changes in crystallographic parameters upon heat treatment with changes in ultrafine pore structure. Unfortunately, the obtaining of quantitative data on crystallite diameter and interlayer spacing is laborious (11) and probably, in any case, not meaningful for samples relatively high in mineral matter. Quantitative crystallite height values can be obtained relatively simply (11), (even on impure samples); they are presented in Table VI. No apparent relation exists between the change in crystallite height upon heat treatment and changes in the ultrafine pore structure. As showed previously for other raw carbonaceous solids (18), the crystallite height of the raw anthracites decreased upon heat treatment at temperatures between 500-900°C. Possible reasons for this have been discussed (19).

It has previously been shown that the closed pore volume in calcined petroleum cokes decreases sharply with increase in crystallite alignment (20). The relative degree of crystallite alignment can be measured for carbons of essentially the same crystallite size from the relative intensity of their (002) x-ray diffraction peak (20,21).  $I(002)$  values for the anthracites are presented in Table VI, normalized to 100 for the raw St. Nicholas sample. Relatively minor changes in  $I(002)$  occurred with increasing heat treatment temperature for the anthracites, showing that significant improvement in crystallite alignment did not occur. Therefore, the substantial increase in helium density upon heat treatment to 900°C (part of which is caused by a decreasing closed pore volume) cannot be attributed to enhanced crystallite alignment.

### Diffusion Parameters

As considered theoretically by Kington and Laing for the diffusion of gases through molecular sieve zeolites (22), when the size of the diffusing species closely approaches the size of the aperture through which it passes, the diffusion becomes activated. Under these conditions a further small decrease in aperture size produces a large increase in activation energy for diffusion. Nelson and Walker showed the validity of this concept experimentally for the diffusion of propane through 4 and 5A Linde zeolites, obtaining activation energies of 8.7 and 0.5 kcal/mole respectively (12). The kinetic dimension\* of propane, calculated using the Lennard-Jones potential and viscosity data is 5.1A (23).

As indicated previously the parameter,  $D^{1/2}/r_0$ , has been calculated from the diffusion results. The diffusion coefficient,  $D$ , has not been given since the value of the diffusion path length,  $r_0$ , is unknown at present. Studies on the change of  $D^{1/2}/r_0$  with anthracite particle size clearly shows that  $r_0$  is not the particle radius (24). In any case, we were primarily interested in the activation energy for the diffusion coefficient. Since  $r_0$  should be independent of diffusion temperature, values of  $D^{1/2}/r_0$  will be sufficient for this purpose.

A thorough study was made of the diffusion of gases from St. Nicholas anthracite heat treated up to 1700°C. For samples heated to 900°C, the diffusion of nitrogen, ethane, and argon was studied. For samples heated to

\*The kinetic dimension is the distance of approach where the potential energy of interaction equals zero.

higher temperatures, it was necessary to use smaller diffusing species in order to have a rate of diffusion which was sufficiently rapid to be measurable in a convenient period of time. Hydrogen and helium were used.

Figure 3 presents Arrhenius plots for the diffusion of nitrogen and ethane out of St. Nicholas anthracite samples heated to a maximum temperature of 900°C. The plots of nitrogen and ethane diffusing from the raw anthracite are not shown, since they fall very close to the 700°C sample. Large decreases in the diffusion parameters of both nitrogen and ethane resulted, however, when the HTT was increased from 700 to 900°C. There also was a significant increase in the activation energy for diffusion of both gases in going from a HTT of 700 to 900°C, indicating a decrease in the average size of the ultrafine pore structure which is determining the diffusion rate. As expected ethane had a higher activation energy for diffusion from comparable St. Nicholas samples than did nitrogen. That is, the kinetic dimensions of ethane and nitrogen are 4.41 and 3.68A respectively (23). It is noted that there was some increase in the difference in activation energy for ethane and nitrogen diffusion when the St. Nicholas sample was heated to higher temperatures. That is, the difference in activation energy was ca. 1.2 kcal/mole for the raw anthracite and ca. 2.7 kcal/mole for samples heat treated to 800 and 900°C. This indicates the possibility of producing sharper molecular sieve effects for different gases by heat treating anthracites.

Figure 4 presents Arrhenius plots for the diffusion of helium and hydrogen out of St. Nicholas samples heated at temperatures between 1200 and 1700°C. Considerable experimental difficulties were encountered in these diffusion rate measurements. The ultrafine pore volume of these samples was low; and, hence, the volume of gas released was low (ca. 0.4 cc at S.T.P. for 25g samples). A slight variation in room temperature affected the rate measurements. Even though the precision of these measurements was less than that obtained for samples heated to temperatures below 900°C, the Arrhenius plots are reasonably good. There was an increase in the activation energy for the diffusion of helium with increasing HTT. The sample heated to 1400°C had the same activation energy for helium diffusion as the sample heated to 900°C had for nitrogen diffusion. This is strong evidence for a continued decrease in the size of the ultrafine pores with increasing HTT in this temperature range. As expected, hydrogen had a higher activation energy for diffusion out of the 1400°C heat treated sample than did helium. That is, the kinetic dimensions of hydrogen and helium are 2.97 and 2.58A respectively (23). It is of interest that the activation energy for helium diffusion from the 3A Linde zeolite is less than 1 kcal/mole (24). This suggests that the ultrafine pores in the St. Nicholas samples heated to 1400 and 1700°C had a size less than 3A.

Figures 5-7 present Arrhenius plots for the diffusion of argon from St. Nicholas, Dorrance, and Treverton samples heat treated up to 900°C. Again, increases in the activation energy for diffusion occurred with increasing HTT. It is of interest, however, that the Dorrance anthracite showed a greater increase in activation energy for argon diffusion than did Treverton or St. Nicholas. Further, the activation energy for the diffusion of argon from Treverton was appreciably higher than the values for the other anthracites, when the samples were heated only to 600°C. Since nitrogen has a kinetic dimension close to that of argon (3.41A), this is consistent with the fact that the nitrogen surface area of Treverton heat treated to 600°C was considerably less than the nitrogen area of the Dorrance sample.

## CONCLUSIONS

Heat treatment of Pennsylvania anthracites in an oxygen-free atmosphere above ca. 700°C is seen to decrease the average size of the ultrafine pores. The result is a sharp decrease in total surface area, as measured by carbon dioxide adsorption for HTT at or above 900°C and a continuous increase in the activation energy for diffusion of gases from the ultrafine pores with increasing HTT.

We appreciate the financial support of the Coal Research Board of the Commonwealth of Pennsylvania which made this work possible.

## REFERENCES

1. Kini, K. A., Nandi, S. P., Sharma, H. N., Iyengar, M. S., and Lahiri, A., *Fuel*, 1956, 35, 71.
2. Walker, P. L. Jr. and Geller, Irwin, *Nature*, 1956, 178, 1001.
3. Anderson, R. B., Hall, W. K., Lecky, J. A., and Stein, K. C., *J. Phys. Chem.*, 1956, 60, 1548.
4. Joy, A. S., Conference on Science in the Use of Coal, Institute of Fuel, 1958, pp. A-67 to A-71.
5. Gregg, S. J. and Pope, M. I., *Fuel*, 1959, 38, 501.
6. Metcalfe, J. E. III, Kawahata, M., Walker, P. L. Jr., *Fuel*, 1963, 42, 233.
7. Emmett, P. H., *A. S. T. M. Tech. Publ.*, No. 51, 1941, pp. 95-105.
8. Kotlensky, M. V., Ph. D. Thesis, The Pennsylvania State University, 1959.
9. Walker, P. L., Jr., Rusinko, F. Jr., and Raats, E., *J. Phys. Chem.*, 1955, 59, 245.
10. Scherrer, P., *Nachr. Ges. Wissensch. Gottingen*, 1918, 2, 98.
11. Short, M. A. and Walker, P. L. Jr., *Carbon*, 1963, 1, 3.
12. Nelson, E. T. and Walker, P. L. Jr., *J. Appl. Chem.*, 1961, 11, 358.
13. Nelson, E. T., Young, G. J., and Walker, P. L. Jr., Special Research Report #3, Coal Research Board, Commonwealth of Pennsylvania, 1958.
14. Worrall, Jean and Walker, P. L. Jr., Special Research Report #16, Coal Research Board, Commonwealth of Pennsylvania, 1959.
15. Walker, P. L. Jr., Rusinko, Frank Jr., and Austin, L. G., *Advances in Catalysis*, Vol. XI, Academic Press, Inc., 1959, pp. 133-221.
16. Anderson, R. B., Hofer, L. J. E., and Bayer, J., *Fuel*, 1962, 41, 559.
17. Walker, P. L. Jr., *Amer. Scientist*, 1962, 50, 259.
18. Gibson, J., Holohan, M., and Riley, H. L., *J. Chem. Soc.*, 1946, 456.
19. Kinney, C. R., Nunn, R. C., and Walker, P. L. Jr., *Ind. Eng. Chem.*, 1957, 49, 880.
20. Walker, P. L. Jr., Rusinko, F. Jr., Rakszawski, J. F., and Liggett, L. M., *Proceedings of the Third Carbon Conference*, Pergamon Press, 1958, pp. 643-658.
21. Walker, P. L. Jr., Gardner, R. P., Short, M. A., and Austin, L. G., *Proceedings of the Fifth Carbon Conference*, Volume 2, Pergamon Press, 1963, pp. 483-492.
22. Kington, G. L. and Laing, W., *Trans. Faraday Soc.*, 1955, 51, 287.
23. Hirschfelder, J. O., Curtiss, C. F., and Bird, R. B., "Molecular Theory of Gases and Liquids", John Wiley and Sons, Inc., 1954, p. 1110.
24. Nandi, S. P., Ph. D. Thesis, The Pennsylvania State University, 1964.

TABLE I

## ANALYSES OF ANTHRACITES

<u>Coal</u>	<u>% Carbon</u> <u>(d. m. f.)</u>	<u>% Volatile</u> <u>(d. m. f.)</u>	<u>% Ash</u>
St. Nicholas	94.0	4.5	9.1
Dorrance	92.7	5.8	9.9
Treverton	92.0	9.0	9.7

TABLE II

## WEIGHT LOSSES UPON HEAT TREATMENT OF THE ANTHRACITES

<u>Anthracite</u>	<u>Heat Treatment</u> <u>Temperature, °C</u>	<u>Loss In</u> <u>Weight, %</u>
St. Nicholas	500	1.7
	700	3.7
	800	4.0
	900	3.6
	1000	4.5
Dorrance	500	0.79
	600	4.2
	700	5.2
	800	6.8
	900	4.6
Treverton	500	4.8
	600	6.6
	700	8.4
	800	9.5
	900	10.2

TABLE III

EFFECT OF HEAT TREATMENT ON THE SURFACE AREAS OF THE ANTHRACITES

<u>Anthracite</u>	<u>Heat Treatment Temperature, °C</u>	<u>Surface Areas, m<sup>2</sup>/g</u>	
		<u>N<sub>2</sub></u>	<u>CO<sub>2</sub></u>
St. Nicholas	raw	32.3	220
	700	24.9	215
	800	9.6	198
	900	5.1	104
	1000	3.7	23.6
Dorrance	raw	34.2	215
	500	38.8	235
	600	23.4	250
	700	10.2	273
	800	6.8	187
Treverton	raw	1.5	131
	500	2.8	222
	600	7.2	243
	700	11.5	216
	800	2.3	208
	900	0.8	61.1

TABLE IV

EFFECT OF HEAT TREATMENT ON THE HELIUM AND MERCURY DENSITIES OF THE ANTHRACITES

<u>Anthracite</u>	<u>Heat Treatment Temperature, °C</u>	<u>Helium Density g/cc</u>	<u>Mercury Density g/cc</u>
St. Nicholas	raw	1.66	1.47
	700	1.73	1.49
	800	1.80	1.50
	900	1.86	1.56
	1000	2.08	1.61
Dorrance	raw	1.63	1.27
	500	1.64	1.35
	600	1.65	1.42
	700	1.79	----
	800	1.85	1.57
Treverton	raw	2.06	1.65
	500	1.58	1.21
	600	1.63	1.27
	700	1.67	1.36
	800	1.75	1.43
	900	2.05	1.54
		2.08	1.65

TABLE V  
EFFECT OF HEAT TREATMENT ON THE SPECIFIC OPEN PORE VOLUME  
AND PERCENTAGE POROSITY OF THE ANTHRACITES

<u>Anthracite</u>	<u>Heat Treatment Temperature, °C</u>	<u>V<sub>t</sub>, cc/g</u>	<u>Porosity %</u>
St. Nicholas	raw	0.07	10.6
	700	0.10	14.2
	800	0.11	16.5
	900	0.10	16.1
	1000	0.14	22.6
Dorrance	raw	0.17	22.1
	500	0.13	17.7
	600	0.10	13.9
	800	0.10	15.2
	900	0.11	18.7
Treverton	raw	0.19	23.2
	500	0.09	11.2
	600	0.14	18.6
	700	0.13	18.3
	800	0.16	25.0
	900	0.13	20.6

TABLE VI  
X-RAY DIFFRACTION RESULTS ON THE HEAT TREATED  
ANTHRACITES

<u>Anthracite</u>	<u>Heat Treatment Temperature, °C</u>	<u>Crystallite Height, A</u>	<u>I(002)</u>
St. Nicholas	raw	15.6	100
	700	10.8	105
	800	10.8	97
	900	11.1	103
	1000	13.0	106
Dorrance	raw	18.0	131
	500	15.8	122
	600	13.2	117
	700	11.3	100
	800	15.2	131
	900	13.0	122
Treverton	raw	18.4	100
	500	14.9	96
	600	11.2	80
	700	11.2	78
	800	11.2	86
	900	10.6	94

## FIGURE CAPTIONS

- Fig. 1 Relationship Between the Volume of Volatile Matter Evolved and Temperature for St. Nicholas Anthracite
- Fig. 2 Relationship Between Volatile Matter Composition and Temperature for St. Nicholas Anthracite
- Fig. 3 Activation Energy Plots for the Diffusion of Nitrogen and Ethane from Heat Treated St. Nicholas Anthracite
- Fig. 4 Activation Energy Plots for the Diffusion of Helium and Hydrogen from Heat Treated St. Nicholas Anthracite
- Fig. 5 Activation Energy Plots for the Diffusion of Argon from Heat Treated St. Nicholas Anthracite
- Fig. 6 Activation Energy Plots for the Diffusion of Argon from Heat Treated Dorrance Anthracite
- Fig. 7 Activation Energy Plots for the Diffusion of Argon from Heat Treated Treverton Anthracite

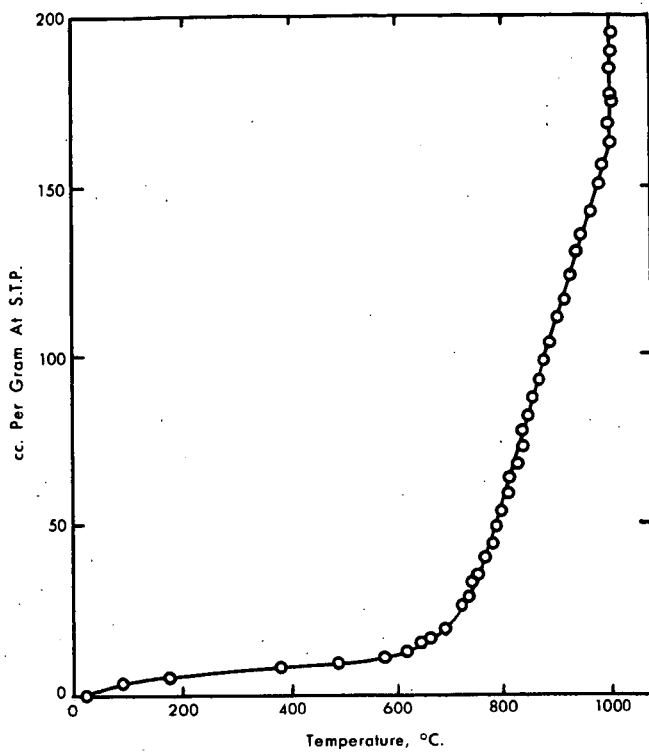


FIGURE 1

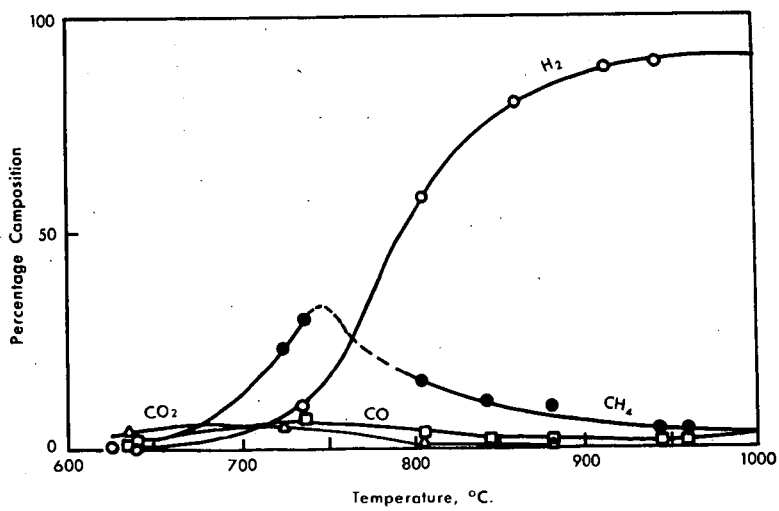


FIGURE 2

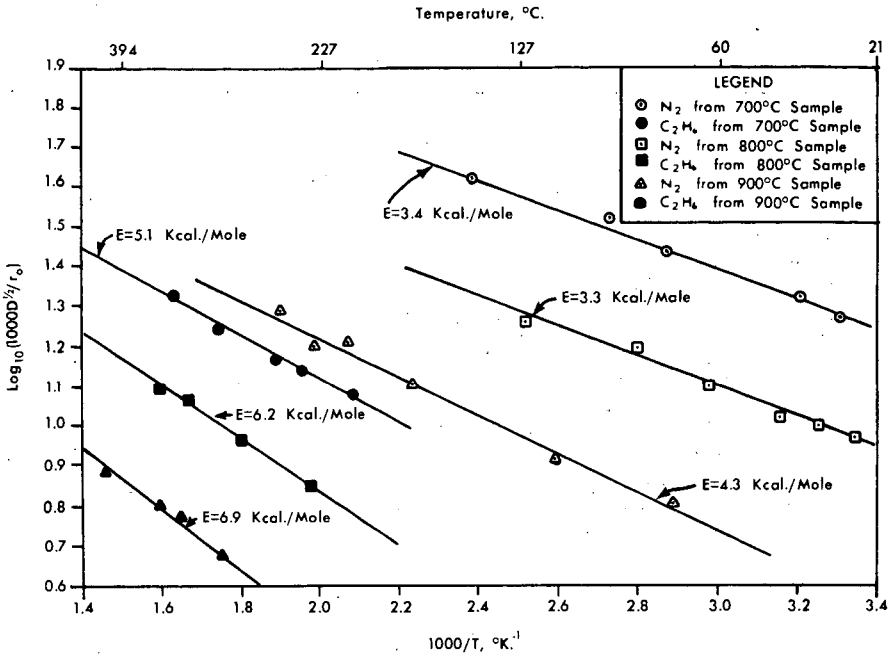


FIGURE 3

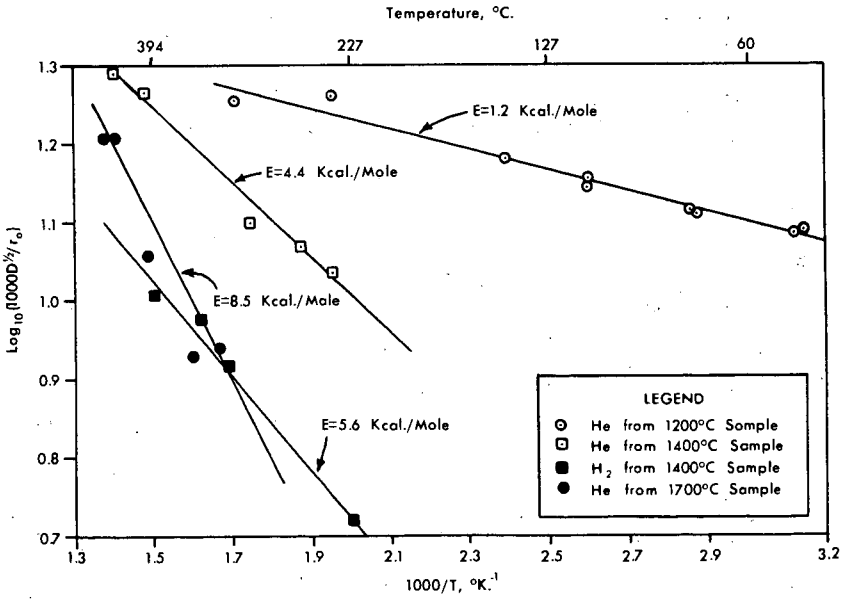


FIGURE 4

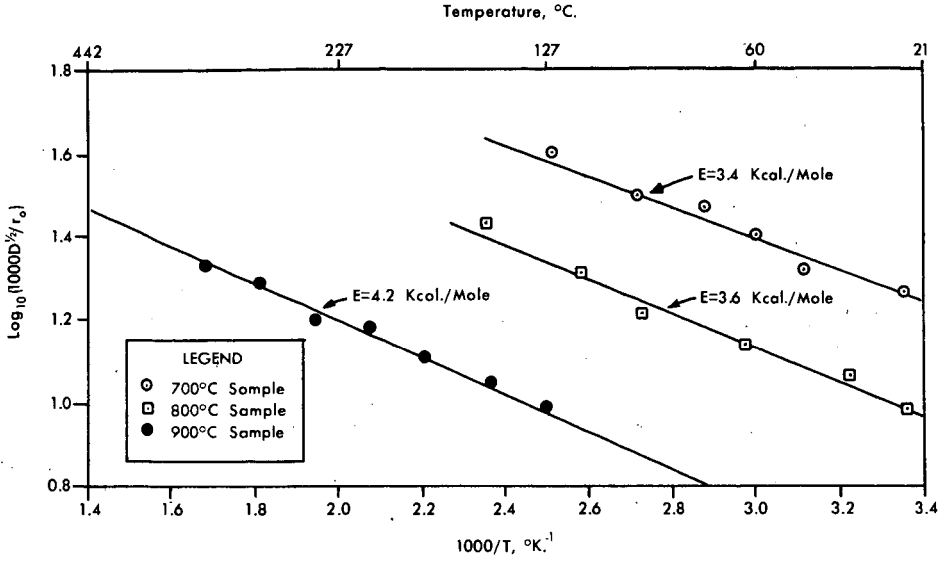


FIGURE 5

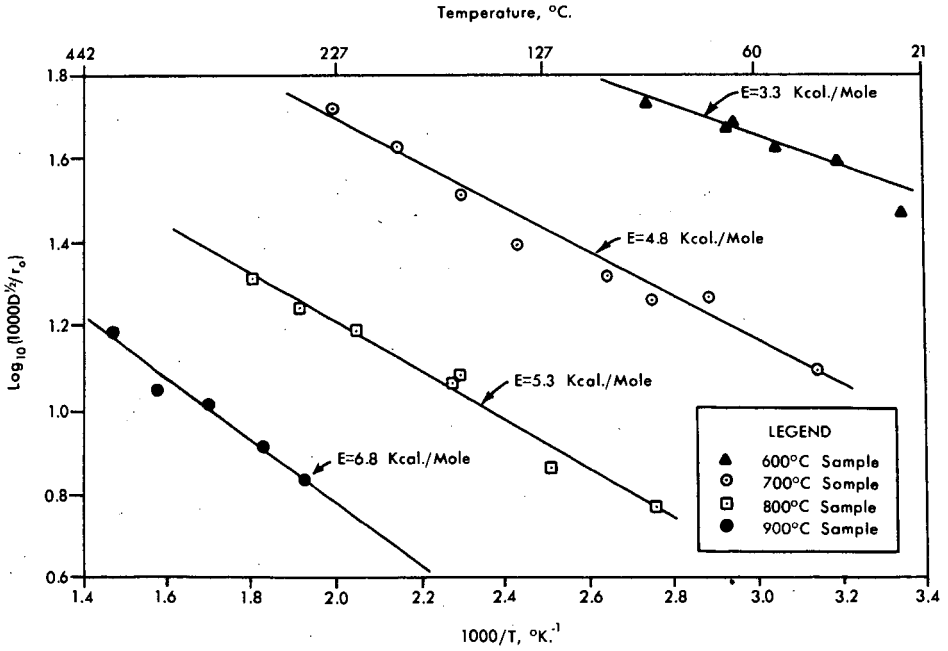


FIGURE 6

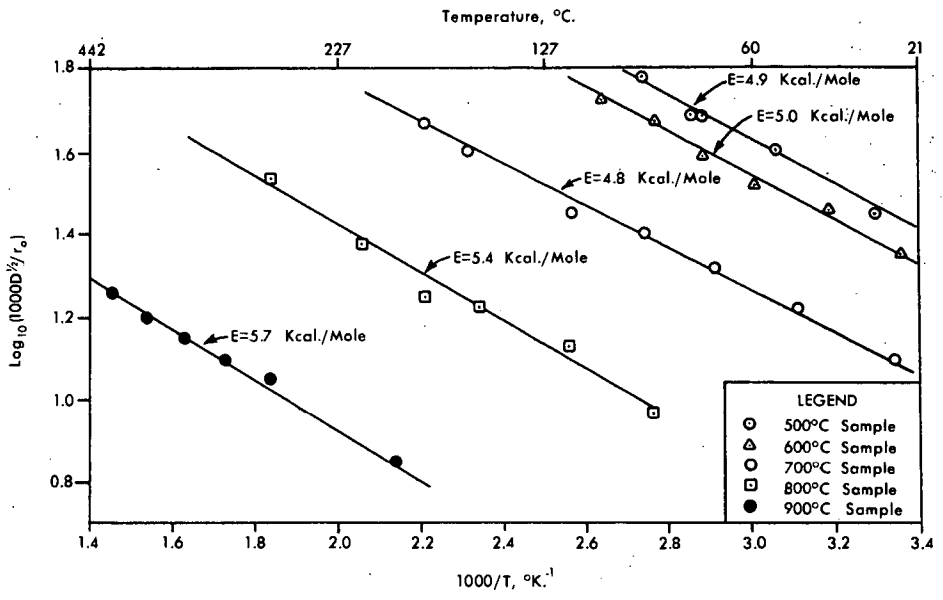


FIGURE 7

Presented Before the Division of Fuel Chemistry  
American Chemical Society  
Chicago, Ill., August 30 - September 4, 1964

## "PYROLYSIS OF COAL AND COAL TAR PRODUCTS"

ROBERT T. JOSEPH  
CONSULTANT\*

### INTRODUCTION

The history of organic chemistry is intimately tied to the history of the production and refining of coal tars. From the heyday of the period when the prime source of organic chemicals (the dye stuffs, the medicinals, the preservatives, the disinfectants) was black coal tar, to the present (when almost any organic chemical whose structure can be conceived, may be synthesis almost directly from carbon, hydrogen, oxygen and nitrogen), the tar by-product from coal pyrolysis has been processed for the 10% low boiling products to supply the fine organic chemicals market. The 90% residue remaining after refining has been channeled to wherever it would fit, from creosote oils for wood preservation to bituminous products for construction and road building, or to fuel for boilers and open hearths whenever the general economy drove the price of the residues into the fuel range.

The work reported herein was done in an attempt to:

1. Upgrade the residue products from coal tar refining.
2. Seek a method of increasing the yield of highly aromatic tar from coal by direct pyrolysis under equilibrium conditions as opposed to pyrolysis under a dynamic temperature situation as found in the slot type coke oven.

To accomplish these aims, certain assumptions had to be made in order to circumvent the prejudice that had persisted for almost a century as to the nature of tar formation in coal processing. These assumptions can be listed as:

1. The products to be derived from coal by pyrolysis are not indigenous to the coal, but are controlled by the process conditions imposed during such pyrolysis.
2. The tar and light oils recovered from carbon-hydrogen-oxygen-nitrogen fragments, of free radical type, along the path of distilling pyrolysis products as these products pushed through the bed of coal maintained at temperatures in the region of 1800° F.

\* Present Address: FMC Corporation  
P. O. Box 8  
Princeton, N. J.

3. The evidence for 2 lay in the fact that while the material collected as tar and oil left the pyrolytic chamber in the vapor phase with a coke residue in the chamber, these tars and oils can not be redistilled under any conditions without leaving a substantial residue of coke similar in nature to the coke left in the pyrolytic chamber wherein the tar and oil had their genesis as a vapor.

#### EXPERIMENTAL - General Attitudes

Unlike research on fine, purified organic chemicals, the field of coal and coal products exploration is characterized by the need of a combined chemist and engineer approach. On one hand, the reactions which occur are obviously governed by the known laws of rates and energy utilization. On the other hand, so little is known of the composition of the starting materials that inference, assumptions as to the specific reactions occurring, thermo-chemical calculations, or model structures, while extremely useful, can lead to serious oversight if taken as gospel over experimental observations, because the large number of components to be dealt with necessitates quantities of materials for test tube operation normally considered as pilot plant studies in the fine chemical field. Furthermore, in order to achieve the extremely short residence times and steady-state operation, a continuous flow system is required.

Accordingly, a rather elaborate description of the ground rules, feedstock identification, apparatus, and operating procedure, is given. The methods of analysis which are not unique are described by reference.

#### EXPERIMENTAL - Ground Rules

With these assumptions in mind, it was decided to attempt to reproduce and apply the pyrolytic conditions found in the slot type coke oven in such a fashion that:

1. The temperature of pyrolysis would remain constant.
2. The heat rate applied to the feedstock would be at a rate approaching 2000° F per second.
3. The pyrolytical action on the feedstock would be imposed for that period necessary to raise the temperature of the feedstock to 1400 to 1800° F.
4. The pyrolytical products would be quenched to ambient temperatures at the same or faster rate as the feedstock was raised to pyrolysis conditions.

#### EXPERIMENTAL - Feedstock Identification

In order to demonstrate the general applicability of the system, it was decided to use the following materials as feedstock:

1. The liquid oil fractions from coke oven tar refining left after the removal of tar acids, tar base, naphthalene, resin and solvents from that fraction of coke oven tar that boils up to 270°C termed by the industry - carbolic oil.
2. The high boiling residues from the distillation refining of the crude quinoline fraction (230 to 250°C) extracted from coke oven tar carbolic oil.
3. A coal tar from low temperature pyrolysis of an Appalachian coal via the "Disco" process.
4. A coal tar from the low temperature pyrolysis of Texas lignite (Rockdale) in the Parry fluid bed process.
5. A bituminous coal of Eastern origin.

#### EXPERIMENTAL - Apparatus Description

The apparatus used is diagrammed as flow sheet and in detail on Figures 1, 2, 3, and 4. Figure 1 represents the apparatus in flow sheet. Figure 2 represents the heating chamber and reforming column for effecting the heating and reforming operations in connection with the pyrolysis of liquid feedstocks. Figure 3 is a horizontal section of the heating chamber taken on the line 3 - 3 of Figure 2. Figure 4 represents the cooled nozzle for spraying liquid feedstocks into the heating chamber.

Referring to Figure 1 of the drawing, the numerals 1 and 1A represent storage tanks for the feedstock, which are suitably provided with the heating jackets to maintain their contents in fluid form, and which are adapted to be alternately connected to the feed line 3 by suitable valved connections 2. The line 3 is connected to the inlet of a pump 4 for the feedstock, which in turn is connected by a suitable conduit 5 to the inlet 6 of the jacketed spray nozzle 7 which is mounted with its spray tip 8 within a heating chamber 9.

The heating chamber 9 is adapted to be heated to temperatures above 600°C by external heat such as hot flue gases, gas flame, or the like, contacting the outer walls 10 of the chamber within a suitable furnace 11. The heating chamber is formed of suitable material to withstand the temperature, such as 310 steel, the inner surface of which is lined with a thin lining of refractory material such as alumina or an alumina-silica fire clay, which functions as cracking catalyst.

Heating chamber 9 is also supplied with an inlet for superheated steam 15 which is supplied through conduit 16 from a steam superheater 17 adapted to superheat by indirect contact steam supplied to the superheater by a conduit 18 from a steam generator 19. Water for generation of the steam is supplied from a suitable reservoir 22 thru valved connection 23 by a pump 24 and a conduit 25.

The heating chamber 9 communicates directly with an elongated reforming column 30 which is suitably heated to temperatures above 600°C by indirect heat, within a heating jacket 31. The chamber 30 is formed of suitable material capable of withstanding the elevated temperatures, such as 310 stainless steel.

The outlet 32 of column 30 is connected to the inlet 33 of a condenser 34 adapted to be cooled by a suitable fluid flowing through a jacket 35. The outlet 36 of the condenser is connected to a primary liquid product receiver 37 which leads to a reflux condenser 38. The vapor outlet 39 of the reflux condenser is connected by a conduit 40 to a condenser 41, the outlet 42 of which is connected by a dip pipe 43 which leads into oil scrubber 44 which is partially filled with mineral oil adapted to scrub the gases and vapors passing through it. The outlet 45 of the scrubber is connected by a conduit 46 to an empty overflow chamber 47 which, in turn, is connected by conduit 48 with a dip pipe 49 which leads into a scrubber 50 partially filled with a suitable mineral acid adapted to remove ammonia and organic bases present in the gas and vapor mixture passing through it. The outlet 51 of the scrubber 50 is connected by a conduit 52 with an overflow chamber 53 which, in turn, is connected through conduit 54 with a dip pipe 55 which leads into a scrubber 56 partially filled with 20% aqueous sodium hydroxide for removal of H<sub>2</sub>S. The outlet 57 of the caustic scrubber 56 is connected by a conduit 58 to an overflow chamber 59 which, in turn, is connected in series with two vessels 60 and 61 which are surrounded by a dry-ice-acetone mixture jackets 62 and 63 to reduce the temperature. The outlet 66 of the chamber 61 is connected by a conduit 67 with a gas sampler 68 which, in turn, is connected by a conduit 69 to a wet test meter 70, the outlet of which is connected to a flare 75 by a conduit 74.

Referring to Figures 2 and 3 of the drawing, the heating chamber 9 consists of a shell 80 formed of 310 stainless steel, mounted in spaced relation within a furnace 81 and surrounded by flues 82, 83, 84 and 85 carrying burner gases from gas burners 87. The exits from the flues are connected to a stack (not shown). The inner surface of the heater 9 is coated with a thin layer of alumina-silica fire clay 79. The heater 9 is provided with a jacketed spray nozzle 7 which is mounted centrally of one wall of the chamber 9 so as to project a fine dispersion of the liquid fed into the chamber onto the hot inner walls of the chamber.

As shown in Figure 4, the jacketed spray nozzle 7 consists of a tube 100 surrounded by two progressively larger tubes 101 and 102 mounted in spaced relation to provide a narrow passage 105 between them and between tubes 100 and 101 for the flow of temperature-regulating fluid, such as water, steam, oil, etc., depending on the temperature to be maintained. Tubes 101 and 102 are provided with couplings 103 and 104 for the entrance and exit of the temperature-regulating fluid. The inner end of the tube 100 is provided with a spray tip 8 which is of the type normally employed for dispersing oil in the form of a cone into an oil burner of the conventional type. Such nozzles are rated according to the number of gallons per hour of No. 2 fuel oil which they are adapted to deliver as spray under a head of 100 p. s. i. g.

The heater 9 is also provided with an inlet 15 for superheated steam which is mounted within the heater on the opposite wall from the spray nozzle 7 so as to deliver superheated steam into the interior of the chamber 9 in intimate contact with the spray of feedstock from nozzle 7.

The reforming column 30 is mounted on the heating chamber 9 in direct communication with the interior thereof, and is surrounded by heating jacket 31. It is provided with a screen 110, 16 mesh stainless steel screen, mounted near the bottom thereof and adapted to retain a column of reforming catalyst 29 within the column 30.

The apparatus is provided with suitable temperature-recording mechanism connected to thermocouples at the following points: 115 within the interior of the heater 9; 116 in the interior of the heating column 30; 117 in the interior of the heating column 30 near the top thereof; 118 in the outlet 32 of the column 30; 119 at the outer wall of the column 30; 120 in the interior of the jacketed nozzle 7; and 121 in the interior of the steam inlet 15.

The apparatus is further provided with means for recording pressures (not shown) at suitable points within the apparatus, such as the interior of the heating chamber 9, the top of the column 30, the steam superheater 17, and the conduit 5 of the spray nozzle inlet 6. Suitable heating jackets (not shown) are also provided for the lines and other parts carrying fluids at temperatures above atmospheric temperature.

#### EXPERIMENTAL - Operating Procedure

In the operation of the apparatus referred to above, with oil feedstocks, the heating chamber 9 and reforming column 30 are first brought to temperature by suitable passage of burner gases through the furnace 11 and heating jacket 31. Water is then introduced into the steam generator 19 and heat is supplied to the steam superheater 17, and superheated steam is pumped into the heating chamber 9. If coke is employed in the reforming column 30, which constitutes the preferred practice, some water-gas is formed in the reforming column and passes through the system and is burned at the flare 75. Operation is continued until the system is cleared of air by the passage of steam, evidenced by condensation of water in the condenser 34 and primary liquid product receiver 37.

Pump 4, supplying the particular liquid feed to be pyrolyzed, is then placed in operation and the temperature-regulating fluid is passed through the tubes 101 and 102 to regulate the temperature of the feed and maintain it at the desired temperature. To prevent the starting material from undergoing undesirable preliminary decomposition, with resultant plugging of the spray nozzle, the feed to the pyrolyzer is preferably maintained at a temperature below 150°C, and usually at a temperature merely sufficient to insure adequate fluidity for spraying through the spray nozzle. Ordinarily the feed is adequately fluid at temperatures lower than 110°C.

Adequate pressure is exerted by pump 4 to secure a fine dispersion of the feed within the heating chamber 9, depending upon the rate of feed desired and the size of the spray tip 8. The rate of feed of superheated steam through inlet 15 is then adjusted to the desired ratio with respect to the feed of stock through the spray tip 8.

Operation is then continued with adjustment of the heat supplied to the heating chamber 9 and reforming column jacket 31; since with continued operation the supply of heat required to maintain operating temperature decreases, presumably by reason of the fact that exothermic as well as endothermic reactions occur in the heating chamber and reforming column.

Tars produced by the process are condensed and collected in the receiver 37 together with unreacted steam which condenses as water. Light oil fractions are absorbed and removed in the mineral oil scrubber 44. Organic bases and ammonia are removed in the acid scrubber 50. Hydrogen sulfide is removed in the alkaline scrubber 56.

The tars do not always form completely in receiver 37, but sometimes tars also are formed farther along in the recovery system. Thus tar has been found to collect in the oil scrubber 44, and in some cases a crystalline material was formed in vessels 60 and 61 which, when warmed to room temperature, formed a tar.

With pulverized coal, the oil feed mechanism was replaced by a screw feeder and the coal was blown into the chamber by superheated steam as it left the water cooled screw within the chamber. The operation of this type of mechanism proved extremely difficult, and in most cases, impossible. This was in 1953.

#### EXPERIMENTAL - Material Balances and Yields

Interpretation of the data demanded accurate account of the distribution of the intake materials. Accordingly, all feedstock, water, sweep gases were measured by weight or volume and subsequently converted to weight. The weight of all samples taken was accounted for and such weight prorated to the proper part of the flow sheet. Wherever possible, quantities were obtained by direct weight before, during, and after each experimental run.

An accurate log of each run was maintained which permitted logical distribution of losses in the calculation of the yields. Yields could then be based on the hydrocarbon feedstock, the steam feed, or a combination. In this fashion, some assessment of the origin of the products could be made.

#### EXPERIMENTAL - Analytical

Composition of the gases was determined by mass spectral analysis (Consolidated Electrodynamics) on samples taken continuously throughout the run.

Composition of the tars and light oils was determined by analysis of component fractions cut from the tar by fractional distillation, using a 1 inch by 36 inch Stedman packed column operated at maximum efficiency. One percent readings were taken for the drawing of boiling curves and fractions were cut to correspond to standard cuts used in the coal tar refining industry - pre-benzene, benzene toluene, solvent naphtha, high flash solvents, naphthalene, crude quinoline, creosote oils and pitches. Analysis of these fractions were by methods standard to the industry and published in the ASTM Specifications, the British\* Methods of Testing Coal Tar Products and publications of tar refiners in the United States.

## RESULTS AND DISCUSSION OF THE RESULTS

Results, along with conditions that produced such results, are given in Tables I thru V. In Tables III and IV, the format is so arranged as to facilitate comparison between individual feedstocks and products derived therefrom. The data presented, of necessity, are selected. In making the selection, considerable effort was made to include representative results where such results were relatively representative. However, wherever observation indicated that an apparent variation could not be assessed against known difficulties in experimental technique, these are recorded and so annotated.

While not shown in all cases where the cracking temperature was below 700°C very little reaction took place other than the formation of coke in the chamber by distillation of the light ends. As indicated in Table I, in all cases the water fed to the reaction reacted to some small percentage. And while there is some indication of straight water gas reaction, there is also evidence that the water may have decomposed and added to the carbon-hydrogen fragments as tar. One thing was noted throughout the experiments - the use of steam drastically inhibited carbon lay-down and coke formation.

In all cases, the most drastic change in composition of the feedstock occurred by gasification. Gas yields varied from 4% for the tar base residues to 41% for the lignite tars. Both low temperature tars produced high gas yields.

The light oils, oils with densities lower than water at room temperature, were produced in about the same quantities regardless of feedstock, and for the most part, were a crude BTX fraction.

Considering Table II, the obvious points of departure are the production of unsaturated gases as opposed to more stable hydrocarbons. Acetylene seems to be the function of the cracking temperature varying from a trace to 2.0% over a temperature range of 750°C to 925°C. However, about 150% more acetylene was derived from coal at 825°C than from lignite tar at

\* Tar Products Test Committee, Gomersal

925°C. No data were collected to differentiate between the reaction temperature and the feedstock as the cause of this difference. However, since at 800°C high temperature coke oven tar yields about .3% acetylene, it seems logical to assess this increase in this product against the feedstock.

A second observation deals with the ease with which primary aromatics are produced. Benzene, while not shown specifically in Table II as such, is the predominant component of the solvents to 200°C. This situation also holds for the tar acids and bases. Pyridine and quinoline form almost 80% of their corresponding fraction while substituents in these genera are absent or present only in minor quantities.

Naphthalene, a most valuable constituent in coal tar, volumewise, forms readily at all temperatures employed. The compound, almost completely absent from tars produced by carbonizing coal in 500°C range, is obtained in yields upward to 14% of the feedstocks. Not shown because of doubtful reliability are yields of naphthalene as high as 28% of the feedstocks charged - using either carbohc oil residues or the lignite tar from the Parry process.

The resulting pitches are peculiar in that for comparable softening points the quinoline insoluble component is low. As they stand, these products are easily employed in saturation operations. No molecular weight distributions were obtained on these materials, but the high benzene insoluble, coupled with the low quinoline value, would indicate a product of low molecular weight in narrow distribution - a product of high uniform quality.

With respect to the effect of this type of treatment on high boiling tar bases, Table II indicates that pyridine, quinoline, and a high nitrogen content pitch can be formed from this heterogeneous low value crude. This type of pitch may well have seeding advantage in the electrode formation process because of the nitrogen backbone in its polymer structure.

Concerning the work with Pond Creek coal, the results should not be taken in any sense other than the indicative. Extreme difficulty was encountered with the feed mechanism and a really reliable set of data could not be obtained. Insufficient tar was recovered for accurate evaluation, but by ordinary smell, the tar would be classified as produced at high, rather than low temperature carbonization.

Table IV lists the proximate analysis of the coal use. No other information, other than the name, was available. The coal appeared dried and aged. However, if it were aged, the aging was insufficient to destroy coking properties.

Since there has been much argument as to the paraffin nature of low temperature tars, a paraffin distribution study was run on the feedstock to Run No. 3. The producer of this tar indicated that yields of 20 to 25% tar might be expected from the coal used. And while this sample contained approximately 40% uncarbonized or partially carbonized coal, he said production would yield

tars of 1 to 5% solids content. This pyrolytic study and the resultant paraffin distribution analysis were run on tar that had been cleaned by filtration.

Table III lists the results of this study. While there is no major paraffin component in this low temperature tar, those that are there appear to be evenly distributed. On pyrolysis, these are cracked to low boilers and fragments which appear to cyclize to aromatics.

Table V attempts a comparison between the pyrolysis products as they are formed on contact with the hot chamber and the flared gases after tar removal by condensation and scrubbing. These samples were taken and quenched immediately in a bath of dry ice and acetone and kept at that temperature until admission to the mass spectrometer.

It can be seen that the hydrogen, methane and acetylene that appear on pyrolysis are rapidly transformed to tar and oil products in the period of time necessary to traverse the apparatus - about 2 seconds. Another observation was noted in this same work. The material withdrawn from the cracking chamber crystallized out as a fine white crystal on the walls of the trap. When allowed to come to room temperature in not less than five minutes, the white crystals first turned to a pale yellow, then a bright brown-red, then a brown. At those stages, melting began and the brown crystals coalesced to form droplets of black tar.

This work is a summary of a much more complete study that covers some 5 years of effort and explored in replication, a wide variety of feedstocks.

Nevertheless, regardless of the source of the feed, the data so obtained fits the general pattern of the results reported here.

TABLE I

## OPERATING CONDITIONS, MATERIAL BALANCES, YIELDS

1. Source of Feedstock	Neutral Oils H. T. Co. Tar		Tar Base Residues H. T. Co. Tar		Appalachian Coal Tar-Low Temp. Carb.		Texas Lignite Tar Low Temp. Carb.		Pond Creek Coal	
	grams <sup>1</sup> wt%	900° C	grams <sup>2</sup> wt%	800° C	grams <sup>3</sup> wt%	750° C	grams <sup>4</sup> wt%	925° C	grams <sup>5</sup> wt%	825° C
2. Run No.										
3. Pyrolysis Temperature										
4. Weight of Feedstock Charged	10,000	50%	20,000	50%	7,920	54%	22,000	50%	309	46%
5. Weight of Water Charged	10,000	50%	20,000	50%	6,800	46%	22,000	50%	475	54%
6. Total Input	20,000	100%	40,000	100%	14,720	100%	44,000	100%	784	100%
7. Weight of Products Recovered	8,730	43.5	19,534	48.7	7,640	52.0	22,510	51.5	319	39.5%
8. Weight of Water Recovered	8,900	44.5	19,000	47.5	6,600	44.7	20,500	46.5	300	39.5% <sup>5</sup>
9. Total Output	17,630	88.5	38,534	96.2	14,240	96.7	43,010	98.0	619	79.0%
10. Material Balance (Line 9/Line 5)		88.5		96.2		96.7		98.0		79.0%
DISTRIBUTION OF PRODUCTS										
11. Tar Recovered	5,783	66.4	17,074	87.3	3,450	45.0	10,700	47.4	35	10.7
12. Light Oil Recovered	680	7.8	900	4.6	455	6.0	800	3.6	4	1.2
13. Trapped Oils	340	3.9	260	1.4	150	2.0	390	1.7	10	3.1
14. Flared Gases	1,052	11.9	780	4.0	2,015	26.4	9,200	41.0	270	85.0
15. Carbon	875	10.0	520	2.7	1,570	20.6	1,420	6.3	---	---
16. Total	8,730	100.0	19,534	100.0	7,640	100.0	22,510	100.0	319	100.0

TABLE II

ANALYSIS OF PRODUCTS

Source of Feedstock	1		2		3		4		5	
	Neutral Oils H. T. Co. Tar	Tar Base Resi- dues - H. T. Co. Tar	Appalachian Coal Tar-Low Temp. Carb.	Texas Lignite Tar Low Temp. Carb.	Pond Creek Coal					
Flared Gases(Below 75°C)	0.00	12.3%	0.00	3.98	0.00	26.61	0.00	40.10	85.0	
Hydrogen	2.88	0.57	0.82	0.82	1.65	0.82	0.00	1.65	47.3	
Methane	3.98	1.00	9.25	1.00	9.79	9.25	9.79	9.79	15.7	
Nitrogen	1.77	0.51	0.43	0.51	10.42	0.43	10.42	10.42	0.0	
Carbon Monoxide	1.74	1.11	8.00	1.11	0.00	8.00	0.00	0.00	17.0	
Acetylene	1.00	0.27	Trace	0.27	1.40	Trace	1.40	1.40	2.1	
Ethylene	0.07	0.01	5.25	0.01	8.73	5.25	8.73	8.73	0.6	
Ethane	0.05	Trace	0.90	Trace	1.16	0.90	1.16	1.16	0.4	
Oxygen	0.00	0.16	0.55	0.16	0.00	0.55	0.00	0.00	0.0	
Carbon Dioxide	0.81	0.14	1.10	0.14	4.23	1.10	4.23	4.23	1.98	
Propylene	0.00	0.00	0.31	0.00	2.70	0.31	2.70	2.70	0.0	
n-Butane	0.00	0.00	0.00	0.00	0.00	0.00	0.00	0.00	0.0	
Total from 75 to 200°C	1.30	7.80	0.00	6.33	7.00	14.70	10.00	11.10	0.0	
Solvents	0.66	4.67	1.36	1.36	1.51	10.54	8.11	9.51	0.0	
Tar Acids	0.34	0.66	0.00	0.00	5.49	4.16	1.50	0.75	0.0	
Tar Bases	0.30	2.47	4.97	4.97	0.00	0.00	0.39	0.90	0.0	
Total from 200 to 250	19.50	22.70	96.00	46.55	22.60	6.30	16.29	9.00	0.0	
Solvents & Oils	13.86	6.32	5.43	6.58	4.30	3.85	12.12	1.00	0.0	
Naphthalene	0.15	13.91	0.00	0.00	0.00	1.44	0.00	7.00	0.0	
Tar Acids	2.22	1.00	0.25	0.05	14.10	1.39	3.17	0.32	0.0	
Crude Quinoline	3.27	1.47	90.32	39.92	0.00	0.00	1.00	0.68	0.0	

No volatile components below 400°C

Apparently normal  
HT CO

TABLE II (Contd)

Source of Feedstock	Neutral Oils		Tar Base Resi-		Appalachian Coal		Texas Lignite		Pond Creek
	H. T. Co.	Tar	dues - H. T. Co.	Tar	Tar - Low Temp.	Carb.	Tar Low Temp.	Carb.	
Run Number	1	2	3	4	5				
Total from 250 to 300°C	76.00	10.90	3.00	10.62	---	---	16.90	0.10	
Solvent & Oils	66.83	8.73	0.30	9.90	---	---	8.91	0.10	
Tar Acids	3.62	1.01	0.00	0.05	---	---	4.67	---	
Tar Bases	5.55	1.16	2.70	8.47	---	---	3.42	---	
Total from 300 to 330°C	0.00	6.40	0.00	6.01	---	---	25.00	4.10	
Solvents & Oils	0.00	4.88	0.00	0.72	---	---	17.13	3.27	
Tar Acids	0.00	1.09	0.00	0.00	---	---	4.46	0.70	
Tar Bases	0.00	0.43	5.28	---	---	---	3.41	0.13	
Total above 330°C	3.00	16.60	1.00	10.98	68.30	31.40	31.80	35.20	
Carbon Produced	0.00	10.60	0.00	2.66	2.10*	20.70	0.00	0.00	

\*Distillation loss -  
Not carbon

TABLE III

ANALYSIS OF THE PITCHES

	No		135°C	46°C	188°C
	98°C	Pitch			
Softening Point(R&B)	Fluid	153°C			
Pitch Carbon Insoluble in CS <sub>2</sub>	0.1%	56.0%	37.7%	8.1%	54.8%
Pitch Carbon Insoluble in Quinoline	0.1%	50.0%	0.5	0.4%	5.0%
Pitch N <sub>2</sub> Content	0.4%	4.0%	0.9	0.7%	1.0%
Pitch Ash Content	0.0%	0.0	0.2	1.0%	0.2%

TABLE IIICOMPARISON OF PARAFFIN CONTENT OF FRACTIONSLow Temperature Tar (Run #3) Vs. Reformed Low Temperature Tar

Fraction by Boiling Point	<u>Feedstock</u>		<u>Product</u>	
	% of Feedstock	% of Fraction	% Product	% of Fraction
75 to 90°C	0.00	0.00	0.00	0.00
90 to 125°C	1.17	17.00	1.42	71.00
125 to 150°C	0.10	17.80	0.00	70.00
150 to 200°C	1.01	18.60	0.01	0.10
200 to 230°C	2.84	18.50	0.04	0.10
230 to 250°C	1.69	22.20	0.00	0.00

TABLE IVANALYSIS OF COAL USED

Name	
Volatile Matter	17.0%
Fixed Carbon	79.0%
Ash	6.0%
Moisture	0.0%

TABLE V.COMPARISON OF GAS COMPOSITION (Run No. 5)Cracking Chamber Vs. Flared Gas

<u>Component</u>	<u>Cracking Chamber (wt %)</u>	<u>Flared Gas</u>
Hydrogen	70.4	55.8
Methane	22.1	18.5
Water	0.2	0.2
Carbon Monoxide	0.0	20.0
Nitrogen	0.0*	0.0
Acetylene	4.2	2.4
Ethylene	0.3	0.7
Ethane	0.3	0.5
Oxygen	0.7	0.0
Argon	0.0	0.0
Carbon Dioxide	1.5	2.2
Benzene	0.2	0.0

\* Not representative since gas was analyzed  
on a nitrogen-free basis

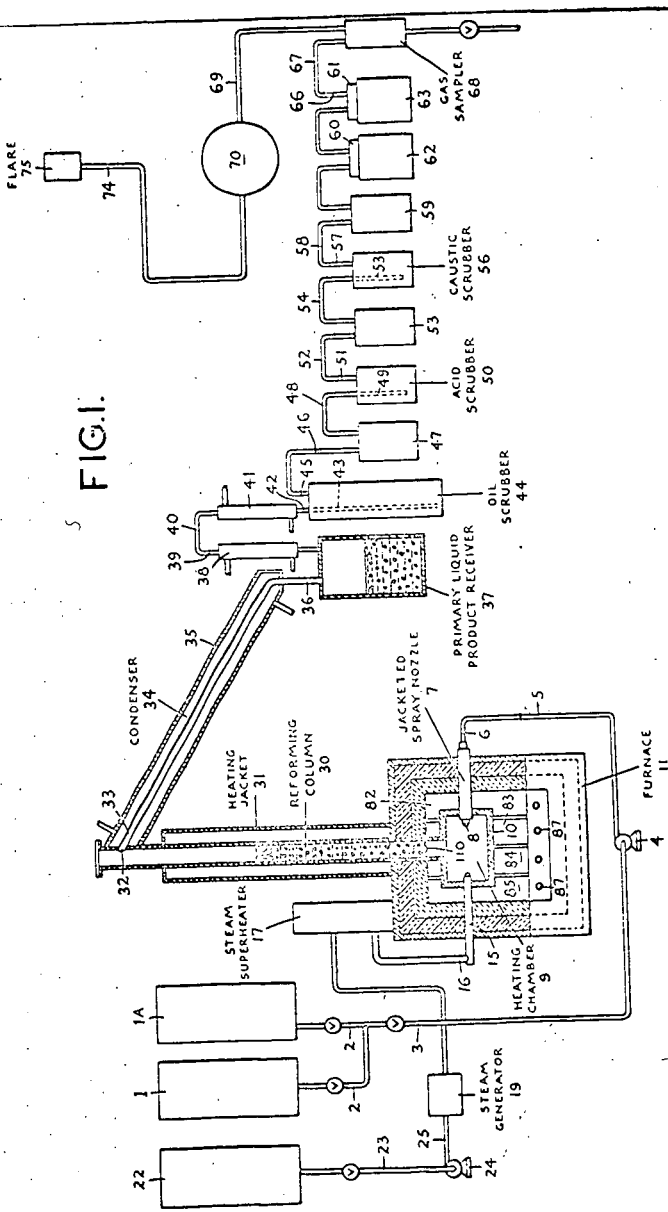


FIG. 1.

FIG. 4.

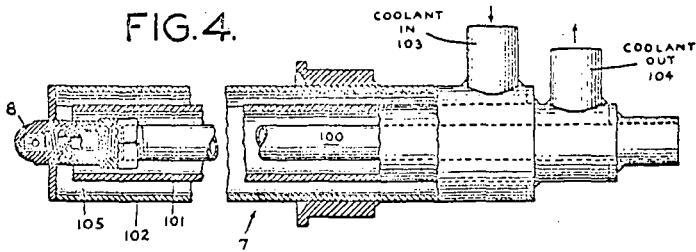


FIG. 3

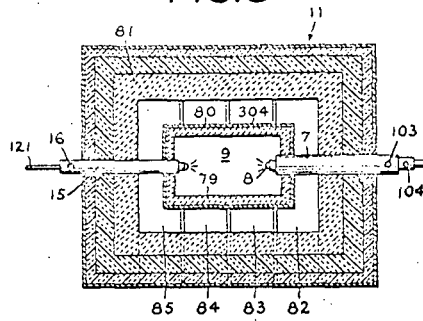
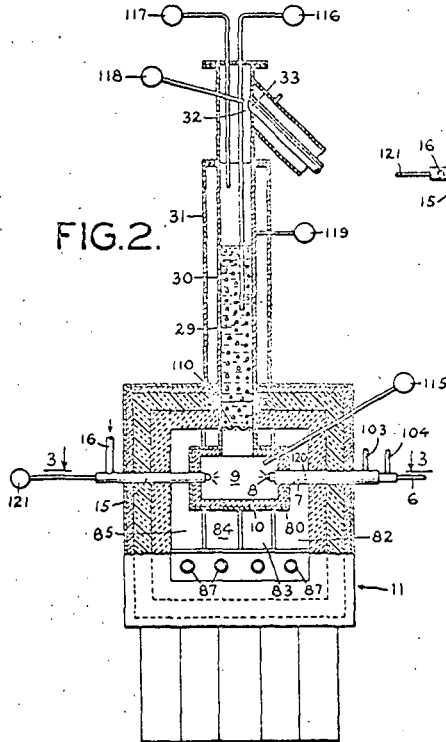


FIG. 2.



Presented Before the Division of Fuel Chemistry  
American Chemical Society  
Chicago, Ill., August 30 - September 4, 1964

## DEVOLATILIZATION OF COAL IN A TRANSPORT REACTOR

L. D. Friedman, E. Rau, R. T. Eddinger

FMC Corp., Chemical Research and Development Center, Princeton, N. J.

### INTRODUCTION

The objective of the Char Oil Energy Development (COED) project, sponsored by the Office of Coal Research, is to develop a process for conversion of coal to a pumpable mixture of char and oil. The work reported herein is part of the Project COED investigation. One approach to developing such a process involves the pyrolysis of coal using very high heating rates and very short residence times. Aside from reducing equipment costs, rapid pyrolysis is also desirable because volatile yields from coal are increased. In fact, under selected conditions, the quantity of material volatilized exceeds the ASTM volatile-matter content of the coal.

Systems most commonly employed to achieve the extremely rapid heating rates needed for maximum devolatilization--shock tubes, flash-heating apparatus and hot-strip microscopes--use such small samples that analysis and characterization of the products is difficult or uncertain. This drawback can be largely overcome by using a dispersed-phase transport reactor. With this system, larger quantities of coal can be heated for short periods at rates of more than 2500°C. per second.

### EXPERIMENTAL AND RESULTS

The transport reactor, shown in Figure 1, is an externally heated tube through which coal is transported by means of an inert gas. Coal is charged from a hopper by means of a Syntron vibrator or a screw feeder. The coal is transported through the reactor by the carrier gas. The reactor is heated by a Global-heated combustion furnace. On leaving the reactor, the bulk of the char is collected in a cyclone; the balance, in a settling vessel along with some tar. Tar mist and ultra-fine particles are collected on glass-wool filters. (These were found to be more effective than an electrostatic precipitator followed by dry ice-acetone and/or liquid nitrogen cold traps.) A cold trap after the filters collects moisture entrained in the gas, and the gas is metered and sampled for mass-spectrographic analysis.

Char collected after the cyclone is washed with acetone to remove condensed tar. The washed char is dried at 110°C. and is analyzed along with char from the cyclone. Acetone is evaporated from the acetone-solution of tar, and the weight of acetone-soluble tar determined. The respective amounts of solids and tars on the filters is determined by quinoline solubility.

Elkol coal, a sub-bituminous B coal from Wyoming was used in these studies. The analysis of this coal is shown in Table I.

TABLE I  
Analysis of Elkol Coal  
Elkol Mine  
The Kemmerer Coal Company

<u>Proximate Analysis, wt. %</u>	<u>As-Received</u>	<u>Dry Basis</u>
Moisture	12.8	-
Volatile Matter	35.5	40.8
Fixed Carbon	47.6	54.5
Ash	4.1	4.7
<u>Ultimate Analysis, wt. %</u>		
Carbon		70.7
Hydrogen		5.4
Nitrogen		1.2
Sulfur		1.0
Oxygen		17.1
Ash		4.7

One of the objectives of this study was to volatilize a maximum amount of coal. From these studies, it was found that the two most important factors in the volatilization of coal were the carrier gas velocity and the furnace temperature.

The quantity of residual volatile matter in the product chars decreases as the carrier gas velocity, calculated at 22°C. and 1 atmosphere, is decreased from 20 to 4 feet per second. This decrease in gas velocity, shown in Figure 2, increases the calculated average residence time of coal in the 8-inch hot zone of the combustion furnace from about 8 to 40 milliseconds. All of these runs were made with the same coal feed rate and with a furnace temperature of 1100°C. The lowest volatile-matter content shown in this figure is about 6 times greater than that obtained when the same coal is heated in a fluidized bed at 1100°C. for 15 minutes. It is not known whether the relatively low devolatilization obtained in the transport reactor at 1100°C. results from insufficient time for devolatilization to be completed or from the char being quenched before it reaches the furnace temperature. Because of the difficulty in determining true char temperatures during devolatilization, all temperatures given herein are furnace temperatures.

Higher furnace temperatures cause increased devolatilization of coal, as shown in Figure 3. This is true for all carrier gas velocities shown in the figure. On the other hand, reducing the carrier gas velocity below 4 feet per second does not increase the amount of coal devolatilized. Because of heating limitations, temperatures above 1500°C. could not be attained with this system. It should be noted that char prepared at 1500°C. with a linear helium velocity of 4.0 feet per second still contains 2.7 percent of volatile components, as determined by the ASTM volatile-matter test.

The foregoing indicates that complete devolatilization of the coal cannot be obtained in the transport reactor when using cold helium as the carrier gas. In an attempt to add additional heat to the system, helium preheated to 550°C. was used as the carrier gas. A comparison of results obtained when using heated and unheated helium as carrier gases is shown in Figure 4. At 1100°C., the product char obtained with heated helium carrier gas contains about four percent less volatile material than that obtained with the cold helium, but the difference decreases at higher temperatures and virtually disappears at 1400°C. With heated helium also, no difference can be found in the amount of coal devolatilized when the linear helium velocity is reduced from 4.0 to 2.5 feet per second.

When steam is used in place of helium as a carrier gas, about 10 to 15 percent less devolatilization is observed. This is attributed to the higher specific heat and lower thermal conductivity of steam, as compared to helium.

Typical product yields obtained with glazed porcelain tubes at 1100 and 1300°C. are shown in Table II. Although more coal is devolatilized at 1300°C. than at 1100°C., as shown in Figure 3 and, in the volatile-matter and ash contents of the chars shown in Table II, more solids are produced at the higher temperature. The gas produced at 1300°C. contains less hydrocarbons than the gas formed at 1100°C. This suggests that volatile hydrocarbons are cracked at the higher temperature to form solids. Confirmation of the cracking reactions was obtained by isolation of vapor-cracked carbon from practically all of the runs made at 1300°C. and higher temperatures. This carbon accumulates in the coarse and fine fractions of the product chars on sieving, or it may be elutriated from the char in a fluidized bed.

Photos of vapor-cracked carbon are shown in Figures 5 and 6.

The quantity of vapor-cracked carbon formed in miscellaneous runs at 1300°C. is shown in Table III. After repeated use, porcelain tubes cause more cracking, as evidenced by the vapor-cracked carbon contents of Runs 89 and 93. The low vapor-cracked carbon content of the solids from Run 95 is attributed to the use of undried coal. Apparently coal moisture delays the temperature rise of coal particles. The high yield of carbon in Run 96 may be partly due to cracking of the hydrocarbons in the carrier medium which simulated a recycle gas.

TABLE II

Product Yields Obtained in Glazed Porcelain Reactors  
 100-x200-mesh Elkol Coal  
 Helium Carrier Gas Velocity, 4.0 ft./sec.

Run No.	88	97
Furnace Temperature, °C.	1100	1300
Feed Rate, gm./hr.	132	124
Coal Charged, gm.	111	62.2
<u>Coal Converted, %, dry basis</u>		
Char	50.1	55.3
Tar	3.6	1.8
Moisture	2.7	2.1
Gas	43.6	40.8
<u>Make-Gas Analysis, mol %</u>		
H <sub>2</sub>	22.5	49.0
CH <sub>4</sub>	18.2	7.7
C <sub>2</sub> H <sub>2</sub>	4.3	7.2
C <sub>2</sub>	10.5	1.1
CO	35.4	28.6
CO <sub>2</sub>	7.5	6.0
C <sub>3</sub> <sup>+</sup>	0.7	0.3
<u>Char Analysis, %, dry basis</u>		
Volatile matter	15.6	5.6
Ash	4.6	6.4

TABLE III

Formation of Vapor-Cracked Carbon at 1300°C.  
 (Basis: Ash Balance)

Run No.	Solids Recovered, wt. %	Percent Vapor-Cracked Carbon	Corrected Char Yield, wt. %
89	46.0	4.8	41.2
93	52.0	14.6	37.4
95 <sup>1</sup>	50.5	6.9	43.6
96 <sup>2</sup>	57.9	16.2	41.7

<sup>1</sup> Undried Elkol coal used.

<sup>2</sup> Recycle gas used as carrier.

The most significant aspect of Table III, however, is that, if the solids recovery is corrected for the calculated carbon content, the corrected char yield is about 41 percent. This figure is considerably lower than the char yield obtained at 1100°C. Thus, it appears that on raising the furnace temperature from 1100°C. to 1300°C. the amount of coal volatilized is increased, but the effect is masked by the simultaneous production of vapor-cracked carbon.

If the true char yield of 1300°C. is 41 weight percent of the dried coal, then 59 percent of this coal must have been volatilized. This is far above the 41 percent indicated by the ASTM volatile-matter determination. Moreover, the char still contains about 6 percent volatile matter which can be removed. Thus, about 60 to 65 weight percent of this coal can probably be volatilized by rapid pyrolysis.

In order to reduce the secondary cracking reactions, the heating zone of the combustion furnace was shortened from 8 to 4 inches by changing the Globars. To get a temperature of 1100°C. with the shorter heating zone, it was necessary to preheat the carrier gas to about 450°C. Results obtained with the 4-inch Globars are presented in Table IV.

The total amount of volatile products produced at 1100°C. in these runs is about one-fourth lower than in Run 88, Table II, but the distribution is different. Thus, tar production is increased substantially and the yield of gas is decreased. The gas has a higher concentration of hydrocarbons and less hydrogen, indicating that less cracking occurs in the shorter hot zone. Also, the yield and volatile content of the chars are higher than from Run 88 shown in Table II, indicating less devolatilization of coal in the shorter heating period.

## DISCUSSION OF RESULTS

The high yield of volatile material from the devolatilization of coal in the transport reactor is believed due to the extremely fast heating rates and the short residence times used. When coal is pyrolyzed, devolatilization and polymerization reactions occur simultaneously. The velocity of the polymerization reactions is slower than that of the devolatilization reactions; and in the short residence times employed in this dilute-phase reactor system, reaction products are quenched and recovered before extensive polymerization of reactive species can occur.

TABLE IV

Devolatilization with 4-inch Globar Heaters  
 100-x200-mesh Elkol Coal  
 Helium Carrier Gas Velocity, 4.0 ft./sec.

Run No.	<u>80</u>	<u>81</u>
Furnace Temperature, °C.	1100	1100
Feed Rate, gm./hr.	120	127.5
Total Coal Charged, gm.	50.1	53.3
<u>Coal Conversion, wt. %, dry basis</u>		
Char	57.1	60.0
Tar	10.6	9.3
Water	6.3	7.0
Gases	26.0	23.5
<u>Make-Gas Analysis, mol %</u>		
H <sub>2</sub>	15.9	17.4
CH <sub>4</sub>	17.9	17.5
C <sub>2</sub> H <sub>2</sub>	1.2	0.6
C <sub>2</sub>	13.9	15.7
CO	37.8	33.6
CO <sub>2</sub>	9.9	12.4
C <sub>6</sub> H <sub>6</sub>	0.4	0.3
C <sub>3</sub>	3.0	2.5
<u>Char Analysis, wt. %, dry basis</u>		
Volatile matter	20.5	21.9
Ash	4.2	4.8

TABLE V

Products Residence Times in Transport  
 and Fluidized-Bed Reactors

<u>Residence Time, seconds</u>	<u>Transport Reactor</u>	<u>Fluidized-Bed Reactor</u>
Gas	0.01-0.04	1-2
Solids	0.01-0.04	900

In Figure 2 it was shown that coal particles do not reach the indicated furnace temperatures, even at the lowest carrier gas velocities (or longest residence times) used. In order to estimate the temperature to which gases and solids were heated in the transport reactor, the char and gas analyses were compared with similar analyses obtained by devolatilizing this same coal in a 3-inch fluidized-bed reactor. This method of determining temperature is less rigid than might be desired, and the residence times of char in the two reactors is very different, as shown in Table V. Based on the analyses of products from the two reactors, the temperatures of the gas and char in the transport reactor were estimated to be about 300 and 500°C., respectively, below that of the furnace. These results are summarized in Table VI.

TABLE VI

Estimated Temperatures Inside Transport Reactor  
Carrier Gas Velocity, 4.0 ft./sec.

Furnace Temperature, °C.	1100	1300
<u>Estimated Temperature, °C.</u>		
From hydrogen content of gas	775	980
From hydrocarbon content of gas	790	980
From VM of char	625	760

The lower char temperature probably results from ablation effects in which the rapid evolution of gases and tars lowers the temperature of the char particle. Similar, though less striking, results are reported by W. Peters<sup>1</sup> in devolatilization studies made with longer char residence times.

In summary, the transport reactor is effective for studying devolatilization of coal. Coal devolatilization reactions proceed very rapidly. With extremely short residence times, the amount of coal that can be volatilized is appreciably greater than that determined by the ASTM volatile-matter determination. Above 1100°C., formation of vapor-cracked carbon becomes extensive, probably due to cracking of tars and gases. Lastly, by varying the residence times within a hot zone, the distribution of products may be altered considerably.

#### ACKNOWLEDGMENTS

The authors wish to thank the Office of Coal Research and FMC Corp. for permission to present this paper. They also wish to acknowledge the help of other members of the project staff. Analyses were made by members of the FMC Analytical Department.

<sup>1</sup> Peters, W., *Chemie-Ing-Techn.* 32 (3) 178 (1960).

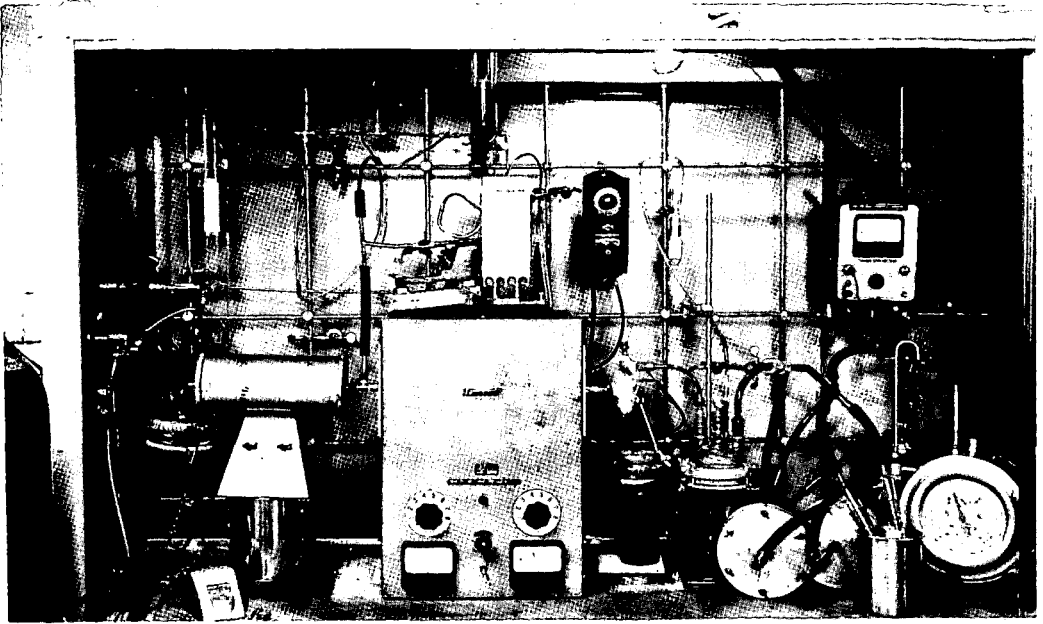


FIGURE 1  
Transport Reactor Assembly

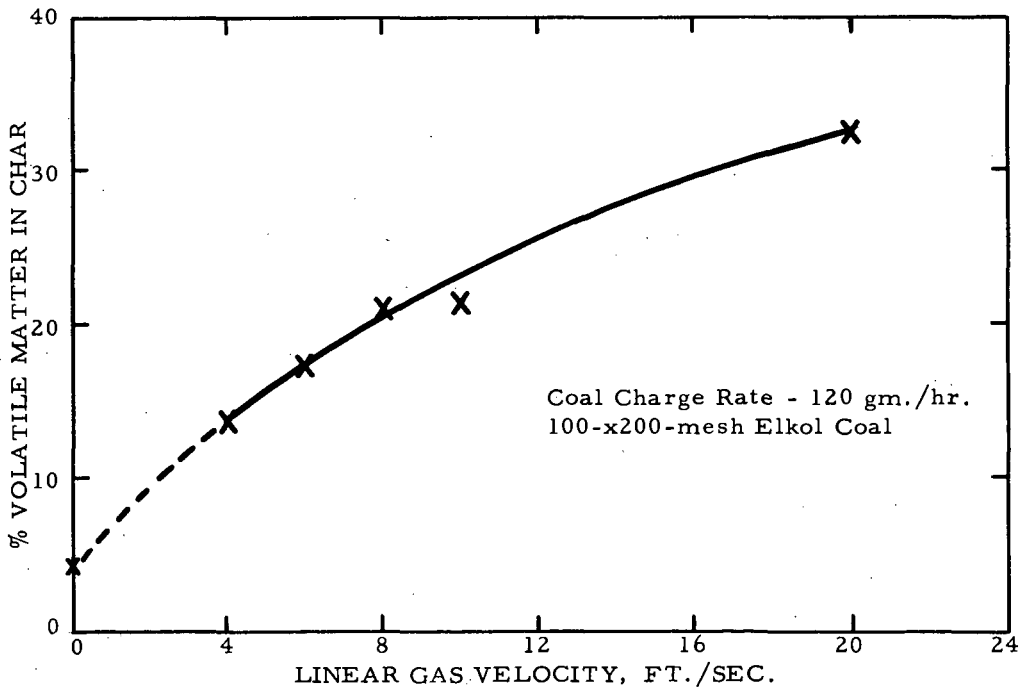
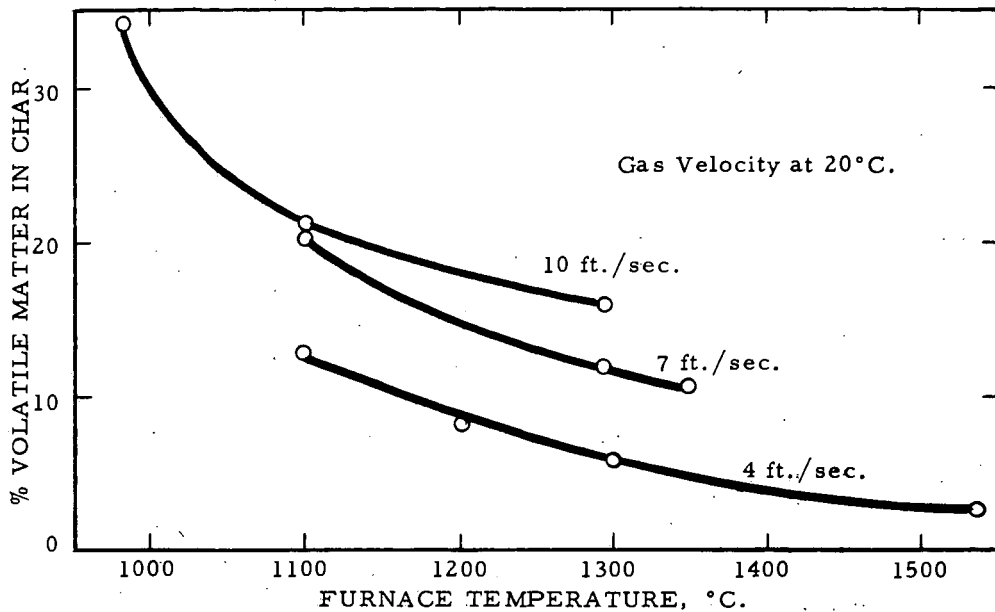
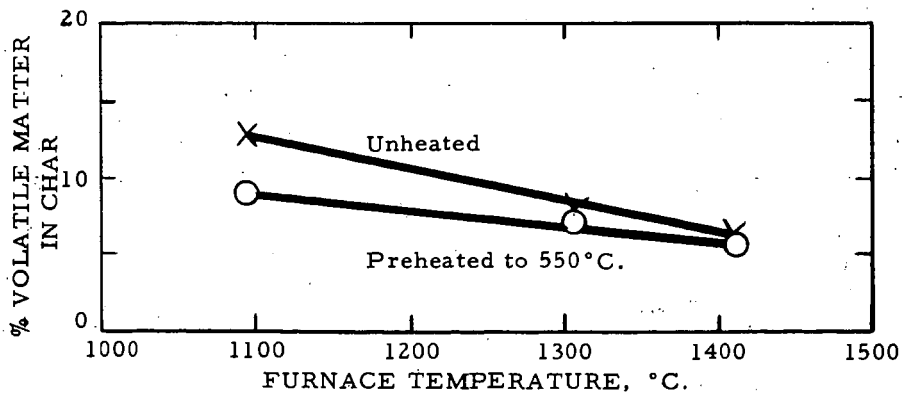


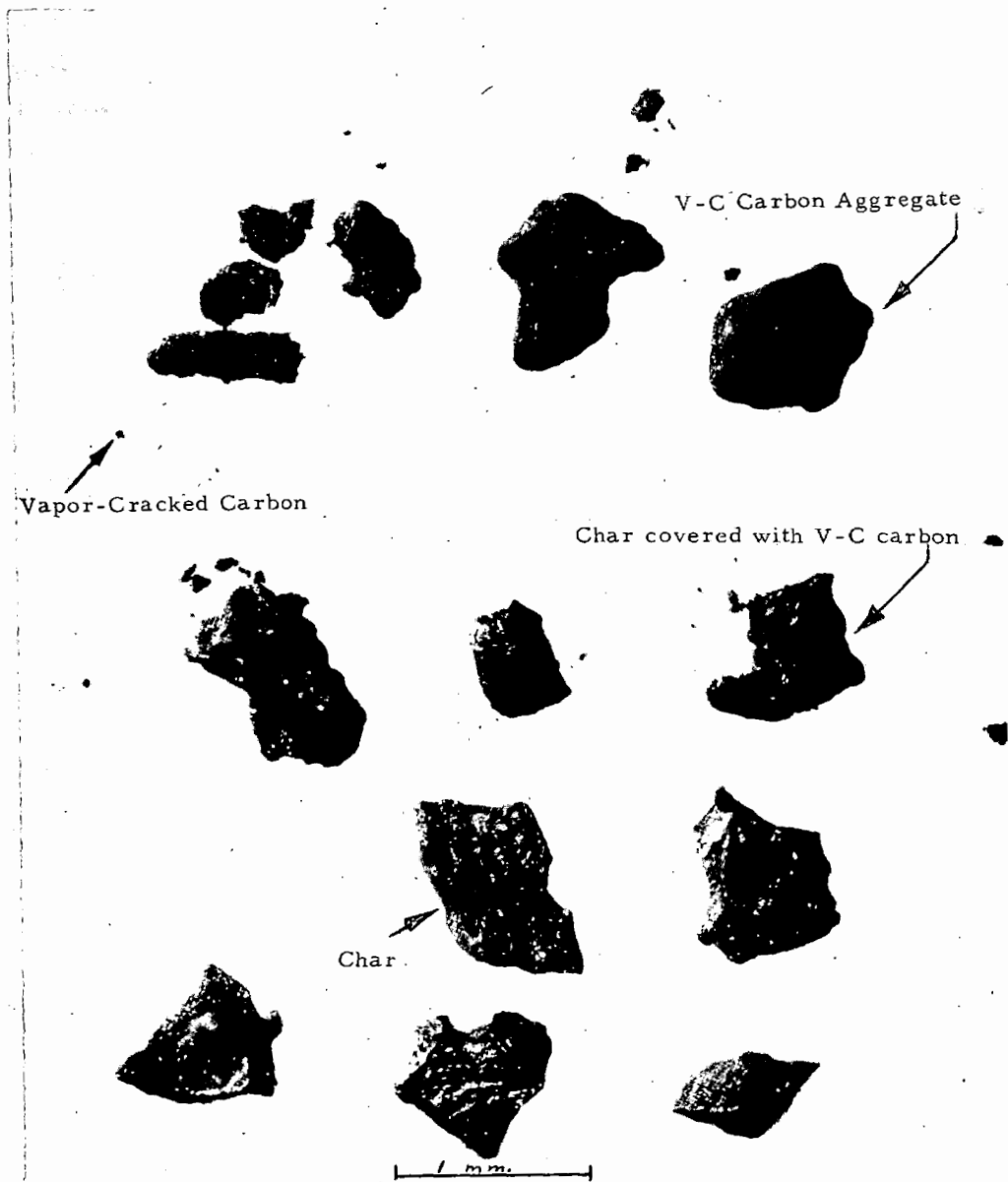
FIGURE 2  
Effect of Carrier Gas Velocity on Coal Devolatilization  
Furnace Temperature 1100°C.



**FIGURE 3**  
Effect of Furnace Temperature on Coal Devolatilization  
 Coal Charge Rate - 120 gm./hr.



**FIGURE 4**  
Effect of Carrier Gas Temperature on Devolatilization



Magnification  $33 \frac{1}{2} X$

28-x48-mesh fraction collected in recovery section

Run conditions: 2400°F. Furnace Temperature

14-x60-mesh Elkol coal

4 ft./sec. He carrier gas

FIGURE 5

Vapor-Cracked Carbon in Coarse Fraction of Char



FIGURE 6  
Vapor-Cracked Carbon in Elutriated Material

Presented Before the Division of Fuel Chemistry  
American Chemical Society  
Chicago, Ill., August 30 - September 4, 1964

Kinetics of the Rapid Degasification of Coals

by W. Peters and H. Bertling

Bergbau-Forschung G.m.b.H., Essen-Kray

1. Introduction

In form of the so-called "LR-Process", developed in team-work by "Lurgi Gesellschaft für Wärmetechnik mbH" in Frankfurt and "Ruhrgas AG" in Essen, the rapid degasification of coal has obtained technical importance.

The basic phenomena of the rapid degasification of coal has been investigated in the laboratory-scale in essential with an equipment shown in figure 1. The most important part of this equipment is the degasification mixing chamber (b). After heating up, the fine-grained heat carriers (coke or sand) are placed into the reactor (b). Immediately behind the inlet of heat carriers, coal of the same granulation is fed into the mixing chamber. Due to the high mixing ratio of heat carriers to coal (about 30 to 6 : 1), each individual coal grain is very rapidly heated and degasified. As the gas development takes place spontaneously and as the mixing chamber is fairly small, the period of sojourn is less than 0.5 sec. After discharge, the products are immediately chilled and partly condensated (f to h). The char coke is transported from the second degasification reactor (d) into the collection reactor (a), from which it is fed, a little overheated, as a heat carrier again to the mixing chamber (b).

The rapid heating and cooling of the products causes a much higher yield of tar. This so-called "rapid degasification effect" is of great interest for the research of coal. It will be the object of this paper to describe the physical-chemical phenomena of this effect. Studying these phenomena, it will be possible not only to describe the reaction kinetics of the rapid degasification, but to draw also some conclusions therefrom on the structure of the substance of coal.

2.1. Heating-up speed of the coal

With the high mixing ratio of heat-carrier:coal, the coal grain, immediately after its entry into the degasification mixing chamber, is surrounded after intensive mixing by hot heat carriers. At the same time it is heated-up presumably very quickly. As it is very difficult to measure the heating-up speed directly, one must fall back on calculations.

The second figure shows the calculated curves at the surface and in the centre of a 1.2 mm  $\varnothing$  coal grain with two different heat transmission ratio related to the temperature of the heat carriers. The heat transmission ratio, of course, is of decisive importance. With a slow heat transmission, the difference between the temperature at the surface and in the centre of the coal grain is relatively small but with a rapid heat transmission it is quite high. This fact will play an important part.

Which of the curves plotted on the figure will most approximate the

true state of affairs, can be decided more easily, when the temporal yield of the degasification products is known, as the thermal diffusivity and the heat transmission ratio cannot be measured directly.

Of these investigations, a mixing chamber with a continuous feeding of coal appeared to be unsuitable. Therefore, a pilot equipment (figure 3) was built which corresponded sufficiently exactly to the conditions in the technical degasification mixing chamber.

A cylindrical tube of 80 mm inside diameter constantly heated from the outside is equipped with a stirring rod with pins. Half of the chamber is filled with fine chips of corundum as a heat carrier. For the test, a sample of coal is blown with nitrogen into the chamber and the time is precisely recorded. An ignitor directly at the free outlet of the gas brings the degasification products leaving the chamber to combustion. The size of the flame is an approximate measure for the quantity of the gases and tar fumes. The flames are photographed together with a watch showing the time in short intervals. Figure 4 shows a series of pictures taken of coking coal grains of the size 1 to 1.5 mm, the temperature of the heat carriers amounting to about 1000 °C. The seconds recorded underneath the photos are counted as from the impact of the coal grains to the corundum chips onwards.

After 0.37 seconds in phase two, a high flame can be seen which, however, is falsified by the nitrogen which still flows out. After that, the cone of the flame is much reduced. Comparing this observation with the calculated temperatures of the coal in fig. 2, much more can now be said about the heating-up process. When coal is heated, the first combustible degasification products develop at a temperature of about 350 °C. Real degasification becoming visible in phase 2, however, occurs at a temperature of 400 °C at the earliest. That means that, after 0.37 seconds, the coal must have temperatures of above 400 °C at its surface. According to fig. 4, a temperature of 400 °C at the surface, i.e. the value  $\delta = 0.4$ , is reached with a heat transmission coefficient of  $\alpha = 100 \text{ kcal/m}^2 \text{ h}^\circ\text{C}$ , in 5 seconds only. In practice, the heat transmission coefficient must be much higher. With  $\alpha = 1000 \text{ kcal/h m}^2$ , 400 °C at the surface will be reached in 0.28 seconds. It can be assumed, however, that degasification started much earlier so that heat transmission coefficients of at least  $\alpha = 1000$  can be reckoned with. The further development of the heating-up curves agrees with the series of pictures, too. This leads to important consequences. With such a high heat transmission coefficient, a steep temperature gradient must be given in the inside of the grain. The reactions of degasification begin at the outside of the grain, when there are still nearly initial temperatures (30 °C) in the inside. The temperature of beginning decomposition in the centre is attained only, when after-coking temperatures have been reached at the surface of the grain already and when the gas yield is already strongly decreasing, as fig. 4 shows.

These rather qualitative statements show clearly that the reactions of degasification and the heating-up are much interdependent. This becomes evident also when lower temperatures of the heat carriers are applied, thus decelerating degasification with the result that more details show up from the diagram. This test can be seen from fig. 5. The phases 2 to 4 give reason to assume, that, during the main phase of degasification, the yield of products is nearly constant. This, however, would again indicate the particular importance of the heat transmission.

## 2.2. Speed of degasification

The extremely rapid heating of the coal with this process promised interesting results with regard to the structure of the substance of coal. The equipment shown in fig. 3 proved to be suitable for such tests, too. However, different devices for the quantitative recording of the temporal yield of the products of degasification had to be connected to the gas outlet. A difference was made between the products condensed at room temperature and gaseous products which were measured, for experimental reasons, separately in parallel tests. The diagrams in the two following figures show the yield of products as a function of the time of sojourn of the coal in the degasification chamber. For instance, figure 6 shows the tar yield of three different coals and figure 7 the gas yield at different temperatures.

The curves of the gaseous products and the condensate products are added, at last, to the degasification curves plotted in fig. 8 for different temperatures.

All these curves show one and the same characteristic development: a linear start until 60 to 70 % of the products have been released, then a bend and, finally, an asymptotic development into the horizontal. After the main yield of products, relatively more gas is increasingly released than tar and, in the development of the curve behind the bend, practically gases with a low molecular weight only are released. Summing up, it can be stated:

With rapid heating, the so-called "rapid degasification" is a reaction of zero order which ends in a different process of second degasification. This statement may be surprising as the coal pyrolysis is composed of decomposition reactions of first order. That we had to do with quite a different process, is proved by the energy of activation found to amount to 2.5 kcal/Mol (1) which is by 10 to 20 times smaller than the values known so far. This low energy of activation is an argument against the assumption that the reactions of decomposition determine the speed.

Presumably, a mutual dependence of transporting processes is decisive for the rapid degasification. A transmission of heat from the heat carriers to the coal and the endothermal degasification process are joined with each other by the flow-off of the degasification products which hinder the inlet of heat. These two processes give an equilibrium as long as still efficient substance for degasification is available in the coal grain.

As for the dependence of the speed of degasification on the temperature of degasification and the grain size, the following equation for the yield of products  $M$  is obtained, considering the fact that we have to do with the reaction of zero order:

$$M = 0,03 (T_a - 330) d^{-0,26} t$$

in which  $M$  means the yield of products in % (by weight),  $T_a$  the temperature of degasification in °C,  $d$  the grain size in mm and  $t$  the time of reaction in seconds (1).

The interpretation of the equation is rendered easier by the fact that the drying of coke represents a similar process. Therefore, processes for the drying of coke were carried out in a modified

degasification mixing chamber. Figure 9 shows clearly, how much the two processes are related to each other. In both cases, there is again the initial straight characterising a stationary process of evaporation, a bend in the curve and, at the end, an asymptotic turn into the horizontal.

The yield of water vapour from the drying of coke was calculated in the same way as the yield of gas and tar from the rapid degasification of coal. This led to the formula (1)

$$M = 0.029 (T - 83) d^{-0.65} t.$$

Again, there is an analogy which gives reason to assume that the two processes are still much more similar than can be recognized directly:

Thus, the rapid degasification of coal represents a process of evaporation the same as a drying process.

The above expositions lead to the following summarizing picture of the degasification processes:

Figure 10 shows the development of the degasification curve in time as well as the calculated temperatures of the coal grain. At first, a fresh coal grain is very rapidly heated up under the influence of the hot heat carriers. After about 0.2 seconds, the surface of the grain reaches a temperature of about 350 °C. The primary bitumen which is then formed, begins to evaporate from the surface. With further heating, more primary bitumen is brought to the surface of the coal grains and evaporates there. The released distillation products now hinder the transmission of heat, and there is an equilibrium of the two processes opposed to each other: with a constant boiling temperature the same quantity of heat per time unit thus flows to the surface from which the bitumen evaporates in constant quantities. During this period, temperature does not increase any more as the amount of new heat covers just the demand for evaporation heat, except the negligible amount flowing-off into the inside of the grain for heating up. A balance of temperature in the grain is established only after a good second.

When not enough primary bitumen flows to the surface of the coal grain any more, the front of evaporation is shifted concentrically to the inside of the grain. This does not yet mean a disturbance of the equilibrium, as the good heat conductivity of the coke affords a good transmission of heat. Besides, the coarse pores of the coke do not offer much flow resistance to the vaporous product. When the front of evaporation shifted far enough to the inside, the equilibrium is disturbed and the curve begins to bend, until the yield of products decreases much in the last course of the curve. In the final phase, the outside zones of the grain heat up essentially. During this process, semi-coke is forming, with the release of gaseous products. Finally, the temperature adapts itself everywhere to the temperature of the heat carriers.

### 3. Yields of degasification

The evaporating substance, called "primary bitumen" in this paper, must not exist necessarily in the coal in the same way. We try to clarify this question by investigation of the degasification products, especially of the tar. In doing so, it was not so much the intention

to identify as many individual substances as possible but rather to obtain a good review of larger complexes of substances.

For the purpose of comparison with products obtained under normal conditions of the pyrolysis of coal, tars were analysed which had been made in the Fischer-retort from the same coal. This was thus a tar which had been formed at a much slower heating-up speed ( $12^{\circ}\text{C}/\text{min}$ ) and a much longer time of sojourn in the reaction room.

The two tars were made at a temperature of  $600^{\circ}\text{C}$  as we obtained at this temperature the highest yield of tar as reported elsewhere (2). Investigations about secondary reactions led us to assume that the decompositions occurring during these reactions at this temperature are much suppressed. But this question, too, can be explained in the following.

The pronounced differences between both methods of degasification become visible already in the next table (fig. 11). Particularly striking is the high yield of tar with the rapid degasification. With the gasification according to Fischer, however, the yield of gas and coke is higher as the longer influence of heat caused, in this case, a cracking and coking of the tar. Very different fractions are obtained from the vacuum distillation of both tars. By virtue of the cracking, the tar according to the Fischer degasification possesses a high fraction of light oil, whereas the tar from the rapid degasification process has the highest yield of pitch. The last column of the table shows the quotient of the different yields from both methods of pyrolysis. According to these figures, the tar products from the rapid degasification process have a much higher molecular weight. This could be determined, however, so far only with regard to the total yield of tar.

### 3.1. Composition of tar

The tars obtained were not to be treated with the usual methods. Therefore, methods of analysis had to be developed which separated the tar products under most mild and gentle conditions, as the tar, already from its origination, is most sensitive against thermal and chemical influences. It is thus very difficult to elaborate suitable methods.

A scheme for the entire preparation of tar in fig. 12 shows, how many steps were required to obtain fractions which could be assumed for the gas chromatographic analysis (4). It proved to be impossible to separate further the undistillable residues of pitch. Therefore, we carried out, after a further extraction, a structural analysis according to van Krevelen (6).

Surely, it would lead too far to mention all results of tar investigations in this paper. It is hoped, however, that the following data of analysis will contribute to elucidate the problem. It is sufficiently known that the pyrolysis of coal is composed of several part reactions which take place partly parallel to each other and partly subsequent to each other. The primary products represent large molecular units which are decomposed in the secondary process into fragments of different sizes. In the end, larger units can develop again by polymerisation and condensation. The composition of the final products depends decisively on the pre-set conditions for the secondary reactions. Especially temperature and the time of reaction are of great importance.

Kröger (3) showed in a paper about the structure of coal macerals that the substance of coal is made up of at least three main complexes of groups of material. These are at first the group of waxes and resins, secondly the group of oxyhumic components and, finally, the group of dehydrohumic substances.

Kröger presumes that the coal represents a structure of solid material built up of many cells, into which bituminous coal components are embedded. He proved this by microscopical photos of a vitrinite before and after cauterization with dimethylformamid. A solvent shows clearly the structure of the cells of the otherwise structureless vitrinite after cauterization. During this process, the material inside the cells (waxes, resins, oxyhumines) - which are probably connected to the skeleton of the cells not without any bonding but also through functional groups - , are released.

If such a structure of cells is slowly heated, gaseous products are formed in the individual cells leading to excess pressure and diffusing to the outside through fissures and pore passages. How far there will be secondary reactions, depends on several parameters such as the structure of the cells and of the pore system as well as type and manner of thermal treatment. Due to such factors of influence, there will always be a different composition of the products of degasification,

With a very rapid heating of the coal, the pressure inside a cell increases very quickly. Then, the walls of the cells are torn up at weak points and the contents of the cells are so rapidly distilled that a cracking and reaction of the material is hardly still possible. On the other hand, it can be observed, that certain groups of substances are decomposed into smaller fragments at the prevailing relatively high temperatures already at extremely short times of sojourn. According to this idea of the process of pyrolysis, it can now be concluded from comparison between the yields of tar obtained from the rapid degasification process and of tar obtained from the Fischer process how these two processes act on the composition of such tars.

As the individual chemical compounds are very different indeed, it is preferable to evaluate them separately, viz. in the condition how they were obtained from the primary separation. In doing so, it is practical to limit this evaluation to the neutral components, moreover as this fraction is the largest. Then, the main two groups are obtained within this fraction: the aliphatic and the aromatic components. The values found by the urea method are partly very significant. Figure 13 shows the yield of aliphates. With hydrocarbons with 14 and 20 C-numbers, there are clearly two maxima which are a little higher for the tar obtained by the Fischer analysis. With high C-numbers, the curve of the tar obtained by the rapid degasification process, however, lies essentially above that for the tar obtained by the Fischer analysis. As products would be proved only up to the C-number of 31, it can hardly be assumed that there will be much longer chains in the substance of coal. There must be mainly hydrocarbons with C-numbers of 20 to 25 in the coal assumed for the tests. The maxima at a C-number of 14 indicate reactions of decomposition of the long chains into 2 halves. This does not mean, of course, that the lower hydrocarbons are formed only by reactions of separation. On the contrary, it must be assumed that these aliphates exist already in the substance of coal in form of waxes of vegetable origin.

By thermal treatment, the paraffins are distilled and diffused from the structure of the cells to the outside. With a "slow heating", they distill successively when reaching their boiling temperatures. With "rapid heating", however, the substances are at once exposed to high temperatures, at which they split up. Only the long-chain hydrocarbons, the boiling points of which lie at higher temperatures, are hardly decomposed. With the Fischer analysis, the longer time of sojourn leads to a cracking into smaller fragments. Therefore, the yields of these hydrocarbons with the slower degasification are lower.

It was much more difficult to determine the aromatic components as shown by a gas chromatogram of a fraction (fig. 14). Both tars contained nearly the same substances, of course, with different concentrations. A clear representation of the percentages of substances is given in the following picture (15), where the percentages of the individual ring systems of both tars have been plotted. Under the conditions of the "rapid degasification", the 3-ring-system arises preferably, whereas mostly 4 rings occur with the "slow" degasification. Besides, the percentage of substituted components of more than 50 % with the rapid degasification process is much higher than the percentage of only about 27 % with compounds obtained from the Fischer analysis.

It has been proved elsewhere (4) that these substances come from the resin in the coal. During the thermal treatment, this component is subject to reactions of decomposition and condensation. As mainly 3- and 4-ring-system could be found in these reactions which can be assigned to the base molecules of resins, the effects of secondary reactions can be small only. Due to the longer time of sojourn in the hot reaction chamber, the reactions of condensation of the tar obtained from the Fischer analysis are more progressed than for the tar obtained from the rapid degasification process. Therefore, the maximum of the ring distribution is with the 4-ring-system. Apart from the reaction of condensation, the low yield of alkylated aromates gives reason to assume stronger reactions of decomposition.

In order to investigate also the high amount of pitch in the tar obtained from the rapid degasification process, a structural analysis of the fractions obtained according to van Krevelen (6) was carried out. The median ring size calculated by this method has been plotted in fig. 16 in percentages. The maximum at the 10-ring-system shows that this is a much higher condensed system. This is indicated also by the median molecular weights between 140 and 554 found by experiment.

As such high molecular units, surely, are not released unchanged from the substance of coal, it can be assumed that the composition of the pitch is much more determined by secondary reactions than the composition of the liquid tar. This is due, above all, to the above mentioned reactions of condensation which, at a sufficiently long time of sojourn, progress to an extent that macromolecules develop which can no more be distilled and coked in the course of the degasification process even if temperature would be further increased. This can be easily derived from the following table (fig. 17). According to this table, 122.9 g of the pitch formed by the rapid degasification of 1 kg coal, has been changed with the degasification according to Fischer secondarily into 98.9 g of coke and 24 g of gaseous products.

The longer period of heat influence with the degasification process according to Fischer thus led to an intensified condensation and decomposition. The macromolecules developed during this process were coked. During the rapid degasification process, however, the reactions of condensation could be interrupted at an early stage by a quick discharge of the degasification products.

These results of investigation are in accordance with the assumption that tar is principally formed by the wax-resin-component of the coal. According to a calculation described by Kröger (5), it could be shown that this complex of substances is being obtained, with the rapid degasification process, nearly entirely in the form of tar, whereas the yield of products obtained by the Fischer analysis is far below the calculated values.

Thus, it is possible by means of the rapid degasification process to obtain this basic complex of the coal completely in the form of tar. It is true, that the degasification products are not portions of the original substances of coal but represent the primary bitumen developed during the primary decomposition of the coal. The primary bitumen is only a little changed by secondary reactions as they are tied up at an early stage by the quick discharge of the degasification products.

#### 4. Summary

By virtue of these results of investigation, the reactions during the rapid degasification of coal can be explained as follows:

Under the conditions of rapid degasification, notably the heating speed at the coal grain and the quick discharge of degasification products, primary bitumen is obtained which developed from the coal during the primary decomposition. During this process, the same regularities prevail as with any process of evaporation.

The substance, most of which are to be assigned to the wax-resin-component of the coal, can be completely evaporated by this process. To which extent the primary bitumen is being changed by secondary reactions, depends especially on the pre-set temperature of the heat carriers. The tests showed that the maximum of the tar yield is obtained at a temperature of about 600 °C.

After numerous analyses of the degasification products evaporated at this temperatures, it can be stated that the substances obtained are hardly decomposed by secondary reactions.

BIBLIOGRAPHY

- 1) Thesis to obtain the "venia legendi"  
by W. Peters, Technische Hochschule Aachen 1963
- 2) W. Peters, "Gas- und Wasserfach" 41 (1958)
- 3) C. Kröger, paper read at the International Coal  
Scientific Congress in Cheltenham, 1963
- 4) Dissertation by H. Bertling  
Technische Hochschule Aachen 1964
- 5) C. Kröger and H. Hortig, unpublished
- 6) D.W. van Krevelen  
"Brennstoff-Chemie" 34 S. 167 (1953)

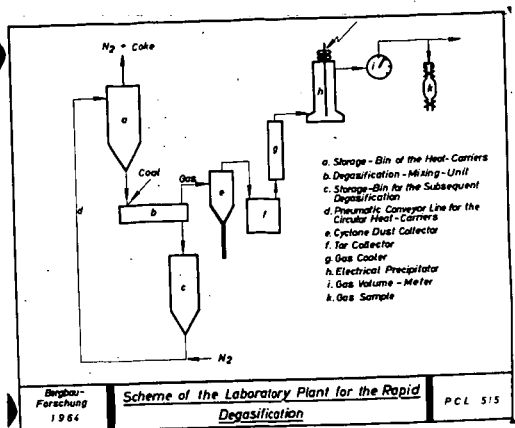


Figure 1

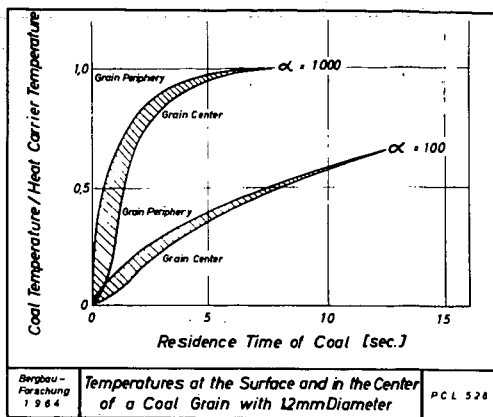


Figure 2

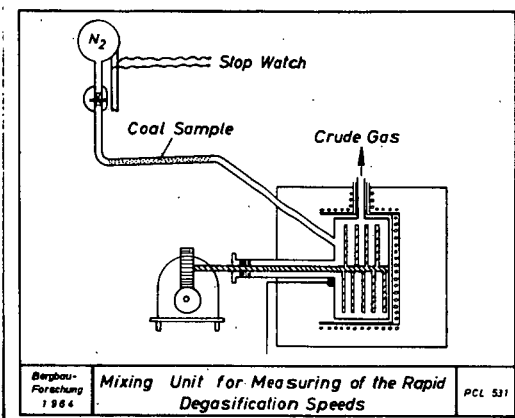


Figure 3

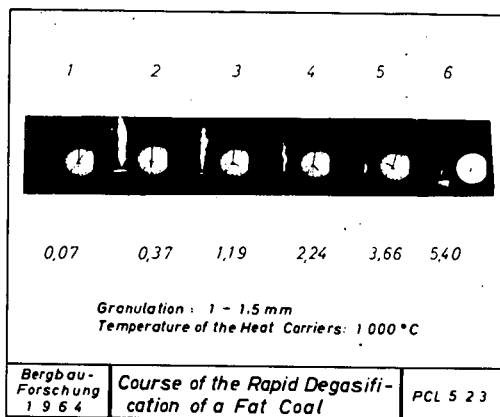


Figure 4

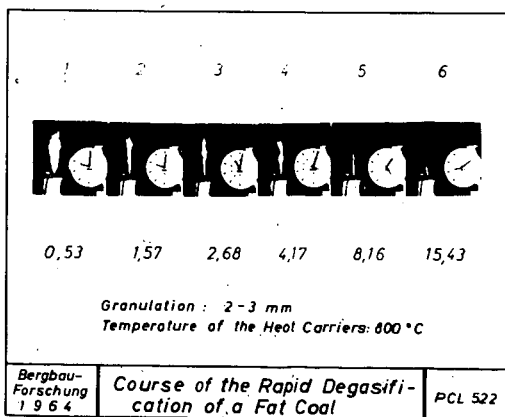


Figure 5

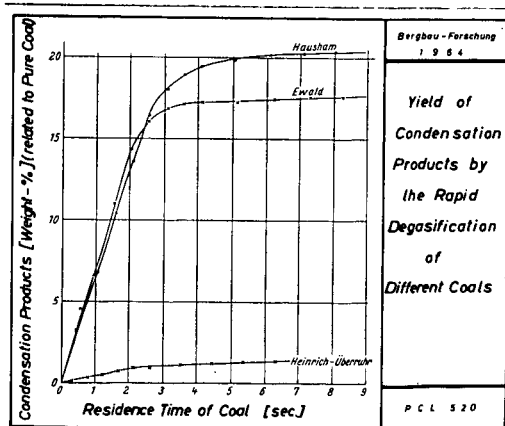


Figure 6

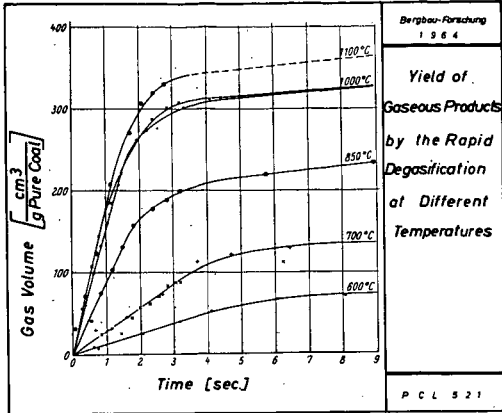


Figure 7

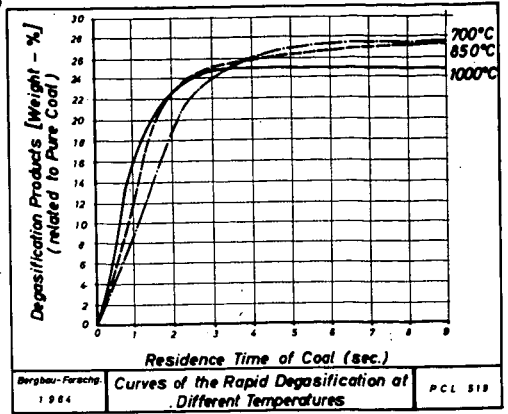


Figure 8

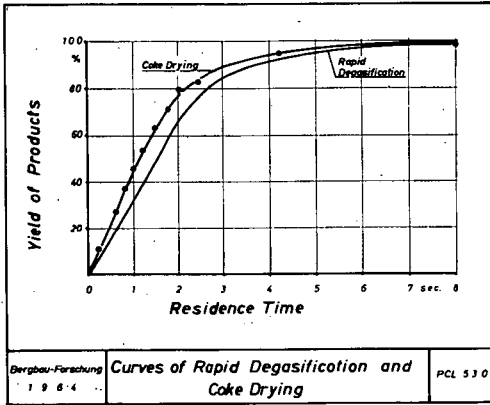


Figure 9

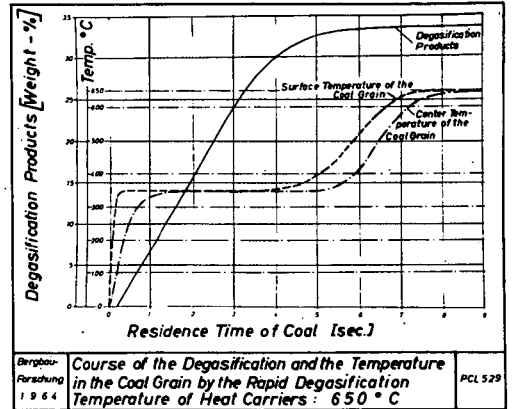


Figure 10

Product	Rapid Degasification	Carbonisation by Fischer	Ratio rapid/slow
Gas	7,25	8,44	0,86
Carbonisation Water	4,10	4,60	0,89
Tar + Carbonisation Benzine	26,40	14,82	1,78
Fraction I up to 140°C/1mmHg	6,50	8,02	0,81
Fraction II up to 140°C/1mmHg	2,87	2,71	1,06
Pitch	17,05	4,11	4,15
Carbonisation Coke	62,25	72,14	0,86

Values are given in Weight-Percent of the Pure Coal

Bergbau-Forschung  
1964

Yields of the Carbonisation Products

PCL 518

Figure 11

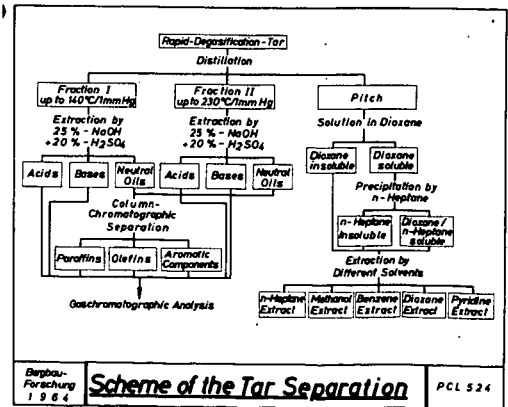


Figure 12

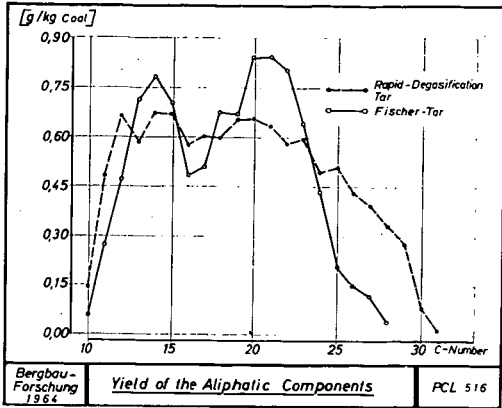


Figure 13

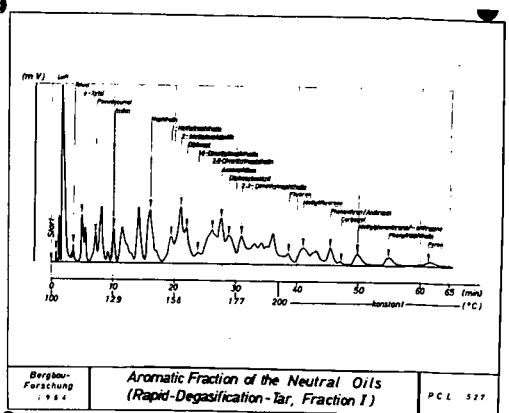


Figure 14

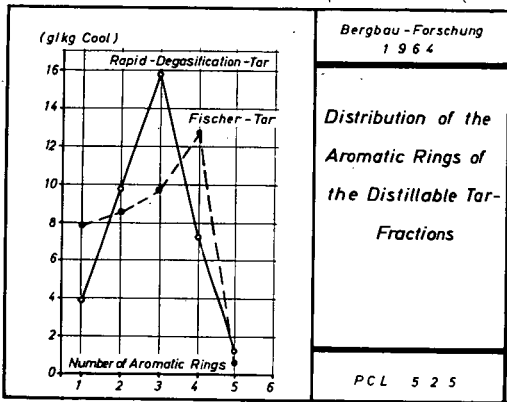


Figure 15

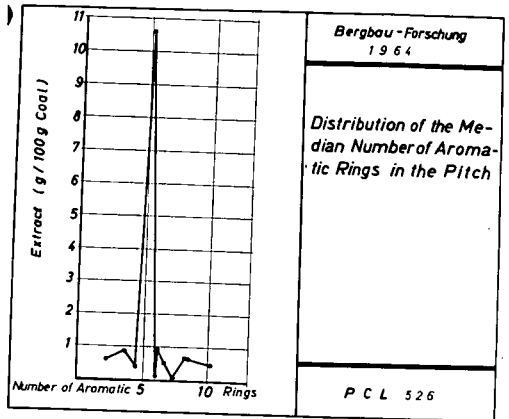


Figure 16

	Pitch	Coke	Sum
Rapid-Degasification-Tar	164,0	+ 622,5	= 786,5 g/kg Coal
Fischer-Tar	41,1	+ 721,4	= 762,5 g/kg Coal
Difference	122,9	99,9	24,0 g/kg Coal

Bergbau-Forschung 1964

**Yields of Pitch and Coke**

PCL 517

Figure 17

## Pyrolysis Kinetics of a Western High Volatile Coal

by Norbert Kertamus and George Richard Hill

Fuels Engineering Department, University of Utah

Although a number of time studies have been made on coal devolatilization, three principal models have been developed to explain the weight loss curves (1).

This study is an attempt to evaluate the mechanism of pyrolysis of a Western U. S. high volatile coal. The weight loss-time curves are interpreted according to the three classical models and as a simple unimolecular reaction. A new mechanism, more in accord with all the data, is proposed.

Several typical pyrolysis curves are plotted in Figure 1. In each instance the weighed coal sample was placed on a quartz spring, thermogravimetric furnace and the weight loss determined as a function of time. In the figure the ordinate is the fractional weight loss  $\Delta W/W_0$ . In the equations that follow, the following definitions apply.  $W_0$  = initial sample weight on an ash free basis.  $x = [W/W_0]$ .  $a = [W/W_0]_{\max}$  (at infinite time).  $Z = x/a$ .  $\Delta H^\ddagger$  = heat of activation.  $\Delta S^\ddagger$  = entropy of activation.  $E$  = activation energy (Arrhenius).  $R^\cdot$  is a reactive intermediate similar to van Krevelen's metaplast.  $B_i$  is the initial concentration of the  $i$ th species in Pitt's pyrolysis mechanism.

The general differential equation defining an  $n$ th order reaction is  $dx/dt = k(a-x)^n$  when  $k$  is the reaction rate constant: In a graph of  $\log(dx/dt)$  vs  $\log(a-x)$ , the slope of the line gives the value of  $n$ . In Figure 2, it is noted that the apparent order of the reaction varies from an initial 4.5 to unity. Obviously the decomposition is not by a simple unimolecular mechanism.

Earlier writers on coal pyrolysis kinetics (2-9) have assumed the basic reaction to be at least one unimolecular decomposition followed by other slower steps which become rate determining. Intuitively (10) bond breaking reactions of organic molecules would be unimolecular and the reaction rate proportional to the remaining undecomposed volatile producing material  $(a-x)$ . To determine whether a region of "first order" kinetics exists the  $\log(1-x/a)$  can be plotted versus time as in Figure 4. All of the curves are linear for the first 10-15 minutes and for times in excess of 200 minutes. If it is assumed that one or the other linear portion of the curve represents true first order rate dependence the slope of the line  $k_i$  (initial) or  $k_f$  (final) would be the rate constant.

The validity of the assumption can be checked by determining the magnitude of the heat and entropy of activation from Arrhenius or Eyring Absolute Reaction Rate plots of the log of the rate versus  $1/T$ . Figure 5 is an Arrhenius plot of  $k_f$  (fit by least squares). The activation energy is 2.4 kcal/mole. This value is considerably less than Pitzer's (11) value of 80 kcal for C-C bond decomposition. The entropy of activation which should be almost zero, is -50 e.u.

Arbitrarily selected times of 150 and 500 minutes were chosen to determine rate constants in Figure 6. The values of "a" determined by extrapolation to infinite time were less than the experimental values in all cases.

Arrhenius plots of the rate constants (Fig. 7) and Eyring plots, fit by the method of least squares give  $E = 10.6$  kcal/mole and  $\Delta H^\ddagger = 9$  kcal/mole respectively.

To a large extent the volatile matter is released from the coal during the first 10 to 30 minutes. The initial rate constants should be the most significant. The least square Arrhenius plot (Fig. 8) gives activation energy of 26.6 kcal/mole. The  $\Delta H^\ddagger$  is 24.8 kcal/mole and the entropy of activation is -10.1 e.u.

It has been suggested by Reed (12) that the intercept at infinite temperature of an activation energy plot may be a more reliable test of a unimolecular mechanism than the activation energy. Daniels (13) states that for most unimolecular bond breaking reactions the entropy of activation in an Eyring plot is almost zero since the activated complex is so much like the original reactants. This means that the frequency factor from an Arrhenius plot should be  $\sim 10^{13}$ . In each region of coal decomposition, initial, intermediate, or final it is seen that energy considerations rule out simple unimolecular decomposition as being rate determining.

Since a simple unimolecular kinetic model does not explain the weight loss curve, or even parts of it rigorously, three extensions have been advanced. The first of these might be roughly defined as the unimolecular approach. This assumes that the weight loss-time curve can be defined by a number of independent unimolecular decompositions. Various writers (2-5) have considered from one to five, although Pitt (6) derives the general case where a great many decompositions take part in the weight loss curve.

The second model was proposed by N. Berkowitz (7). In his representation, he assumes as coal is placed in a hot environment, that a rapid pyrolytic reaction occurs. This reaction produces a large volume of volatile material that is stuffed into the inter-porous space of the coal particle. He postulates a slow diffusion of volatile matter from the inter-porous volume as giving rise to the kinetics. He considers the initial decomposition as unimolecular and estimates appropriate rate constants to fit the slow diffusion controlled process.

The third approach is that defined by van Krevelen and co-workers (8, 9). They postulate a mathematical scheme to define not only the pyrolytic weight loss curves, but other coal pyrolytic phenomenon. This approach assumes that the decomposition of a bituminous coal can be distinguished into three successive reactions; formation of an unstable intermediate phase (metaplast) which is (partly) responsible for the plastification and transformation of this intermediate into semi-coke and finally into coke with three individual rate constants.

In addition to the assumption of one unimolecular decomposition the following assumptions are made in the three models. Case I, Berkowitz; (1) an undefinable equation of state of the product gases in the pore structures, (2) a diffusionally controlled rate loss which can not be treated rigorously, and (3) an assumed time of completion of pyrolysis which determines the activation energy. Case II, Pitt; (1) a value for the frequency factor "a", (2) the initial concentration of all volatile species is the same, (3) a large number of independent unimolecular decompositions of different activation energies. Case III, van Krevelen; (1) an initial depolymerization to unstable intermediate (metaplast) which decomposes to give gas, (2) equality of rate constants for formation and decomposition of metaplast and (3) the occurrence of a second (semi-coke) decomposition which produces additional gas.

Berkowitz found that significant differences existed between the weight loss-time curves for a -10 to +28 mesh coal and a -60 mesh coal. In our laboratory representative samples of -40 to +60 and -200 to +250 mesh coals were pyrolyzed. The weight loss time curves were identical. It is possible that heat distribution and thermal conductivity may be important with larger particle sizes.

In Pitt's model (Case II) it is assumed that the independently decomposing coal molecules have a distribution of activation energies for decomposition between E and E+dE. The number of undecomposed molecules remaining after some time t is given by the equation:

$$n_t = n_0 \int_0^{\infty} f(E) e^{-At} e^{-E/RT} dE$$

Mathematically assuming an energy distribution from zero to infinity and plotting a range of activation energies, the data give a broad maximum in the distribution curve in the energy range 50 to 55 kcal/mole.

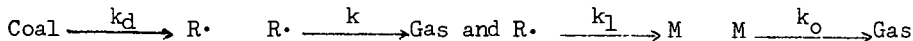
An alternate treatment using Pitt's model gives the equation:

$$x = \sum_{i=1}^j B_i - \sum_{i=1}^j B_i e^{-k_i t}$$

where j decompositions occur. Using Pitt's assumptions of equal initial concentration of volatile matter a curve analogous to Figure 4 can be constructed. From  $k_1$  for our run 17/R (682°K), an activation energy of 51.6 kcal/mole is obtained. From  $k_2$  the activation energy is 55.2 kcal/mole. For run 24/R (770°K), the respective values are 55.2 and 61.4 kcal/mole. The one disadvantage of Pitt's model is the assumption of equal initial concentration of all the volatile species. If the species pyrolyzed were large a more tenable assumption is equal  $k_i$ 's (equal activation energies). If so, the above equation reduces to simple first order kinetics and the initial concentration of  $B_1$  is unimportant.

In van Krevelen's model (Case III), the assumption that the rate constants  $k_1$  and  $k_2$  are equal and that one half of the gas evolved is from each of two steps does not result in a good fit of the experimental curve, according to Pitt (6). The problem can be solved by modifying

slightly the van Krevelen model to permit an estimation of the gas produced in each step. Mathematically the final expression is the same as the integrated form for a consecutive reaction except that the fraction of gas produced is defined by a ratio of rate constants. The modified model consists of the following steps:



and  $M \xrightarrow{k_2} \text{Coke}$ , where  $R \cdot$  is a reactive intermediate similar to van Krevelen's metaplast and  $M$  is equivalent to semi-coke; a steady state is assumed for  $R \cdot$ . By making certain simple approximations  $k_d$  can be determined from Figure 4. From the points of an Arrhenius plot, the variation in  $k_d$  with temperature gives the least square equation of  $\log_e(k_d) = -11.1/T + 12.7$  which gives an activation energy of 22.1 kcal/mole and a frequency factor of  $3.3 \times 10^5$ . If  $k_o \cong k_2$ , then  $k_o + k_2$  corresponds roughly to  $k_3$  of the van Krevelen model or  $k_f$  discussed previously. This means that the activation energy for the second step is very small ( $\sim 2.4$  kcal/mole). Pyrolysis could not account for the second step.

A new model which fits the experimental data involves the following two assumptions. The decomposition follows a simple first order rate law; the decomposition exhibits first order dependence upon the number of surface sites ( $S$ :) available at any time.

This model is based upon the earlier worker's observations and data cited and upon additional experimental data. In the pyrolyses conducted in this laboratory, the calculated residence time of volatile products is 9.3 seconds. Analyses of the nitrogen carrier gas stream utilizing an F and M model 720 Chromatograph and a Consolidated Electrodynamics Model 21-620 Mass Spectrometer showed no detectable low molecular weight hydrocarbons. The usual distillate was a tar mist. The product gases were frozen out in a liquid nitrogen cooled trap and analyzed. The total hydrocarbon and carbon dioxide concentration was determined to be 1.8% with  $\text{CH}_4$ ,  $\text{C}_2\text{H}_6$ ,  $\text{C}_3\text{H}_8$ ,  $\text{C}_4\text{-C}_6$  and higher hydrocarbons being present in the ratio 80:60:62:129. The gas analysis indicates that in addition to the  $\text{CO}_2$  and  $\text{H}_2\text{O}$  produced, the principle primary decomposition products were of high molecular weight. The light gases found may be due to secondary reactions. These analytical data strongly suggest that large molecules in the coal are fragmented to produce the primary products, probably in a single bond breaking, unimolecular reaction.

The second postulate involves a first order dependence upon surface sites; the pyrolysis reaction would be written  $S: + (1-Z) \xrightarrow{k_o} Z + S:$ . The differential equation defining the rate is:  $dZ/dT = k_o (1-Z)(S:)$ . The second postulate requires that  $d(S:)/dZ = -b(S:)$  which on integration gives  $(S:) = e^{-bZ}$ . Substituting one obtains  $dZ/dT = k_o(1-Z)e^{-bZ}$ . From Eyring's rate theory (14) the rate constant  $k_o' = \frac{kT}{e} \frac{-\Delta F^\ddagger}{RT}$  where  $k$  is Boltzmann's constant and  $h$  is Planck's constant. <sup>h</sup>If the free energy of activation varies in a linear manner with the amount pyrolyzed,  $\Delta F^\ddagger = \Delta F_o^\ddagger + qZ$ . If  $q$  is a function of the entropy of activation only, i.e. of the relative complexity of the activated complex to the undecomposed

reactant, the temperature dependence of entropy cancels when this equation is substituted into Eyring's equation. If this is substituted into a unimolecular rate equation, the equation  $dZ/dT = k_0 (1-Z)e^{-bZ}$  results where  $b$  is an entropy dependent term or  $dZ/dT = (kT/h)e^{-\Delta F^\ddagger/RT}(1-Z)e^{-bZ}$ . A plot of  $\log \frac{dZ/dT}{T(1-Z)}$  versus  $Z$  should give a straight line of slope  $b/2.3$ .

If the model is correct the slope should not be temperature dependent. In Figure 9 the appropriate plots are represented from 0 to 75% completion. As can be seen, excellent point linearity and slope agreement at different temperatures, are found, especially for the lower temperature curves.

At the lower temperatures linearity is observed for 90% of the pyrolysis. At higher temperatures a departure from linearity occurs at 75% completion. This might indicate a break down of the coal surface at higher temperature (6) or an increase in secondary reactions.

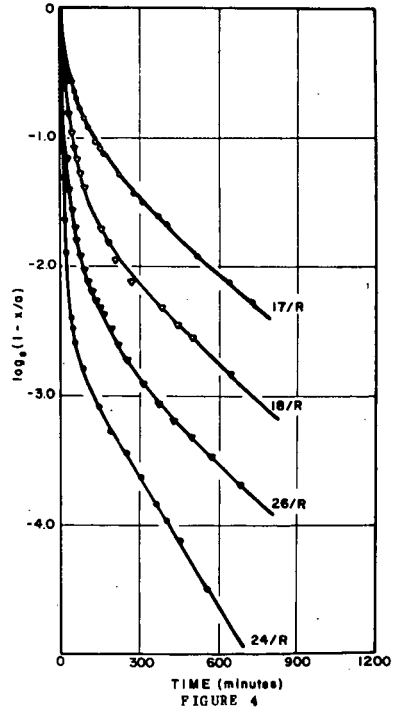
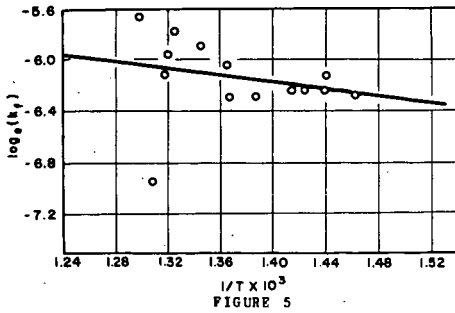
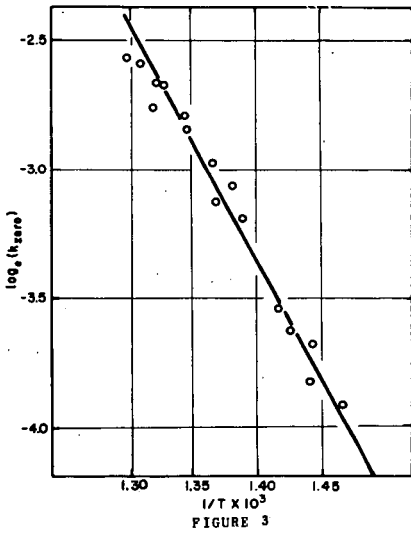
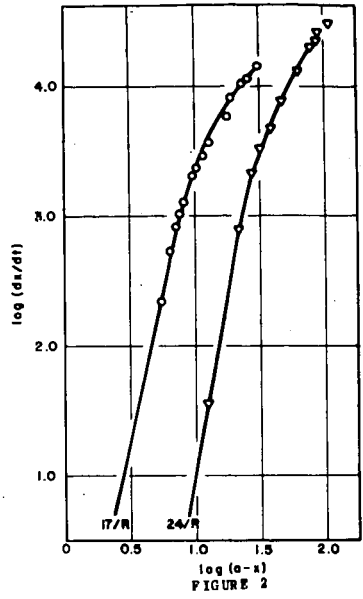
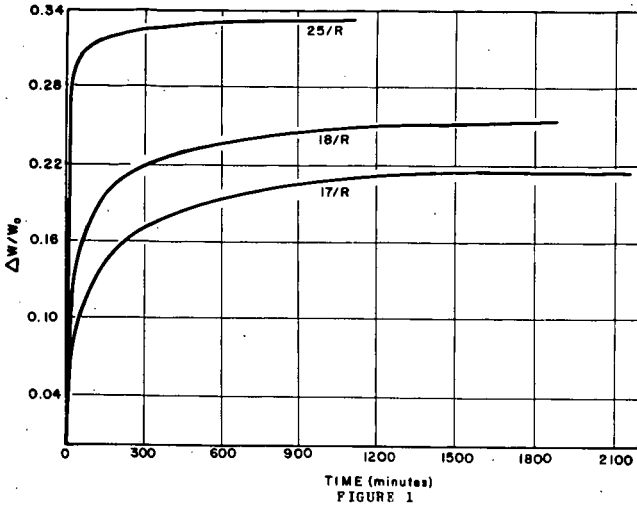
From the intercepts of Figure 9, Figure 10 was constructed. The heat of activation was found to be 55.8 kcal/mole. The intercept is 13.51. This corresponds to a very small positive entropy of activation or to a frequency factor of about  $10^{14}$ , a value to be expected from theoretical considerations. The activation energy is of the right magnitude for bond breaking reactions.

Van Krevelen's observation is most germane: "Any kinetic interpretation is much too simple to provide a complete description of the complicated decomposition process; therefore, it is more correct to regard it as a mathematical model which does not pretend to be more than an aid for obtaining a semi-quantitative description of the experimental results."

Appreciation is expressed to the Office of Coal Research which, with the State of Utah co-sponsors this research. We are grateful also for the advice and counsel given by Dr. R. I. Reed and Dr. Larry L. Anderson in the interpretation of the data.

## BIBLIOGRAPHY

1. W. I. Jones, *J. Inst. Fuel*, 37, 3 (1964), Abstr. in "Fuel Abst. and Curr. Titles" 139 (1964) pp 136.
2. W. Fuchs, and A. G. Sandhoff, "*Ind. Eng. Chem.*", 34, 567 (1942).
3. E. A. Shapatina, V. V. Kalyuzhny, and Z. F. Chukhanov, "*Dokl. Akad. Nauk. S. S. S. R.*", 72, 869 (1950).
4. H. N. Stone, J. D. Batchelor, and H. F. Johnstone, "*Ind. Eng. Chem.*" 46, 274 (1954).
5. S. F. Tschuchanow, "*Brennst. Chemie.*", 37, 234 (1956).
6. G. J. Pitt, "*Fuel*", London, 41, 237 (1962).
7. N. Berkowitz, "*Fuel*", London, 39, 47 (1960).
8. H. A. G. Chérmin, and D. W. van Krevelen, "*Fuel*", London 36, 85 (1957).
9. D. W. van Krevelen, "*Coal*", Elsevier, New York (1961), pp 287.
10. Ibid. pp 289.
11. Pitzer, "*Quantum Chem.*", Prentice-Hall, New York (1953) pp 170.
12. Suggestion from Dr. R. I. Reed, Univer. Glasgow.
13. F. Daniels, and A. Alberty, "*Physical Chemistry*", John Wiley and Sons, Inc., New York, (1955) pp 353.
14. H. Eyring, "*Theory of Rate Processes*", McGraw-Hill, New York (1941), pp 14.



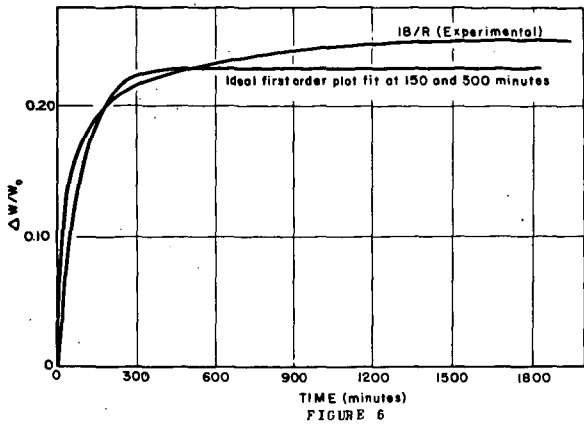


FIGURE 6

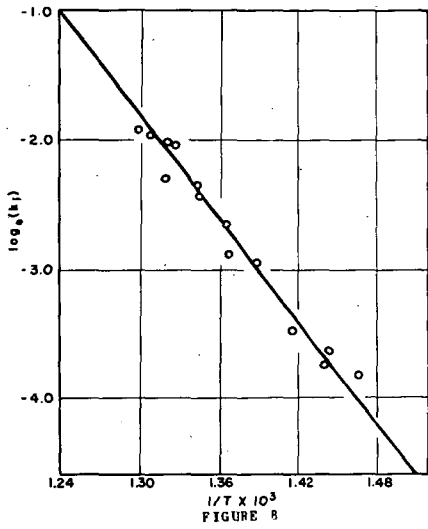


FIGURE 8

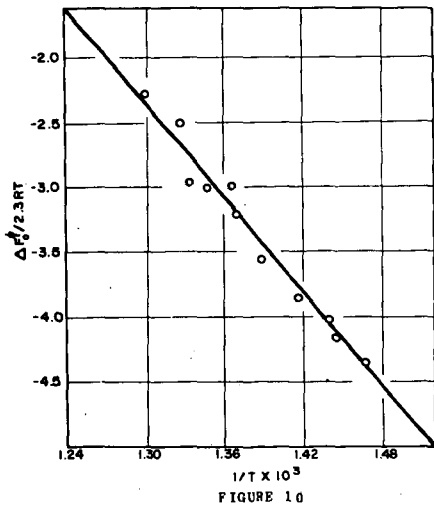


FIGURE 10

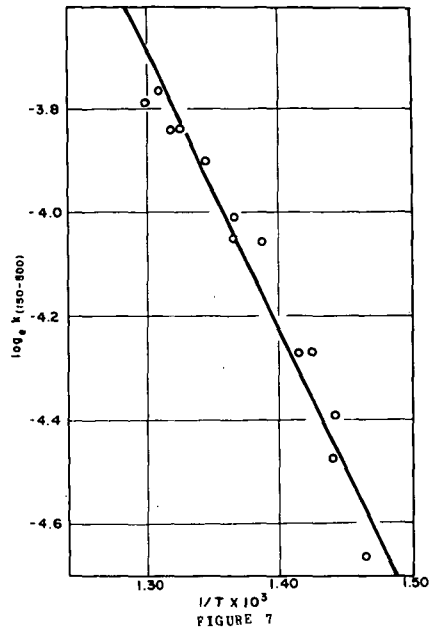


FIGURE 7

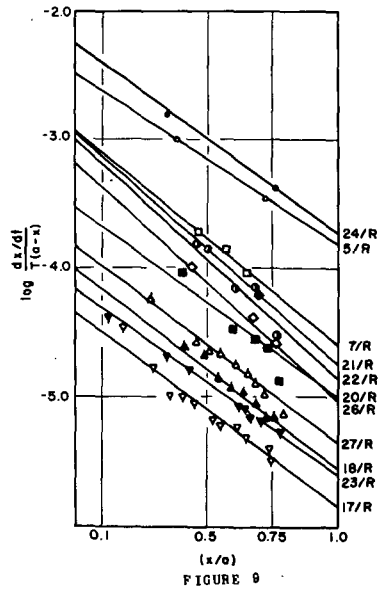


FIGURE 9

Presented Before the Division of Fuel Chemistry  
American Chemical Society  
Chicago, Ill., August 30 - September 4, 1964

### BOND RUPTURE PROCESSES IN COAL PYROLYSIS

H.M. Brown and N. Berkowitz  
Research Council of Alberta  
Edmonton, Canada

The purpose of this paper is to report some preliminary findings of a study which, while primarily concerned with the kinetics of carbon crystallite growth at  $T > 650^{\circ}\text{C}$ , is also beginning to delineate a major route by which unpaired electrons (i.e. so-called "free radicals") form in coal chars. The results are of particular interest inasmuch as they demonstrate that skeletal C-O and C-C bond rupture processes are not - as is commonly thought - confined to the temperature region between  $400^{\circ}$  and  $650^{\circ}\text{C}$  (in which tar forms by elimination of naphthenic structures).

#### Experimental

Experimentally, the investigations here under discussion centre on (i) heat treatment of a coal sample in vacuo at a series of pre-selected temperatures; (ii) rapid quenching after such heat treatment; and (iii) measurement of the magnetic mass susceptibility and pure diamagnetic susceptibility of the quenched residue.

For the experiments so far completed, cleaned (-65 +200 mesh) samples of a low volatile bituminous coal (ash <0.5%; Ref. 1) were chosen. These were vacuum-carbonized at  $<10^{-5}$  mm Hg and  $6^{\circ}\text{C}/\text{min.}$ , held at the selected final temperatures for periods varying between <5 seconds and 0.5 hr., and then rapidly cooled by external air jets. Figure 1 exemplifies a typical heating and quenching program. When the carbonized residues had attained room temperature, the furnace assembly was flooded with purified nitrogen, and the residues removed and transferred to a continuously evacuated desiccator.

Immediately prior to their use in the magnetic balance (cf. below), and always within less than 24 hrs. after preparation, samples were rapidly filled into the upper chamber of a compensated specimen holder (cf. Detail B, Figure 2) and the loaded holder re-evacuated in order to allow proper settling of the char. After 30 minutes' pumping, the holder was again flooded with purified nitrogen, removed, weighed and inserted into the vacuum chamber of the specially constructed Gouy-type balance. Sample weights were usually of the order of 1.0 gm.

The assembly in which magnetic susceptibilities were measured is diagrammatically shown in Figure 2. It consists of (i) a custom-made quartz fibre balance\* (Detail A, Figure 2) suspended in a shielded vacuum chamber V; (ii) a specimen tube suspension S extending from V into an evacuated tube fitted with the necessary temperature control and measuring equipment; and (iii) a Cambridge electromagnet capable of creating fields of up to 16,000 gauss across a one-inch gap between conical pole pieces. Balance readings were taken with a cathetometer M after major weight changes had been compensated by adjusting the current to a carefully calibrated solenoid coil C. Calibration of the balance and magnet at current densities from ca. 2 to 15 amp. was carried out with pure specimens of rhombic sulphur for which  $\chi = -0.490 \times 10^{-6}$  cgs units per gm. over the temperature range from 25° to -196°C.

Measurements of  $\chi$  with coal chars were made at 25°C, while  $\chi_{\text{dia}}$  was obtained from plots of  $\chi$  vs.  $1/T$ , i.e. by assuming Curie's Law to be operative and extrapolating  $\chi$  vs.  $1/T$  to zero. To permit construction of the necessary graphs, determinations of  $\chi$  were also made at -78.5°C (the sublimation temperature of CO<sub>2</sub>) and at -196°C (the boiling point of nitrogen)\*\*. The linearity of the resultant  $\chi$  vs.  $1/T$  plots, and the accuracy with which it proved possible to estimate  $\chi_{\text{dia}}$  from these plots, can be gauged from Figure 3.

Individual values of  $\chi$  cited below represent averages of 5 determinations which were, in turn, each replicated by measurements at several different field strengths in the range 6000 - 14000 gauss. Maximum deviation within any one set of 5 determinations was always less than  $0.005 \times 10^{-6}$  cgs gm<sup>-1</sup>.

Experimental data so far available are summarized in Figures 4 and 5. Figure 4 shows the variation of  $\chi$  and  $\chi_{\text{dia}}$  with heat treatment time  $t_H$  at 500°, 600° and 750°C, while Figure 5 shows the corresponding variation of  $\Delta\chi$ , i.e. of  $\chi_{\text{dia}} - \chi_{25^\circ}$ . On the assumption that the entire paramagnetic component of  $\chi$  is associated with unpaired electrons on carbon atoms, i.e. that residual mineral matter makes no significant contribution to  $\chi$ ,  $\Delta\chi$  affords a direct measure of the "free radical" concentration.

#### Comments on Procedure

The temperatures at which coal samples were pyrolyzed in the present series of experiments were selected to correspond to particular points in the behaviour pattern of equilibrated specimens, i.e. of specimens which were, in each case,

---

\* Manufactured by Worden Laboratories, Houston. The instrument used by us had a total capacity of better than 10 gms. and a sensitivity of 5 micrograms at full load.

\*\* These temperatures were checked with a calibrated chromel/p-alumel thermocouple.

held at the final temperature for 2 hr (1). The 500°C point thus corresponds to the onset of active thermal decomposition (as evidenced by a sharp downward turn of the  $\chi/T$  plot, by increasing rates of weight loss, and by an increasing d-spacing and decreasing  $\bar{c}$ -dimension of the crystallite). The 600°C point corresponds to the near-end of active decomposition. And at 750°C, marked growth of the carbon lamellae (as evidenced by large increases in their  $\bar{a}$ -dimension) is in progress.

This dependence of behaviour on temperature - and the fact that heat treatment temperatures in the present series of experiments were approached gradually - imposes an important limitation on the data shown in Figure 4. Since transient processes at temperatures below the final heat treatment temperature will take place while the coal sample approaches this final temperature, both the form and location of individual  $\chi$  vs.  $t_H$  graphs within the coordinate system must be seen as extensions of changes which commence at "negative" times (i.e. to the left of the  $\chi$ -coordinate in Figure 4) and at correspondingly higher  $\chi$  values than the nominal initial values shown in the diagram at  $t_H = 0$ .

This recognition, which accounts for the inverse relationship between the "initial" susceptibility and heat treatment temperature and which also explains the fact that the  $\chi$  vs  $t_H$  curve at 750°C passes through so much shallower a minimum than the 600°C curve, necessarily complicates a kinetic interpretation of the data\*. But it is pertinent to note here that the problem is essentially unavoidable - that it arises from the nature of coal per se. Theoretically, the best alternative to the heating schedule chosen in this study would be shock-heating, i.e. an approach to the final temperature in minimum time. However, with diffusion control over disengagement of volatile pyrolytic products (2, 3), such a course - followed by short heat treatment periods - would produce chars containing an indeterminate residue of undischarged pyrolytic matter making an indeterminate contribution to  $\chi$ . The measured value of  $\chi$  would here, in other words, be meaningless.

#### Discussion

So far as we are aware, only H. Honda (4) has published data on the variation of  $\chi$  with  $t_H$ . He does not, however, seem to have concerned himself with the detailed form of this variation - Figure 4 of his paper (4) shows results for  $t_H = 15, 30, 60$  and 120 minutes only - and while the text of the paper refers to "diamagnetic mass susceptibility", it is clear that the reported values refer to the uncorrected mass susceptibility, i.e. to  $\chi$  rather than  $\chi_{dia}$ . For these reasons (and also because of the uncertainty attaching to the conditions under which Honda pyrolyzed his samples), the results summarized in Figures 4 and 5 cannot be viewed against an established background. But subject to the recognition that they represent initial data (and bearing in mind the limitations referred to above), they nevertheless allow of some important tentative conclusions.

---

\*Efforts to develop graphical methods by which the necessary corrections can be interpolated seem to be meeting with some success. They will be reported in due course.

In principle, a fall in  $\chi$  may be associated with either (a) the formation of unpaired electrons by any mechanism, or (b) a decrease in the size of the average aromatic area of the statistical structure unit (or lamella). (b) itself may or may not be accompanied by formation of unpaired electrons and would, if not so accompanied, cause a fall in  $\chi$  by reducing the so-called London contribution to the observed mass susceptibility. Conversely, a rise in  $\chi$  can be attributed to either a removal of unpaired electrons from the system (by  $\sigma - \sigma$  or  $\sigma - \pi$  coupling) or simple growth of aromatic lamellae. The fact that variations of  $\chi$  and  $\chi_{dia}$  with  $t_H$  follow virtually parallel courses (which are only displaced with respect to each other along the  $\chi$  - coordinate), i.e. the relative insensitivity of  $\Delta\chi$  to changes in  $t_H$  (cf. Figure 5), is in these circumstances highly significant. Bearing in mind transient processes at "negative" time values (cf. above) and noting that  $\Delta\chi$  itself increases with the heat treatment temperature, it implies that, for short heat treatment periods at least, a modified (b) operates, i.e. that  $\chi$  and  $\chi_{dia}$  fall as a result of lamellar size reductions and simultaneous formation of unpaired electrons, but that unpaired electrons are subsequently "frozen" into the structure without actually being eliminated by pairing. In view of Figure 5, the rise in  $\chi$  and  $\chi_{dia}$  must clearly be ascribed to lamellar growth only.

The corollary of this conclusion is, of course, that unpaired electrons are created by rupture of  $\sigma$  - bonds, i.e. by rupture of C-C and/or C-O lattice bonds.

It might usefully be observed that such an identification is in general harmony with certain other findings. It is, for example, qualitatively supported by Mrozowski and Andrew's observation (5) that the "free radical" concentrations in polycrystalline graphitized carbons can be greatly increased by prolonged grinding in inert atmospheres (or in vacuo). And it also lends support to the suggestion (6) that ultimate elimination of unpaired electrons by extended heating at  $T > 650^\circ\text{C}$  can be associated with a change in the semiconductor mechanism at  $650^\circ - 700^\circ\text{C}$  - from excess electron to excess "hole" conduction (7) - by postulating a progressive  $\sigma - \pi$  electron interaction.

But more immediate interest attaches to the fact that conclusions derived from the data contained in Figures 4 and 5 bear directly on descriptions of the overall coal pyrolysis process.

The gross features of this process are conventionally described in terms of a 3-stage sequence which, successively, involves (i) elimination of peripheral functional groups at  $T < 400^\circ\text{C}$ ; (ii) skeletal breakdown and reorganization between  $\sim 400^\circ$  and  $650^\circ\text{C}$ ; and (iii) progressive growth and ordering of aromatic lamellae at  $T > 650^\circ\text{C}$ . It is, in other words, supposed that only the second stage involves more than peripheral reactions\*.

---

\*A recent study concerned with the kinetics of hydrogen formation at temperatures in the range  $600^\circ - 800^\circ\text{C}$  has led to the conclusion (9) that rates of H-elimination are controlled by lamellar mobility and that abstraction of hydrogen from positions at the peripheries of the lamellae is the immediate precursor of crystallite growth.

In the light of evidence now available, this view requires some revision. In particular, it must now be concluded that skeletal reorganization can extend well into the third stage and that it is here connected with the elimination of residual oxygen from coal chars.

Investigations into the kinetics of water formation at temperatures in the range 650°-850°C (8) have shown that all (or almost all) oxygen lost in this range ultimately appears as water; that the reactions leading to formation of water (which must itself be regarded as a secondary or tertiary product) are all relatively fast; and that kinetic control over water formation is exerted by bond rupture processes (which, insofar as they involve non-quinoid oxygen, must partially disrupt lamellae and result in a fall in  $\%$  even if no unpaired electrons are formed in the process). If it is now borne in mind that elemental hydrogen (deriving from peripheral H-atom abstraction) and water (at least partly deriving from carbonization of ether-structures and heterocyclic O-bearing aromatics) are the only products actually formed by decomposition of coal at  $T > 650^\circ\text{C}^*$ , association of reductions in  $\%$  (and  $\%_{\text{dia}}$ ) with oxygen-breakout at these temperatures is virtually inescapable. The fact that oxygen-breakout is, as already noted, fairly fast (and generally 90% complete within 10 minutes from the start of reaction; Ref. 8) and that  $\%$  and  $\%_{\text{dia}}$  undergo rapid changes at correspondingly low values of  $t_{\text{H}}$ , may be seen as additional support for such a view.

It is, however, in this connection of interest to observe that measurements of rates of water formation between 650° and 850°C indicate sequential oxygen removal by at least two reactions. If the association between oxygen elimination and changes in  $\%$  here suggested is accepted, plots of  $\%$  vs.  $t_{\text{H}}$  would therefore be expected to pass through at least two corresponding minima - with the second tentatively placed at  $t_{\text{H}} \approx 7-8$  minutes. This point is currently being checked.

#### References

1. P.A. Cavell and N. Berkowitz; *Fuel*, 39 (1960), 401.
2. N. Berkowitz; *Fuel*, 39 (1960), 47.
3. H. Luther and S. Traustel; *Brennstoff Chemie*, 44 (1963), 65.
4. H. Honda; *Proc. 3rd Conf. on Carbon* (Pergamon Press, 1957), 159.
5. S. Mrozowski and J.F. Andrew; *Proc. 4th Conf. on Carbon* (Pergamon Press, 1960), 207.
6. N. Berkowitz, P.A. Cavell and R.M. Eloffson; *Fuel*, 40 (1961), 279.
7. E.A. Kmetko; *Phys. Rev.*, 82 (1951), 456.
8. Lynne F. Neufeld and N. Berkowitz; *Fuel*, 43 (1964), May.
9. N. Berkowitz and W. den Hertog; *Fuel*, 41 (1962), 507.

---

\*The (relatively small) quantities of methane and oxides of carbon disengaged from coal chars at these temperatures appear to be formed by autohydrogenation and steam gasification of the chars (8) and therefore to be basically unrelated to the decomposition of coal per se.

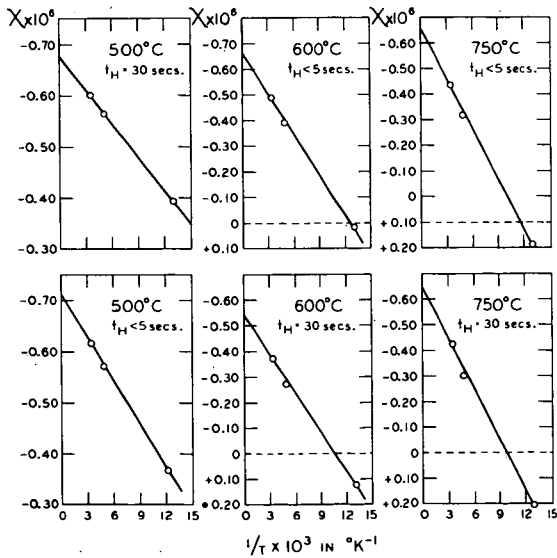
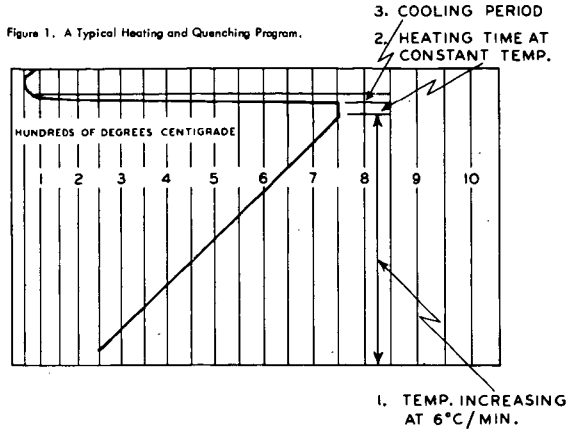


Figure 3. Some Typical Plots of  $X_c$  vs.  $1/T$ . ( $X_{c,0} = X_c$  when  $1/T = 0$ .)

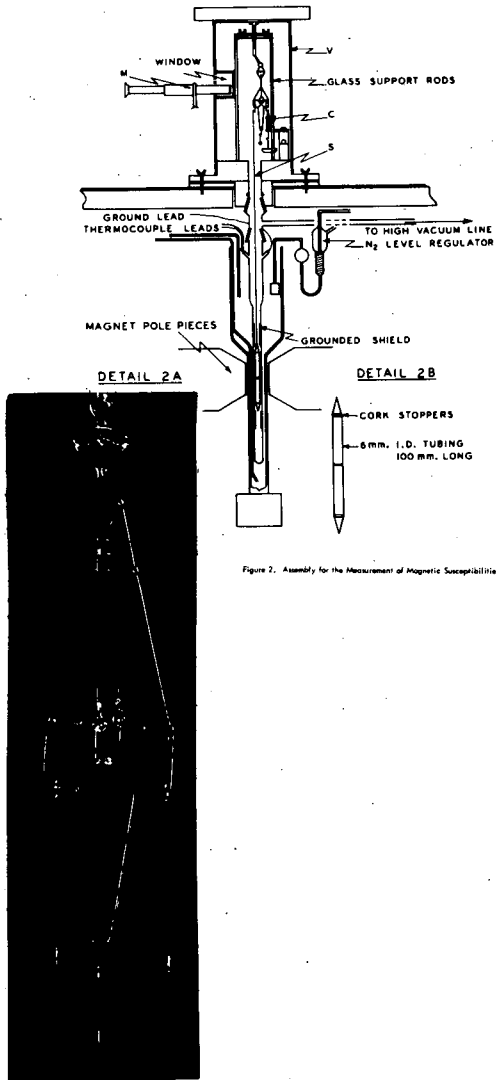


Figure 2. Assembly for the Measurement of Magnetic Susceptibilities.

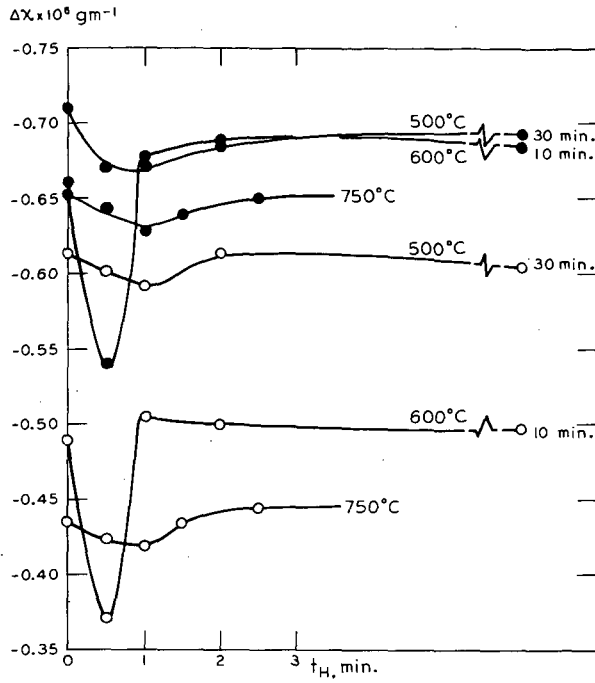


Figure 4. The Variation of Magnetic Susceptibility with Heat Treatment Time  $t_H$ . (Full circles denote  $\chi_{dip}$ ; empty circles  $\chi$ .)

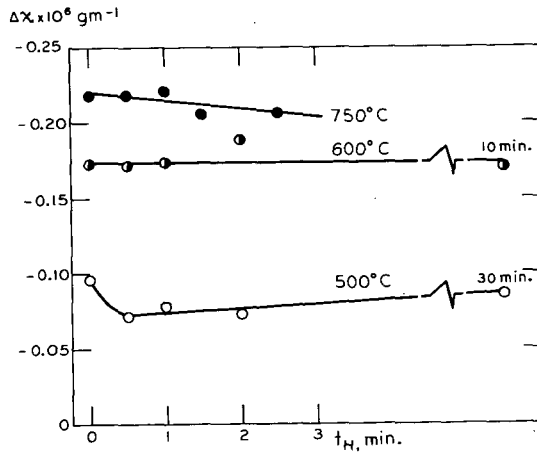


Figure 5. The Variation of  $\chi$  with  $t_H$ .

Presented Before the Division of Fuel Chemistry  
American Chemical Society  
Chicago, Ill., August 30 - September 4, 1964

## THE USE OF THE MICROSAMPLE STRIP FURNACE IN COAL RESEARCH

E. Rau and J. A. Robertson

FMC Corp, Chemical Research and Development Center, Princeton, N. J.

### INTRODUCTION

The pyrolysis and carbonization behavior of coal has been studied intensively since the industrial revolution. Many techniques have been developed, but most require relatively large quantities of material; they are time-consuming and expensive to perform. The Microsample Strip Furnace described in this paper uses only a few milligrams of material and evaluations can be carried out in a matter of minutes. Techniques have been developed to study coking behavior on heating, weight loss on heating, the nature of the product evolved during the heating sequence, and ash distribution and properties.

These techniques generally yield qualitative information. The observations assist in the interpretation of the phenomena involved, and serve as a guide in setting up more quantitatively precise experiments. Qualitative differences in pyrolysis behavior can readily be observed and problems such as sample heterogeneity readily detected.

### APPARATUS

The Microsample Strip Furnace (or often called simply a hot-stage microscope) has been described in previous publications<sup>1</sup>. The model available at Princeton (Figure 1) is similar except that manual temperature controls are employed. Essentially, the unit consists of an enclosed microstrip furnace and swing-out, stereoscopic, variable power microscope. The microscope is fitted with a vertical illuminator, so that an optical pyrometer can be used to

---

<sup>1</sup>A. R. Conroy and J. A. Robertson, "Controlled Atmosphere Hot Stage for Microscopic Observations of Glass Melting Phenomena. Part I," *The Glass Industry*, 44, 76-9, 139-43 (1963).

measure the temperature of the hot strip. The furnace consists of a strip of platinum, molybdenum or other refractory metal held between two water-cooled electrodes. Power for resistance heating is supplied by a 4-volt, 100 ampere step-down transformer. The temperature can be raised slowly by manually adjusting the autotransformers or quickly by presetting the autotransformers and then snapping the switch on. The furnace assembly is covered with an envelope consisting of a piece of three-inch Pyrex pipe to the top of which is sealed a plane piece of optical quartz. The sample is viewed through the quartz plate, and since a long working distance objective is used at 7-30 X total magnification, cooling of the microscope is not required. The enclosed area can be flushed with any gas desired. This gas is introduced so as to sweep across the quartz window and thus prevent fogging by condensibles.

The temperatures that can be reached depend mainly on the resistivity and thickness of the strip material. We used 3-5 mil thick, 8 mm wide platinum or molybdenum in this study. The maximum temperature obtainable is limited by the melting point of the material, 3190°F for platinum and 4750°F for molybdenum.

#### PRELIMINARY OBSERVATIONS

Microscopically, coal is a heterogeneous composite of macerals. It is desirable to make a preliminary microscopic observation to determine the minimum particle size which is representative of the material under study. If the heterogeneity is large with respect to the size of the particle preferred for microscopic study, then the various components can be separated and studied individually. The final conclusions are then weighted accordingly. Or, a composite of fine particles can be studied as representative of the total composition. If the heterogeneity is of fine structure, so that individual particles of the desired size are representative, the sample can be considered as homogeneous for the tests described. The latter was the case in the coals used in this study.

The individual behavior of the various macerals on heating can be observed, if desired, by heating a thin section, in which the macerals have been identified, in direct contact with the strip. The thin section must be carefully cleaned to remove the cement used in its preparation. Also, the cement-solvent system chosen must not modify the section.

Slow oxidation of the coal particle in air often brings out the structural discontinuities which are difficult to see in the untreated particle. This oxidation can be carried all the way to the final ash skeleton, showing the distribution of ash-forming minerals.

A few minutes spent in this preliminary examination will permit the selection of more meaningful samples for subsequent studies, and will provide a better understanding of the phenomena to be observed later.

### CARBONIZATION OF COAL

Different ranks of coal show great differences in behavior under fixed heating conditions, and coals of the same rank show different behaviors if heating rates or atmospheres are varied. For example, it can be readily seen that a lignite which undergoes excessive particulate shrinkage, through loss of gas only, can be processed in equipment that would be completely unable to handle a coking coal. Observations of this nature before designing of laboratory or pilot set-ups reduce later problems. The time required for such observations is minimal.

Observations made before designing laboratory equipment should be followed by periodic examination of intermediates and products prepared in laboratory, pilot and shake-down plant runs. Often a product characteristic not apparent, except by microscopic study, can indicate needed process changes. The anomaly can often be duplicated under the microscope and the remedy checked for effectiveness before being applied on a larger scale.

Experiments in which heating rate was varied have been especially informative. The hot stage offers a much wider range of available heating rates than most pyrolysis equipment and so allows one to determine what might happen beyond the limits of the larger equipment. This is illustrated in experiments involving shock heating of various coals.

A small piece of coal, about 1-2 mg, was placed on the strip and shock heated to about 1000°C by snapping the switch with the transformers preset for 1000°C. Coking coal, such as Federal melts, exudes tars and vapors which condense on the glass vessel, and forms a coke button. A non-coking subbituminous coal such as Elkol does not melt, but puffs out into a porous structure with the loss of light vapors (Figure 2). A simple test for coking is to heat two particles of coal in contact with each other. Coking coals will fuse while non-coking coals will not. The strength of the bond after cooling can be easily estimated by probing with a needle while observing through the microscope.

### WEIGHT LOSS

It had been thought that the observed volume changes could be used to estimate the percentage of coal volatilized. However, because of density and porosity changes in the char, this was not

possible. It was therefore decided to attempt a semi-quantitative approach by weighing a coal particle before and after exposure on the hot stage. It was found that, with care, particles of coal weighing one to three milligrams could be handled. Weighing was performed on a microbalance sensitive to 10.000001 gm (1 microgram).

Considerable technique development was necessary to reduce the experimental scatter found initially. Direct handling of coal particles with forceps proved impractical as the chars tended to be too friable. Microcrucibles about 2 mm on the edge were folded from platinum foil or gauze. The tared crucibles were then used to contain the coal. Besides increasing reproducibility, this system allowed the evaluation of fine-grind particles on the hot stage. However, the metal of the crucible did not make perfect contact with the metal strip, even though the strip was bent to the shape of the crucible and the latter was held as by a spring. Also, the total weight of metal that had to be heated was about doubled. As a result, the maximum temperature obtainable was reduced from 3200°F to 2200°F.

Heat transfer to the sample was from the heated strip only. Thus, heat flow was essentially unidirectional, with the bottom heated first. This phenomenon could be clearly observed in coking coals, where liquefaction and coking occurred in waves starting from the heat source.

The time to reach set temperature was estimated from the current pulse observed on an ammeter. When the switch was closed, the current rose quickly to a high value. As the metal strip heated, its resistance increased, decreasing the current. It was presumed that, when the current had decreased from the peak value to a steady state, the strip had reached temperature equilibrium. The effect of crucible and coal on time to steady state could be observed. It was estimated that it took 1.5 to 2.5 seconds to reach a temperature of 1830°F.

Weight-loss curves for several coals are presented in Figures 3-7. All curves reflect increased volatilization with increasing temperature. Further, the amount volatilized is often greater than that obtained in the ASTM volatile-matter test. The amounts volatilized at 1742°F are compared in Table I. In Figure 4 the number beside each point represents the number of experiments averaged to obtain it.

These findings are similar to those of Loison and Chauvin<sup>2</sup>.

---

<sup>2</sup>R. Loison and R. Chauvin, "Rapid Pyrolysis of Coal," Cerchar, Cheltenham International Coal Science Conference, 1963.

Since volatilizations by shock heating are for the most part greater than those obtained by the ASTM technique, the heating rate must be responsible for the increase. At the time the results were obtained, the possibility that error inherent in the technique was responsible for all the variation was considered. Now this can be discounted because of other data obtained in Project COED which supports the conclusion concerning the dependence of volatilization on the heating rate<sup>3</sup>. However, the data obtained here gave us the confidence that increased volatilization could be obtained, and therefore guided the experiments which quantitatively proved this finding.

### TAR AND LIQUOR YIELD

In order to estimate more quantitatively the amount of tar and liquor formed, a measured amount of coal was placed in a melting-point capillary tube. The hot strip was bent into a loop to hold the coal-containing end of the capillary. On shock heating, it was found that the vapors exuded and condensed in the upper regions of the capillary with the heavier material condensing nearer the coal. The nature of the exudate, whether tar, liquid, or gas, could be easily observed through the microscope and its condensation behavior followed. As shown in Figure 8, coking coal such as Federal tended to have more heavy tar, while the product from non-coking coals such as subbituminous Elkolare lighter and more mobile. A semi-quantitative comparison of yield can be made by measuring the lengths of capillary containing the various fractions.

The capillary tube technique has been found to be particularly useful in the rapid screening of unknown coals. By using a standard fill (0.5 cm) of a sized coal (40-60 mesh), an unknown coal can be compared with known standards with regard to water content, melting (coking) behavior, volume change on heating, tar evolution, tar character (light or heavy) and sometimes gas evolution (made visible by entrained tar). The entire observation takes about five minutes and requires only a few milligrams of sample.

### ASH DISTRIBUTION AND PROPERTIES

Considerable information can be gained by observing the burning of a single particle of coal under the microscope. If desired, the oxidation can be carried out slowly, avoiding visible flames thus making possible the observation of the slow removal of carbon from the ash skeleton; or the combustion can be forced to determine its

---

<sup>3</sup>J. F. Jones, M. R. Schmid, R. T. Eddinger, Chem. Eng. Prog. 10, No. 6, 1964.

influence. By regulating the oxygen content of the atmosphere, the rate of oxidation can be controlled and the influence of temperature isolated.

When a coal particle is slowly oxidized, the ash-producing minerals are left at their original sites and a skeleton structure is retained. The original minerals may be converted to oxidized forms, e.g., pyrite converted to hematite, but in the absence of liquifaction, the converted minerals remain distributed in space about the same as their predecessors. This allows the observer to decide if beneficiation techniques would be useful in upgrading the coal and to what degree of size reduction the coal must be ground before separation could be expected.

After the ash structure has been studied, the temperature can be raised and the ash melting characteristics observed. The ash melting point or melting range can be easily measured and the reaction or fluxing of ash components noted. The behavior of the ash on heating gives clues as to problems that might be encountered in commercial use of the coal, such as clinker formation, fluxing of fire brick, or fly-ash control.

#### CONCLUSIONS

The techniques just described show that the hot-stage microscope can be a very useful tool in coal research. It can be used for qualitative observation of coal-structure carbonization behavior, and ash characteristics. Semi-quantitative results can be obtained, providing reasonable guide lines for scale-up work.

#### ACKNOWLEDGEMENT

The authors thank FMC Corporation for permission to publish this paper. Part of this work was supported by the Office of Coal Research through the United States Government Contract 14-01-0001-235 (Project COED).

ER:hvh  
6/3/64

TABLE I

Comparison of Volatilization at 1742°F (950°C), Dry Basis

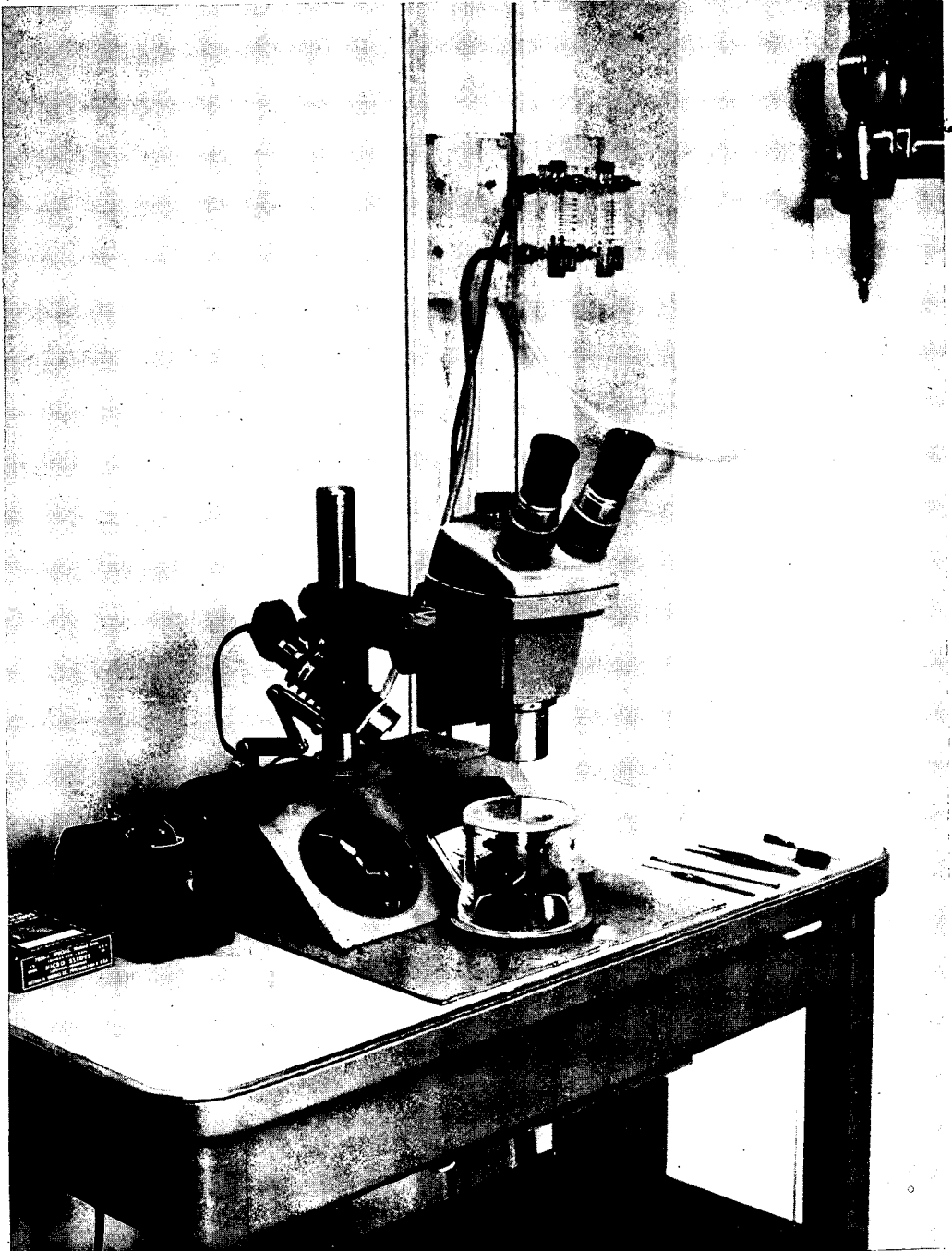
	<u>ASTM Procedure</u>	<u>Hot Stage</u>	<u>Percentage Increase</u>
Elkol <sup>1</sup>	40.7	48	17
Federal <sup>2</sup>	37.7	49	30
Kopperston No. 2 <sup>2</sup>	31.6	36	14
Colver <sup>2</sup>	25.3	19	neg. -25
Orient No. 3 <sup>2</sup>	44	41	neg. -7

<sup>1</sup>Kemmerer Coal Company, Frontier, Wyoming

<sup>2</sup>Eastern Associated Coal Corp., Pittsburgh, Pa.

<sup>3</sup>Freeman Coal Mining Corp., Chicago, Illinois

Figure 1



Microsample Strip Furnace with Microscope  
Note glass envelope covering the electrode posts.

Figure 2



A. Federal Coal before shock heating



B. Federal Coal after shock heating. Residue formed from a tarry liquid which solidified.



C. Elkol Coal after shock heating. Material cracked open to release gases.

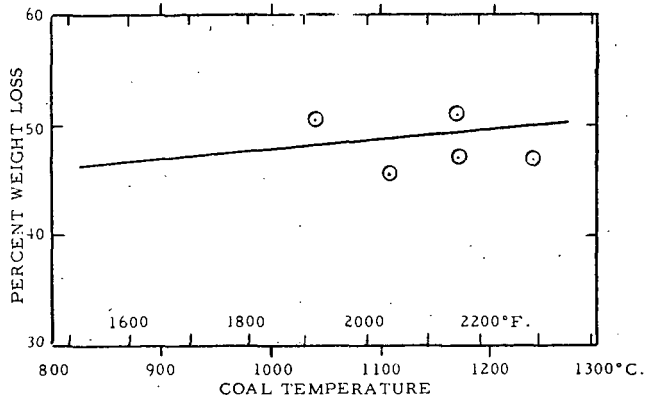
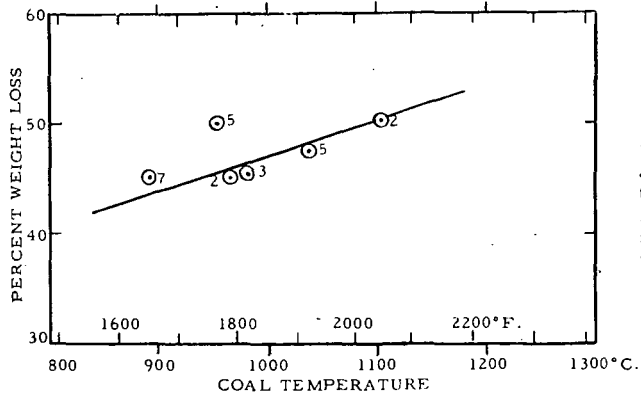


FIGURE 3

Weight Loss of Elkol Coal on Hot Stage



Points are average of tests, (number indicates how many tests were made).

FIGURE 4

Weight Loss of Federal Coal on Hot Stage

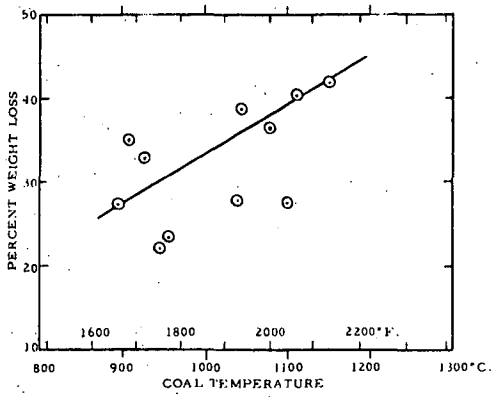


FIGURE 5

Weight Loss of Kopperston No. 2 Coal on Hot Stage

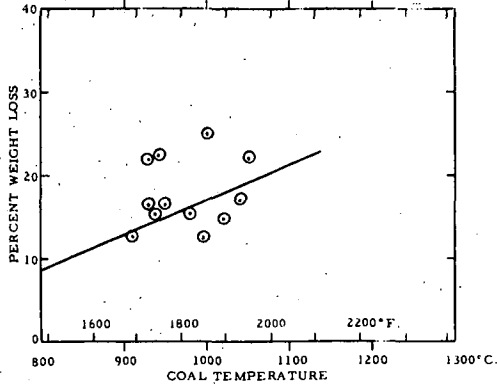


FIGURE 6

Weight Loss of Colver Coal on Hot Stage

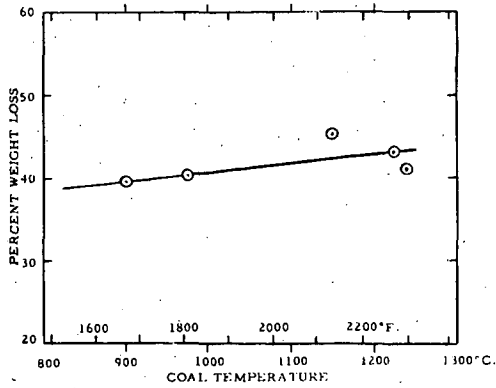
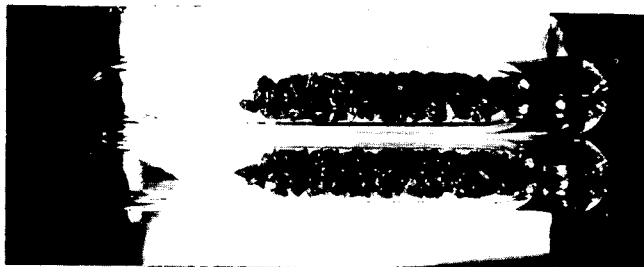


FIGURE 7

Weight Loss of Orient No. 3 Coal on Hot Stage

Figure 8



A. Before shock heating.  
Federal on right,  
Elkol on left.



B. After shock heating.  
Federal has given more  
of a heavier tar than  
Elkol.

Figure 9



Elkol coal after mild oxidation. Ash is uniformly distributed throughout particle.

Presented Before the Division of Fuel Chemistry  
American Chemical Society  
Chicago, Ill., August 30 - September 4, 1964

### Reactions of Coal in a Plasma Jet

R. D. Graves, W. Kawa, and P. S. Lewis

U.S. Bureau of Mines, 4800 Forbes Avenue  
Pittsburgh 13, Pennsylvania

### INTRODUCTION

The Bureau of Mines has made an exploratory study of the reaction of coal in a plasma jet in which plasma temperatures up to about 15,000° C can be attained. The objective was to obtain new knowledge of coal chemistry which may lead to new methods of producing chemicals from coal. Plasma consists of more or less ionized gases or vapors, and is present in any electrical discharge. Temperatures generated in electrical discharges are high enough for molecular bonds to be broken and for the resultant atoms to dissociate into ions and electrons. The complex mixture of ions, electrons, neutral atoms, and excited molecules produced is called a plasma and is referred to as the fourth state of matter. It conducts electricity, is a good heat conductor, and is luminous. The highly excited species that exist in plasmas can react to produce compounds whose formation is thermodynamically unfavorable at conventional conditions.

A plasma jet is formed when plasma generated from a fluid flowing through an electrical arc confined within a chamber is made to flow out of the chamber through a nozzle or orifice. Various plasma jet devices have been used in recent years to study high-temperature chemical syntheses. Leutner and Stokes<sup>1/</sup>, using a consumable graphite anode, produced acetylene by reacting the graphite with hydrogen in an argon-hydrogen plasma. About 34 percent of the carbon consumed was converted to acetylene. Adding graphite in powdered form did not increase the yield of acetylene. These same investigators also reacted methane in argon plasmas and converted 80 percent of the carbon in the methane to acetylene. Acetylene synthesis has also been reported by Freeman and Skrivan<sup>2/</sup>, who reacted methane in argon and argon-hydrogen plasmas, and by Baddour and Iwasyk<sup>3/</sup>, who reacted hydrogen with carbon vapor obtained from a consumable graphite electrode.

The plasma-jet device used in the present study was a commercial plasma gun designed for spray-coating applications. Experiments were made with high-volatile A bituminous (hvab) coal using argon as the working gas and also as a carrier gas in which coal was entrained and fed into the plasma gun. The effects of coal rate, coal particle size, and plasma temperature on yields and product composition were determined.

### EXPERIMENTAL PROCEDURE

#### Apparatus

The plasma-jet unit consists of a plasma gun, product recovery system, coal feeder, power supply, cooling water facilities, and a control console. Direct current used to operate the plasma gun is supplied by two 3-phase alternating current transformers and selenium rectifiers. This system is rated at 28 kw and

is capable of delivering 700 amp at 40 volts or 350 amp at 80 volts. It also contains a high-frequency oscillator used to start an arc. The electrical potential required to sustain an argon plasma was about 20 volts.

The plasma gun, shown schematically in figure 1, has a 3/16-inch thoriated tungsten cathode and a 1/4-inch id cylindrical water-cooled copper anode. The working gas enters the gun radially near the cathode and flows downward into the anode. The gas is converted to a plasma as it flows through the electrical discharge between electrodes. Coal entrained in the carrier gas enters the plasma through an inlet in the side of the anode. The reaction mixture leaves the bottom of the anode as a luminous jet and flows down through the water-jacketed cooler which consists of a 3-inch copper tube about 12 inches long. The residence time of coal in the plasma is less than a millisecond. Reaction products leave the cooler at several hundred degrees C and enter the solids receiver via a dip tube. The receiver is 6 inches in diameter and 12 inches long and contains about 3 inches of water. Most of the solids collect in the bottom of the receiver, while the gases and finer solid particles at near room temperature bubble up through the water and a tubular baffle. Gases flow through a cloth filter, which collects additional fines, and are sampled, metered, and vented.

### Operating Procedure

The system is assembled, purged with argon, and pressure tested. Flows of cooling water and working gas are established, and then the electrical discharge between electrodes is started. The flow of carrier gas is established, and the coal feeder is started. Coal is fed into the plasma gun for 10 minutes unless a coal feed stoppage or other system failure causes a premature termination of an experiment. Initially, the system is at a pressure of about 3 to 4 psig but gradually increases several psi as solids accumulate on the filter. Temperatures of cooling water entering and leaving the plasma gun are measured. Product gases are sampled after steady state conditions are reached. At the conclusion of an experiment, solid products are washed from the cooling system, receiver, filter, trap, and interconnecting lines with water. The washings are combined, and then the solids are filtered and dried in air at 70° C for 20 hours.

### Calculations

Total power input is determined from electrical current and voltage measurements at the gun, whereas net power input to the plasma is calculated as the difference between total power input and the power loss to the cooling water. The enthalpy of the primary gas and the average plasma temperature are determined from the net power input into the plasma, the working gas flow rates, and a plot of specific enthalpy as a function of temperature. This calculation assumes no energy loss other than that to the cooling water.

Yields of solids are determined from weighings of coal fed and solids recovered. Yields of gaseous products are calculated from analyses of product gas and the known coal and argon feed rates. This calculation assumes constant coal feed rate and steady state conditions at the time the gases were sampled.

## RESULTS AND DISCUSSION

### Reactions of 70 x 100 Mesh Coal

Experiments with 70 x 100 mesh coal (U.S. sieve) were made using feed rates of about 3.1 and 1.1 pounds per hour. Argon rates were constant at 1.17 scfm as the primary gas and 0.26 scfm as the carrier gas. The power input at each coal rate was varied to give average plasma temperatures ranging from 3,400° to 7,700° C

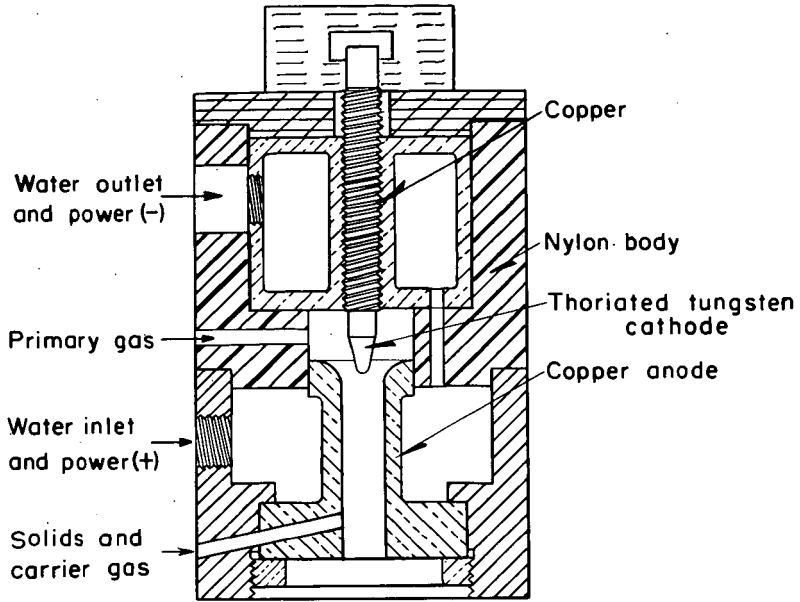


Figure 1.- Schematic diagram of the plasma generator.

at about 3.1 pounds per hour and from 3,900° to 8,600° C at about 1.1 pounds per hour. Reaction products were a solid residue and a gas containing hydrogen, methane, acetylene, diacetylene, and carbon monoxide.

Operating conditions, yield data, and analyses of the coal feed and residues produced are shown in table 1. Yields are expressed as weight-percent of moisture- and ash-free (maf) coal. At a coal rate of 3.1 pounds per hour, increasing the power input (or average plasma temperature) had only a slight effect on the extent of coal decomposition. Yields of solid residue decreased from 92.2 percent at 3,400° C to 89 percent at 7,700° C. Yields of hydrogen and acetylene increased almost linearly from 0.4 to 1.1 percent and from 2.6 to 4.5 percent respectively. The yield of methane was constant at about 0.2 percent, while the yields of diacetylene showed no significant trend. With a coal rate of about 1.1 pounds per hour, the effect of increasing the plasma temperature on yields was similar. Yields of residue decreased while yields of hydrogen increased from 0.4 to 1.7 percent, yields of acetylene increased from 2.2 to 6.0 percent, and yields of diacetylene increased from 0.1 to 0.6 percent with increasing temperature. The amount of methane produced was again constant at about 0.2 percent. At both coal rates, yields of carbon monoxide increased with increasing temperature.

The effect of decreasing the coal feed rate from 3.1 to 1.1 pounds per hour can be seen by comparing the results from experiment 9 with experiment 18 and experiment 10 with experiment 14. Estimated plasma temperatures in each pair of experiments were comparable. At the lower coal rate, higher coal heating rates, higher average coal temperatures, and, hence, more extensive coal decomposition would be expected because there was more heat available per unit weight of coal. However, there was no significant effect of coal rate on yields of gaseous products in these experiments. Although the yields of solid residue were about 5 percent lower at the lower coal rate, this is not necessarily an indication of more coal decomposition. Carbon recoveries were also lower by about the same amount, and it is possible that losses of solid products were higher at the lower coal rate.

Analyses of the solid residues showed that extensive thermal decomposition did not occur in any of the experiments because the coal was not heated sufficiently. Ultimate analyses of the coal and residues did not differ appreciably, and the residues contained only 3 to 6 percent less volatile matter. It is possible that most of the coal particles, because of poor mixing, remained in the periphery of the plasma where temperatures are much lower than along the axis.

The distance between the coal entry port of the anode and the discharge port is 1/4 inch. This may be considered as the coal-plasma mixing zone. To improve the mixing of coal and plasma, an anode was modified to give a threefold increase in the length of the mixing zone. Experiments were then performed at conditions similar to those in experiments 14, 16, and 18 (1.1 pounds of coal per hour). However, as yields and ultimate compositions of the residues produced in the two sets of experiments were similar at comparable conditions, this change was ineffective. Assuming that better mixing was achieved with the extended nozzle, it appeared that heat transfer rate rather than the degree of mixing limited the temperature rise and extent of coal decomposition.

#### Reaction of -325 Mesh Coal

To reach higher coal temperatures, the particle size of the coal feed was decreased to -325 mesh. Experiments were made with power input as a variable, and average plasma temperatures of 4,800°, 7,300°, and 8,800° C were obtained. Argon rates were constant at 1.17 scfm as working gas and 0.26 scfm as carrier gas. Average coal rates were 1.03, 0.84, and 0.74 pounds per hour although intended to be 1.0 pound per hour. Product distributions and the analyses of the coal feed and

TABLE 1.- Reactions of 70 x 100 mesh hvab coal in argon plasmas  
Effects of power input and coal feed  
rate on yields and residue compositions  
(1.17 scfm argon as primary gas, 0.26 scfm argon as carrier gas)

Experiment number	9	10	4	18	14	16	
Average coal rate, lb/hr	3.11	3.06	3.14	1.20	0.99	1.11	
Average plasma temp., ° C	3,400	6,300	7,700	3,900	6,600	8,600	
Total power input, kw	3.8	7.3	9.4	4.1	7.5	12.6	
Net power input, kw	1.7	3.2	3.9	2.0	3.3	4.7	
<u>Products, wt pct maf coal</u>							
Solid residue, maf	92.2	89.2	89.0	87.7	84.0	78.3	
Hydrogen	0.4	0.8	1.1	0.4	1.0	1.7	
Methane	.2	.2	0.3	.2	0.1	0.2	
Acetylene	2.6	3.5	4.5	2.2	4.3	6.0	
Diacetylene	0.3	0.3	-	0.1	0.4	0.6	
Carbon monoxide	4.1	5.3	5.6	3.8	5.6	11.0	
Total	99.8	99.3	100.5	94.4	95.4	97.8	
Carbon recovery, pct	96.8	96.8	97.1	91.3	92.3	92.8	
Hydrogen recovery, pct	96.4	98.0	105.4	94.2	100.3	104.1	
<u>Analyses, wt pct</u>							
Material	Coal	-----Solid residue-----					
Moisture	0.8	0.8	1.3	0.4	0.1	0.6	
Ash	3.8	4.4	5.4	5.1	4.7	4.2	
<u>Ultimate composition, maf basis</u>							
H	5.6	5.2	5.1	5.0	5.3	5.2	
C	84.3	83.3	87.5	87.0	83.4	87.4	
N	1.7	1.7	1.6	1.5	1.6	1.6	
S	0.9	0.9	0.9	1.0	0.8	0.8	
O (by difference)	7.5	8.9	4.9	5.5	8.9	5.0	
Volatile matter, maf basis	37.6	34.8	31.2	32.6	34.4	33.9	
						31.1	

solid residues produced are shown in table 2. As power input was increased, yields of solid residue decreased from about 74 to 45 percent and yields of hydrogen and acetylene increased. No trends were observed in the yields of methane and carbon monoxide. Trace quantities of diacetylene were formed in each experiment.

There was considerably more decomposition in all experiments with -325 mesh coal than in experiments with 70 x 100 mesh coal. The -325 mesh coal evidently reached higher temperatures. Volatile matter contents of the residues from -325 mesh coal were much lower, and yields of gaseous products were much higher. In experiments with 70 x 100 mesh coal in argon plasmas, the highest yield of acetylene obtained was 6 percent. The solid residue produced from this experiment contained 31 weight-percent volatile matter on a maf basis. As shown in table 2, acetylene yields obtained from -325 mesh coal were about 10, 12, and 15 percent, and the residues contained about 17, 10, and 12 percent volatile matter. These results clearly show that particle size had a pronounced effect on the extent of coal decomposition. However, the -325 mesh coal was still not completely devolatilized although it is estimated that coal temperatures of about 2,900° to 6,300° C would have been reached if thermal equilibrium had been attained. Complete devolatilization would be expected at a temperature somewhat above 1,000° C.

Total yields and carbon and ash recoveries were low in experiments 40 and 41 (table 2), possibly because of losses of extremely fine solid residue that filtered through the recovery system. In all three experiments, the recoveries of hydrogen and oxygen were high, and in experiments 38 and 40, the yields of carbon monoxide obtained would not be possible even if all the oxygen in the coal had been converted to carbon monoxide. It is likely that some leakage of cooling water into the plasma had occurred. The reaction of this water with coal or coal decomposition products would account for the high hydrogen recoveries and the high yields of carbon monoxide.

#### CONCLUSIONS

Acetylene was the principal hydrocarbon gas produced when hvab coal was injected into argon plasmas and was obtained in yields as high as 15 weight-percent of maf coal. However, the coal was not heated to temperatures high enough for complete devolatilization to occur. To obtain higher coal temperature and yields of gaseous products, changes in plasma generator design and/or operating techniques that will result in more efficient utilization of the heat available in plasmas will be required.

#### REFERENCES

1. Leutner, H. W. and C. S. Stokes. Producing Acetylene in a Plasma Jet. *Ind. and Eng. Chem.*, v. 53, No. 5, May 1961, pp. 341-342.
2. Freeman, M. P. and J. F. Skrivan. Plasma Jet...New Chemical Processing Tool. *Hydrocarbon Processing and Petroleum Refiner*, v. 41, No. 8, August 1962, pp. 124-128.
3. Baddour, R. F. and J. M. Iwasyk. Reactions Between Elemental Carbon and Hydrogen at Temperatures Above 2,800° K. *Ind. and Eng. Chem. Process Design and Development*, v. 1, No. 3, July 1962, pp. 169-176.

TABLE 2.- Reactions of -325 mesh hvab coal in argon plasmas  
Effect of power input on yields and residue compositions  
 (1.17 scfm argon as working gas, 0.26 scfm argon as carrier gas)

Experiment number	38	41	40
Average coal rate, lb/hr	1.03	0.84	0.74
Average plasma temp., ° C	4,800	7,300	8,800
Total power input, kw	4.8	7.5	10.2
Net power input, kw	2.4	3.7	4.9
<u>Products, wt pct maf coal</u>			
Solid residue, maf	73.6	62.9	45.3
Hydrogen	2.4	3.0	3.9
Methane	2.7	0.5	0.6
Acetylene	9.5	12.3	15.4
Diacetylene	trace	trace	trace
Carbon monoxide	18.1	11.4	24.3
Carbon dioxide	1.4	0.0	0.0
Total	107.7	90.1	89.5
Carbon recovery, pct	103.2	89.4	80.9
Hydrogen recovery, pct	126.6	115.8	130.5
<u>Analyses, wt pct</u>			
Material	Coal	----Solid residue----	
Moisture	1.1	0.7	0.5
Ash	8.3	11.2	11.4
Ultimate composition, maf basis			
H	4.9	3.2	2.5
C	81.9	89.2	90.0
N	1.5	1.5	1.1
S	1.5	1.1	1.1
O (by difference)	10.2	5.0	5.3
Volatile matter, maf basis	37.2	17.4	10.2

Presented Before the Division of Fuel Chemistry  
American Chemical Society  
Chicago, Ill., August 30 - September 4, 1964

Evaluation of the Moisture Content of a Coking Coal  
for the Heat Consumption During Carbonization

by Dr. rer. nat. K. G. Beck,  
Dr. rer. nat. R. Beckmann  
and Dr. Ing. W. Weskamp

of Steinkohlenbergbauverein,  
Essen, Germany

On an invitation by the American Institute of Mining, Metallurgical, and Petroleum Engineers three years ago, we had the opportunity to present to the Blast Furnace, Coke Oven, and Raw Materials Conference in Philadelphia a report on carbonization tests, which specifically dealt with the more essential coke characteristics and how they are affected by carbonization conditions<sup>1)</sup>. The results of these tests had been obtained in a semi-industrial scale coke oven with a charging volume of 11.1 cu. ft.. Such test ovens are used with good success both in Europe and the USA for the determination of coke characteristics<sup>2)</sup>. However, it is not possible to carry out thermo-technological investigations with such ovens, because the considerable surface and waste gas losses prevent an exact evaluation of the underfiring heat, which can be related to practical operation. Such thermo-technological investigations, however, are of particular significance for the West-German coke oven plants, since the expenses for underfiring constitute by far the largest factor of all costs which can be influenced by the mode of operation. Steinkohlenbergbauverein, thus, decided to build a test plant to be erected on a large coke oven plant in commercial operation. The test plant consists of an oven block with five industrial-scale semi-divided flow controlled coke ovens of underjet design. A bricked-up bulkhead of 59.1 in. width connects the test ovens (Fig. 1) with the adjoining oven group. On the other side there is a buttress of the usual type, with bricked cooling duct and concrete end. The dimensions of the ovens in cold condition and the hot dimensions determined during operation are shown in the following table (Fig. 2). In order to be able to heat all oven walls uniformly, "quantometers" and needle valves have been incorporated in each set of heating flues on the coke and ram side. The heat for underfiring the central oven can be measured individually. This separate gas feeder and measuring system proved necessary, because a comparison of the heat consumption ascertained

1) Size Distribution, Strength and Reactivity of Coke and how they are affected by the Coking Process

H. Echterhoff, K. G. Beck and W. Peters, 1961

2) Doherty, J. D., R. J. Hodder, L. N. Anthony  
Some Effects of Moisture in Coking Coal,  
Blast Furnace and Steel Plant 1962, pages 3/16

from the five test ovens with the heat consumption of newly constructed larger oven groups revealed great differences. This is in agreement with the results obtained by the British Coke Research Association at their test plant at Wingerworth. From the report by D.A. Hall, W.J. Pater, and F.K. Warford<sup>3)</sup> on "The effect of drying coal charge and filter cake on coke oven performance and the yield and properties of the products" it can be seen that even an industrial-scale coke oven of 10 t. capacity, which is operated separately from a coke oven battery, has a thermal efficiency of only 50%, as compared with the usual 70-80% efficiency of coke ovens arranged in batteries.

The coke is classified in a special screening plant (Fig. 3) and tested for its strength. A condensation plant (Fig. 4) serves to determine the amount and composition of the raw gas. This plant is designed in such a way that both the gas evolved from the five ovens, and the yield of by-products can be followed over the carbonization time of one oven. All measured data are centrally registered in a control station to monitor the operation.

From among the various serial tests so far carried out to ascertain the effects of heating flue temperature and moisture in the coking coal, the influence of the moisture content of the coal on high-temperature carbonization will be illustrated in the following.

Similarly to the method adopted by Brisse and Price<sup>4)</sup>, who used a wooden chamber, the distribution of the bulk densities as dependent on the moisture content of the coal was investigated in a test chamber of steel, prior to the commencement of carbonization tests (Fig. 5). Altogether 37 sampling points were arranged at three different levels. The coal used had a volatile content of 25.3% (free of water and ash), a size consists of 72% under 0.08 in. and 34% under 0.02 in., its ash content was 7.1% (free of water). Fig. 6 shows the distribution of bulk densities at moisture contents of 10%, 8%, and 6% at the three measuring levels. Due to the effect of dropping, the bulk density below the charging holes is always substantially above the bulk density between the charging holes. Naturally, this difference is reduced with the height of dropping. In the upper section of the

<sup>3)</sup> Hall, D.A., W.J. Pater, F.K. Warford  
Journal of the Inst. of Fuel (1963), pages 3/11

<sup>4)</sup> Brisse, A.H., J.G. Price  
Explorations in coke making research with a full scale coke oven model  
Blast Furnace and Steel Plant 1959, pages 1285/90

Hock, H., M. Paschke  
Archiv Eisenhütten 3 (1929), pages 99/102

Koppers, H., A. Jenkner  
Glückauf 66 (1930), pages 834/38

Eisenberg, G.A.,  
Glückauf 68 (1932), pages 445/61

Ejdelman, A.B., F.Z. Elenkij, G.D. Butuzov  
Coke and Chemistry (USSR) 1961, pages 3/6

chamber there is also a more uniform distribution due to levelling. The following Fig. 7 shows the distribution of bulk densities under charging hole 1 and between charging holes 1 and 2. The hatched area is a measure of the inequality of the bulk densities. It illustrates the difficulty of heating an oven chamber with coal of high moisture content in such a way that the same carbonization rate is attained throughout the chamber. The results show how important it is for coke oven plants to lower the moisture content of the coking coal and, thus, to bring about an equalization of the bulk densities in the oven chamber in order to warrant a uniform carbonization of the chamber contents resulting in coke of homogeneous structure and strength.

After charging, the bulk density of the coke does not at all remain constant, but it changes during carbonization. Immediately after charging the coal, it starts shrinking. This shrinking phenomenon continues for 2 hours. It is caused by an intrinsic oiling effect inherent with coal. During the distillation, part of the gas evolves through uncarbonized coal. This gas, let us call it internal gas, carries with it about 122 gr./cu. ft. compounds from the plastic zone which are solid or liquid under normal conditions. They are partially precipitated as an oily film on the surface of the coals. To initiate the first shrinkage it only requires a stimulus which is created by the gases and vapours passing through the coal.

The second shrinkage does not begin until after the formation of the first semi-coke. It should be due to the relaxation of tensions in the structure of the coke, and subsidence of the coke, caused by cracks.

Fig. 8 shows the duplication of the shrinkage effect between 10 and 6% moisture, its reduction at 4% to a value lower than at 10%, and the almost complete disappearance of shrinkage at 2% moisture content. If the bulk density is calculated after the initial shrinkage, it turns out to be the same between 10% and 4% moisture content. Thus, the first shrinkage is effective until the same bulk density (wf) is reached. In the case of coals with swelling properties a reduction in the moisture content will not have any influence on the mode of operating the ovens. At 2% moisture content, the bulk density (wf) of the coal is so high that the coal grains cannot, of their own weight, become more compacted. The second shrinkage of the coal tested was not large enough to regain the initial coal volume. The coal struck to the wall, and pushing the coke was difficult.

There are generally two possibilities of investigating the effect of the moisture content of the coal on heat consumption. Either the heating flue temperature is kept constant for all tests and the influence of differences in the moisture content is balanced by modifying the carbonization time, or the tests are made at equal carbonization times, while a change in the heating flue temperature will compensate for differences in the moisture content.

The first mode of operation was chosen for our investigations, i. e. at a heating flue temperature of 2280°F. the carbonization time according to the respective moisture content of the coal was determined in preliminary tests. The serial tests comprised 6 tests in which the water content of the coal was changed in steps of 2% between 2 and 12%. A new test with modified moisture content was not commenced until the battery was surely at an equilibrium. The duration of the test, at each moisture content, was at least 5 times 24 hours.

The coking coal, in a thermal drier, was adjusted to the desired moisture content. No larger deviations than 0.1% from the desired moisture content of the coal were determined in the larry car.

Fig. 9 illustrates the bulk densities, carbonization times and throughputs in their dependency of the moisture content. The bulk density (moist) has a minimum at 4 to 6% moisture content of the coal. This minimum, in the curve of the bulk density (wf) is shifted towards the higher moisture content. The curve of the carbonization time has about the same tendency as the curve of the bulk density (moist). The negligible differences can be accounted for by modifications in the carbonization conditions owing to the influence of the moisture content of the coal. In this case, it is particularly the great dependency of the heat conductivity on the water content which makes itself felt. The dependency of bulk density and carbonization time on the moisture content of the coal are also reflected in the throughput. The hatched area between the curves for moist and water-free throughput is a measure for the amount of water which must be processed as a ballast during carbonization. Referred to the coke yielded  $wf/wf$  an increase in the throughput of 18% will result, when the moisture content of the coal is reduced from 12 to 2%.

In discussions about the heat consumption for carbonization, as dependent on the moisture content of the coal, the question is always raised how much energy is required for expelling the moisture of the coal in the oven and if under certain circumstances it may be more economical to reduce the moisture content of the coal in a special drying process<sup>5</sup>). The heat consumption figures measured in our test ovens with the coal described above have been illustrated in Fig. 10. They change from 832 Btu/lb. at 2% moisture content of the coal (moist) by 70 Btu/lb. to 902 Btu/lb. at 12% moisture content of the coal (moist). As the illustration further reveals, the differences in the heat consumption figures are by no means equal for each 2% change in the moisture content. At higher moisture contents they are essentially larger than at lower ones, although the changes in the amounts of moisture and coal at 0.02 lb. are the same.

Before following up the reasons for the non-linearity of the course of the heat consumption curve, the calculated heat consumption figures likewise illustrated in Fig. 10 should be mentioned which result from operating the ovens at equal carbonization time and at a heating flue temperature as modified in correspondence with the moisture content of the coal. The data necessary for the re-calculation have been taken from an earlier investigation into the effect of the heating flue temperature on high temperature carbonization<sup>6</sup>). The carbonization time of 20 hours which results from coking a coal with 10% moisture at a heating flue temperature of 2280°F. has

<sup>5</sup>) Wollenweber, W., Glückauf 57 (1921), pages 987/92

Koppers, H., Koppers-Mitteilungen 14 (1932), pages 3/8

Baum, K., Glückauf 68 (1932), pages 1/8, 40/45

Litterscheid, W., Brennstoff-Chemie 13 (1932), pages 386/91

Hofmeister, B., Glückauf 88 (1952), pages 367/70

<sup>6</sup>) Weskamp, W., W. Dressler, E. Schierholz, Glückauf 98 (1962), pages 567/77

been taken as the basis. The heat consumption differences for any 2% change in the moisture content are larger than they are at constant heating flue temperature. Table 2 (Fig. 11) compares the results of the two modes of operation. When reducing the moisture content of the coal from 12 to 6% a saving averaging 14.4 Btu is attainable for each 1% reduction in the moisture content at constant carbonization time, while an average of only 9.0 Btu could be determined at constant heating flue temperature.

On the other hand, when operating at constant heating flue temperature, a larger increase in the throughput of the coke ovens can be achieved by changing the carbonization time.

The question about the real heat requirement for the evaporation of the moisture led us to further investigations and observations regarding the heat economy of a coke oven and how it is influenced by differences in the moisture content. In carrying out these further investigations it appeared expedient to extensively break up the individual thermo-technological mechanisms in a coke oven. By means of a section through a coke oven (Fig. 12), an explanation of the individual items should be given initially. The underfiring heat  $Q_1$  fed through the heating flue is only partially utilized for carbonization. Items  $Q_2$  and  $Q_3$  represent the total losses. Item  $Q_2$  collects the waste gas and surface losses of the lower part of the oven up to the coal line. Item  $Q_3$  includes the surface losses above the coal line. The heat amount  $Q_1$  minus  $Q_2$  is largely transferred to the chamber charge ( $Q_{10}$ ). Only a negligible portion, through heat transfer, flows into the area above the coal line  $Q_4$ . This heat, depending on the temperature condition prevailing in the gas collecting space, can be transferred to the gas or is lost as surface loss. During carbonization, together with external  $Q_6$  and internal  $Q_7$  gas, a substantial amount of heat reaches the gas collecting space and leaves it again with the developed mixed gas  $Q_5$ . Item  $Q_8$  is constituted of the evaporation heat of the water, the tar and the light oil at 32°F. and the gas formation energy (Gasarbeit) of the gaseous distillation products at 32°F. At the time of pushing, the coke possesses the sensible heat, item  $Q_9$ . The chemical processes occurring during the carbonization have an overall heat inherence which is considered under Item  $Q_{11}$ . A sensible heat  $Q_{12}$  is brought into the coke oven by the feed coal, the underfiring gas and the combustion air.

During the tests, all temperatures for the calculation of the sensible heats have been measured excepting the temperature of the external gas and internal gas when entering into the gas collecting space. For these measurements special suction pyrometers had to be designed because it is very important not to disturb the flow conditions prevailing in the measured range during measurements. The suction pyrometer to measure the temperature of the external gas was equipped with a narrow hood which on the one hand keeps off the radiation of the wall and on the other offers a screen against the internal gas. The hot must at least have the width of one piece of coke in order to be independent of the geometry of the coke lumps. Suction must be so dimensioned that the same velocity will prevail inside and outside the hood. When the suction is too strong, the temperature will drop immediately which indicates that gas from other sources is simultaneously sucked in which can only be colder in any case.

A similar procedure was adopted for measuring the temperature of the internal gas. In a pipe with a diameter of 3.94 in. a second pipe with a diameter of 1.97 in. is inserted to screen off the heat influx from the gas collecting space. The space in between the two pipes is filled with asbestos and a gas inlet is created by a conical shell. The distance of the thermocouple from the coal surface can be changed at random by using an adjusting screw.

Since the internal gas will surely have a temperature exceeding a  $212^{\circ}\text{F.}$ , the system was heated above  $212^{\circ}\text{F.}$  to avoid condensation of steam. Approximately 1 minute after the commencement of measuring, a temperature of approximately  $392^{\circ}\text{F.}$  was reached; 6 to 8 minutes later, the temperature continues to raise further. By this time, the asbestos, heated up by the gas from the gas collecting space has attained a temperature higher than  $392^{\circ}\text{F.}$  and superheats the internal gas.

Further measurements revealed that the internal gas has a temperature of  $212^{\circ}\text{F.}$  immediately after charging. After one hour, the temperature has risen to  $302^{\circ}\text{F.}$ , to remain constant at  $392^{\circ}\text{F.}$  from the 2nd to the 7th hour of carbonization. With these temperatures, all variables required for the establishment of a detailed heat balance are known.

At a temperature of  $59^{\circ}\text{F.}$  of the coal input, 1210 Btu/lb. water is required for heating up, evaporation and superheating to  $392^{\circ}\text{F.}$  At an efficiency of the underfiring system of 80%, 1510 Btu will be required in terms of underfiring heat per lb. moisture. The further heating up of the steam is effected almost exclusively by heat exchange with the hotter external gas.

This value of 1510 Btu/lb. water now serves to calculate the heat consumption for dry coal. This turns out to be approximately 810 Btu/lb. for the coal used, at a constant heating flue temperature of  $2280^{\circ}\text{F.}$  At a moisture content of 6% it is lowest and raises by 12.6 Btu towards coals with 2% and 12% moisture content.

If an attempt is made at calculating the heat consumption at a change in the moisture content by 2%, it must be taken into consideration that in case of moist coal as used in practical operation, a change in the moisture content is automatically connected with a modification in the amount of coal, for the carbonization of which additional heat is required. The savings in terms of underfiring heat for the reduced moisture of 0.02 lb. can be calculated at 30.2 Btu if the above two pyrometers are taken into consideration. On the other hand, an additional heat consumption of 16.2 Btu is required for the additional 0.02 lb. dry coal. From the difference of these 2 values of  $30.2 - 16.2$  results a constant reduction in consumption of 14 Btu/lb. for each 2% reduction in the moisture content.

If this calculated value of 14 Btu is compared with the measured differences in heat consumption illustrated in Fig. 10 it can be shown that the calculated and the measured differences agree when reducing the moisture content from 8 to 6%. Below 6%, the measured difference is smaller, below 8% larger than 14 Btu. Now, what are the reasons for these deviations from the calculated figures?

A quantitative treatment of these phenomena would become too complex at this point. Therefore, our report will be confined to an explanation of the results. In a balance in which all items stated in Fig. 12 have been considered it can be shown that the curve of the sensible heat of the total gas is responsible for the tendency of the underfiring curve. This heat results from the sensible heat of the external and internal gas and from a portion absorbed by heat exchange from the vault of the gas collecting space. The curve of the sensible heat of the total gas runs through a minimum at 6% moisture content of the coal. Its rise towards higher, and lower moisture contents has different reasons.

At 6% moisture content of the coal the sum of the sensible heat of the external and internal gases is equal to the sensible heat of the total gas. Thus, in the wall, there flows only such heat as is lost as a surface loss. Since in this range there is no heat exchange in the vault of the gas collecting space, the heat consumption difference calculated from changes in the amounts of moisture and coal is equal to the measured difference.

At higher moisture contents, the mean wall temperature in the area of the charge drops, and with it the sensible heat of the external gas. As the amount of steam in the internal gas, moreover, has a rising tendency, the temperature of the total gas decreases. By convection and radiation, heat from the vault of the gas collecting space is transferred to the total gas, which, through heat conduction in the wall is transferred from the area of the charge into the area of the gas collecting space and must, therefore, be fed as underfiring heat.

Below 6% moisture content of the coal, the reasons for the rise of the sensible heat of the total gas are of different nature. With the reduction in the moisture content there is an increase in the average chamber wall temperature and, thus, in the sensible heat of the external gas. However, since the internal gas, owing to the decreasing amount of moisture, demands less heat for superheating, a high temperature of the total gas is attained. The lower the moisture content the earlier the time when the total gas has a higher temperature than the vault of the gas collecting space, and thus yields heat. The temperature gradient between the wall in the area of the charge and above the charge is now very much smaller and hence less heat flows as item  $Q_4$  into the area of the gas collecting space. The heat determined as surface loss below 6% moisture content of the coal is, thus, partially supplied by external gas. This heat need no longer be fed via  $Q_4$  through underfiring, and so the measured heat consumption difference becomes smaller than the calculated one.

Let us briefly survey the results of these investigations:

The steam evolved from the moisture of the coal reaches the gas collecting space at a temperature of 392°F. This required 1510 Btu underfiring heat per lb. water at a thermal efficiency of the coke oven of 80%. The heat for further superheating of the steam is supplied by the hotter external gas. With the aid of this value, a detailed heat balance of the coke oven can be established permitting to critically observe the measured heat consumption and to scrutinize the correctness of the chosen carbonization time at constant heating flue temperature. Besides, the non-linear course of the heat consumption curve has been interpreted.

The economic significance of reducing the moisture content will be different according to the conditions of coke oven operation and can only be seen within the total economy of a mining company. If potential savings by reducing the moisture content of the coal are not referred to coal with a coal ready to be charged but to a dry coal amount of 0.9 lb. which corresponds to a coking coal with 10% moisture and which constitutes the figure used in economic calculations by German coke oven operators, savings in the heat consumption averaging 17 Btu, for each 1% reduction in the moisture content of the coal are revealed in the range of 10 to 6% moisture content which is the range of primary technical interest. For expelling 1 lb. moisture, in the range of 10 to 6% moisture content at an efficiency of 80%, an average of 1530 Btu or, at an efficiency of 70%, an average of 1840 Btu will have to be expended. For a modern drier one likewise calculates with a heat expenditure of 1710 Btu/lb. moisture, if a flotation concentrate is for instance dried from 22% moisture content to 6% moisture content. The savings in heat consumption are thus absorbed or even surpassed by the expenses for previous drying. However, the reduction of the water content brings about other advantages which are apt to exert a favourable influence on the economy of a coke oven plant. The question of drying can gain vital significance if the basis of raw materials can thus be extended considerably, as it happened in the case of the Lorraine coking plants after the process using dried coal had been successfully developed at the Marienau test plant and proved in practical operation at the Hagendingen coke oven plant<sup>7)</sup>. An effect which cannot be underestimated will be the influence of a lower moisture content of the coal on the life of a battery. An essential advantage is a possible increase in the throughput which permits savings in the capital service and a reduction in other overheads.

There is a substantial difference between the conditions prevailing in USA and in Germany which must be considered in judging the importance of the moisture content of the coking coal for the economy of coke oven plant operation.

In the Federal Republic of Germany more than 80% of the total coke outputs is produced at coking plants located in the immediate vicinity of collieries supplying coking coal. Our investigations confirmed that in terms of thermal economy there is no advantage in reducing the moisture content of a coking coal in a thermal drying unit prior to its carbonization. Accordingly, the average moisture content of the feed coal used in German coking plants located at collieries is at 9 to 10%. However, if the coking coal has to be transported to the coking plant over long distances, as it happens in many cases in the USA, there will be freight savings which can be significantly higher than the expenditure for thermal drying<sup>8)</sup>. Thus, it is understandable that, as a rule, American coking coals have a lower moisture content.

7) Loison, R., P. Foch  
Revue de l'industrie minerale (1961), pages 593/618

8) Doherty, I.D., J. Griffen  
Blast Furnace, Coke Oven, and Raw Materials  
Conference, 1960, pages 117/37

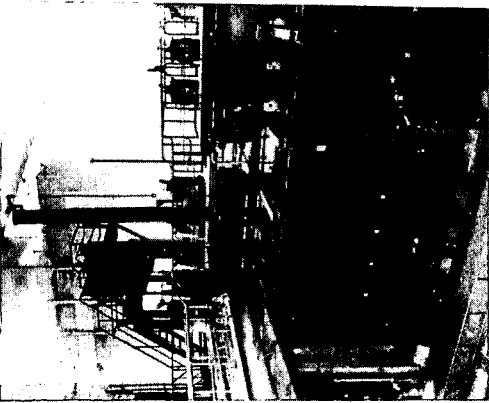


Fig. 1

	Cold Dimensions In.	Hot Dimensions In.
Length between buckstays	500	509
Length between door plugs	468	477
Height of chamber	164	167
Charging height (Coal line)	152	-
Width of chamber (Machine side)	16.5	16.2
Width of chamber (Coke side)	18.9	18.5
Mean chamber width	17.7	17.3
Thickness of oven roof	39.4	-
Pitch	45.3	-
Capacity of oven	Cu.ft. 729	
BWV 1964	Oven Dimensions	VK 150

Fig. 2

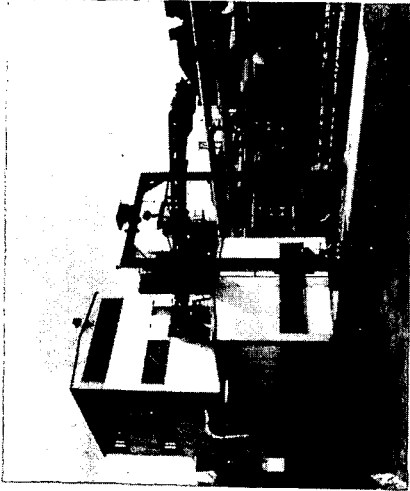


Fig. 3

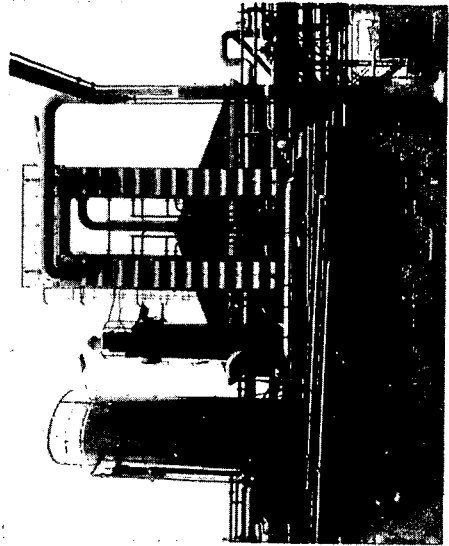


Fig. 4

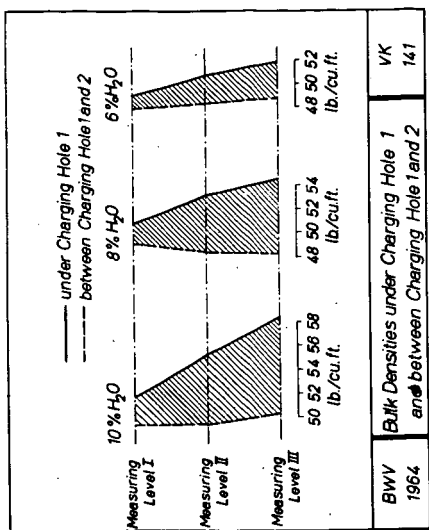


Fig. 7

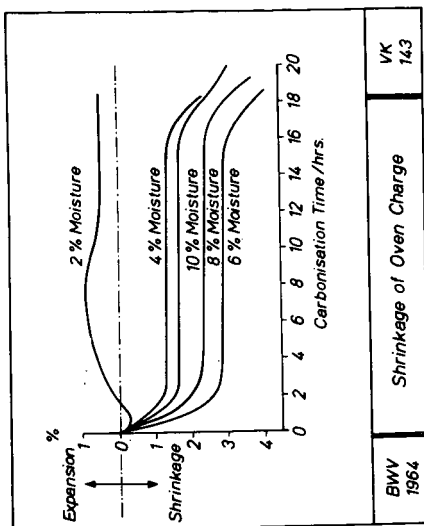


Fig. 8

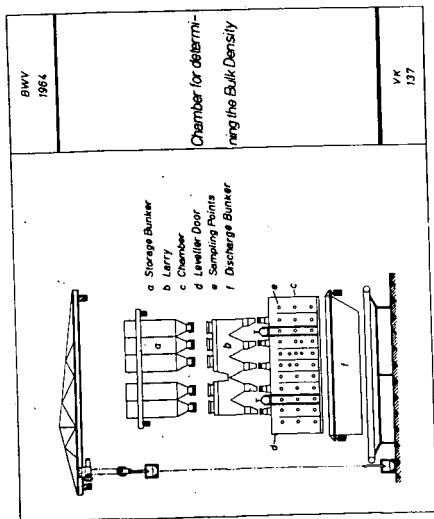


Fig. 5

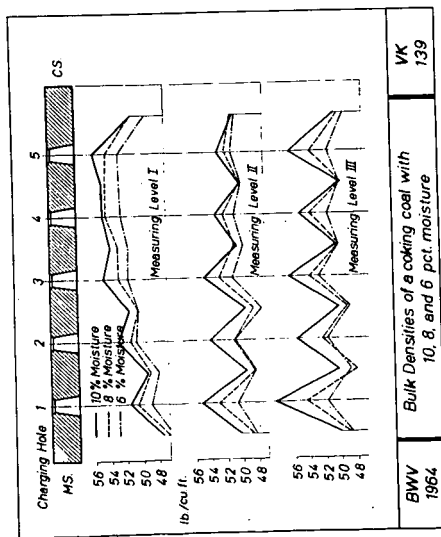


Fig. 6

Mode of Operation	1 per cent reduction in the moisture content of the coking coal, in the range of 12-6% H <sub>2</sub> O results in:		VK 157
	a change in Throughput i.e.	reduction in Heat Consumption referred to 1 lb coal, moist (efficiency of oven = 80%)	
	Constant Carbonisation Time	14.4 Btu	
Constant Heating Flue Temperature	- 0.9 % by a change of Bulk Density		VK 157
	+ 1.5 % by a change of Bulk Density and Carbonisation Time	9.0 Btu	
BWV 1964		Moisture Content of Coal Throughput, Heat Consumption	VK 157

Fig. 11

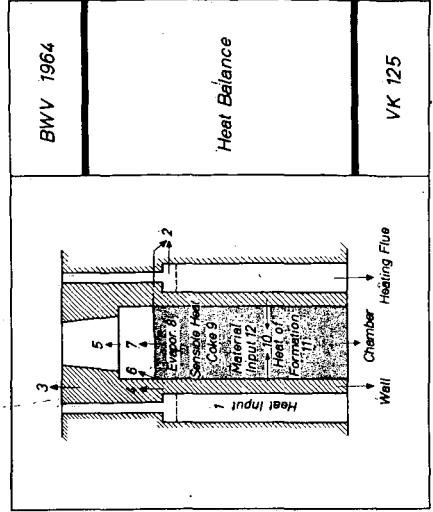


Fig. 12

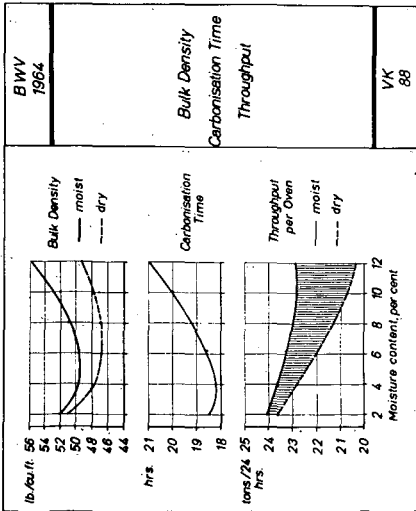


Fig. 9

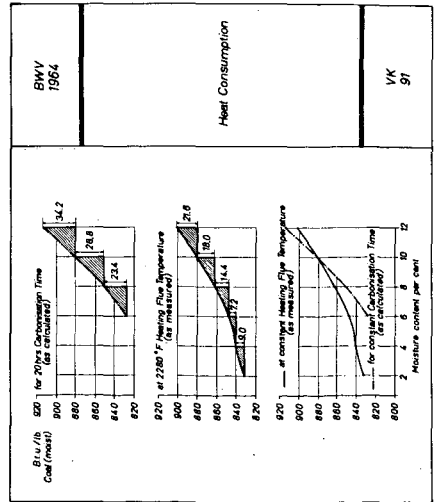


Fig. 10

Presented Before the Division of Fuel Chemistry  
American Chemical Society  
Chicago, Ill., August 30 - September 4, 1964

Devolatilization Studies on Coal Vitrinoids  
By Use of a Thermobalance

R. W. Shoenberger and E. F. Strickler

United States Steel Corporation  
Applied Research Laboratory  
Monroeville, Pennsylvania

The petrographic entities, which originate from the vegetation making up coal, help to establish the properties of coal that influence its mining, preparation, and use. Consequently, the properties of these entities should be known if the potential use of petrographic techniques and of the coal itself is to be made. Various physical and chemical properties of coals have been determined with significant contributions to the basic knowledge of coal and with practical application in industry, particularly in the carbonization of coal. To further exploit these entities, a study was initiated to determine their pyrolytic and plastic properties. In the initial phase, the vitrinoids of different rank coals were chosen for this study since vitrinoids are the most abundant and easiest entity to obtain from coal.

The thermal-decomposition behavior of entities has been visually examined in the hot-stage microscope. These observations are mostly qualitative. To obtain more quantitative results, the authors used a thermogravimetric balance (thermobalance) to determine the pyrolytic properties of the vitrinoids. The thermobalance, which has been used satisfactorily by numerous investigators,<sup>1,2,3,4</sup>\* was selected because it continuously records the weight and temperature of the sample in respect to time as the sample is heated automatically.

When coal is heated, it not only devolatilized but also becomes fluid. Consequently, the plastic properties of coal have been associated with its pyrolytic properties. By using the rate of devolatilization and plastic properties, Soth and Russell<sup>5</sup>) explained the coking pressure developed by coal blends. Van Krevelin,<sup>3,6</sup>) Berkowitz,<sup>7</sup>) and Brown<sup>8</sup>) used the pyrolytic and plastic properties to present concepts of coal structure and the mechanism of carbonization. The relative plastic properties of the vitrinoids were obtained when possible, to determine the relationships that exist with their pyrolytic properties.

This paper presents the results of the thermogravimetric study on vitrinoids of various rank coals and the relationships of these results to the rank and plastic properties of the vitrinoids.

Materials and Experimental Work

The samples, high in vitrinoids, were selected from coking coals representing different ranks of coal. Because vitrinoids can be distinguished from the other coal entities by their bright luster in banded coals, these bright bands were removed with a table saw. The samples were then selected from these specimens with a dissecting needle under a magnifying glass. These samples, listed in Table I,

\* See References

were then pulverized to 100 percent minus 60 mesh. The volatile-matter content of these samples, determined by standard procedures (ASTM Test Designation D 271-58), are included in Table I. The petrographic analyses conducted by the procedures used at the U. S. Steel Corporation's Applied Research Laboratory (ARL)<sup>9</sup> are shown in Table II. These analyses indicate that the samples contained high concentrations of vitrinoids. Only Wellington and Donegan coal samples contained less than 90 percent vitrinoids, but even they contained more than 83 percent. The average reflectances were also determined on these samples, Table I.

The devolatilization measured by the weight loss was determined on a Stanton thermogravimetric balance, Model TR-1. This thermobalance continuously records the temperature and the weight of the samples that were automatically heated at a rate of 6 degrees C per minute. The 0.5-gram sample was contained in a silica crucible supported by a silica weighing mechanism attached to the balance and heated by a tube furnace. The balance is sensitive to 1 milligram.

The plastic properties were determined in the Gieseler Plastometer by the standard procedures used in ASTM Test Designation D 1812-60T. The results of these tests are listed in Table III. The amount of sample was limited and, therefore, only single tests were made. Furthermore, the stirrer broke loose on some of the low-rank coals and no values could be obtained.

### Results and Discussion

The data obtained from the thermobalance show the cumulative weight losses at corresponding temperatures. These "S"-type curves are presented in Figure 1. The initial level of weight loss reflects the total moisture content and amount of occluded gas in each sample, the low-rank coals containing high percentages of inherent moisture. In all samples the weight loss increased slightly for a short time after the first devolatilization; the temperature of the initial devolatilization increased with the rank of vitrinoids. Very rapid devolatilization then occurred for a considerable time (about 100 minutes) until the weight loss gradually decreased. Most of the volatile matter was driven off by the time the temperature reached 900 C.

To obtain additional information, the differential pyrolysis curves were then determined from these data. The graphs that show the rate of devolatilization with respect to temperature are shown in Figure 2. The maximum rates of devolatilization for the low-volatile coals are lower than those for the high-volatile coals. A summary of the maximum rate of devolatilization and the temperature of this maximum rate is listed in Table IV. The relationship between the maximum rate of devolatilization and volatile matter is shown in Figure 3. This relationship appears to substantiate published results which show that maximum devolatilization rates are obtained with coal containing about 35 percent volatile-matter content.<sup>3</sup>) High-rank coals have much less volatile matter and, therefore, would be expected to have low rates of maximum devolatilization. However, since the low-rank high-volatile coals decompose at the lower temperatures because of their aliphatic structure, the devolatilization is distributed over a longer initial time or temperature range; therefore, the maximum rate would decrease after a certain rank coal was reached.

The results also indicate that the temperature of maximum rate of devolatilization increased as the rank of the coal increased. A good correlation is shown in Figure 4 where average reflectance is used as a rank parameter. A similar correlation is shown in Figure 5 where volatile matter is used.

Because plastic properties are related to rank, the temperature of maximum fluidity was related to the temperature of maximum rate of devolatilization. This relationship, shown in Figure 6, indicated a difference of about 50 degrees C between

these values. Published work on whole coals indicates that these values should be about the same.<sup>3,6,7)</sup> However, the data reported by van Krevelen<sup>3)</sup> show that the difference of 3 degrees per minute in the heating rate would account for about 20 degrees in the temperature of the maximum rate, since the faster the heating rate the higher the temperature.

The plastic properties and thermogravimetric analyses indicate that the vitrinoids start to decompose before they soften. However, the rapid devolatilization occurs at temperatures higher than the softening point for coal. In these vitrinoid samples, the maximum fluidity as measured in the Gieseler Plastometer occurred before the maximum rate of devolatilization. The relationships found in this study indicate that the thermal-decomposition characteristics can be estimated from the rank and plastic properties of the coal.

#### Summary

The results of this study indicated that the vitrinoids started to decompose before they became fluid. The initial temperature of devolatilization increased as the rank of the sample increased. Rapid devolatilization then occurred after the coal softened. From the differential pyrolysis curves, a good correlation was obtained between the temperature of maximum rate of devolatilization and the rank of coal. The maximum rate appears to be greatest for coals containing volatile matter (dry basis) of about 35 percent. The maximum fluidity of the vitrinoids was reached shortly before the temperature of maximum-rate devolatilization, and a good relationship was found between the temperature of maximum fluidity and the temperature of maximum rate of devolatilization.

The relationships obtained in this study indicate that the pyrolytic properties of coal can be estimated from its rank and plastic properties. This information should be useful to show what changes occur to coal when heated in the various processes used in industry.

#### References

1. H. C. Howard, "Pyrolytic Reactions of Coal," Chemistry of Coal Utilization, H. H. Lowry, Ed., Supplementary Volume, John Wiley & Sons, Inc., New York, pp. 363-394 (1963).
2. P. L. Waters, "Recording Differential Balances for Thermogravimetric Analysis," Coke and Gas, July 1958, pp. 289-291, and August 1958, pp. 341-343.
3. D. W. van Krevelen, F. J. Huntjens, and H. H. M. Dormans, "Chemical Structure and Properties of Coal XVI — Plastic Behaviour on Heating," Fuel, 35, 1956, pp. 462-475.
4. H. Luther and B. Bussmann, "Die Theomische Zersetzung von Steinkohlen in Abhangigkeit van de Korngrosse l. Mikroskopische und Thermogravemetrishe Untersuchungen," Brennstoff-Chemie, Vol. 43, No. 12, December 1962, pp. 353-361.
5. G. C. Soth and C. C. Russell, "Sources of Pressure Occurring during Carbonization of Coal," Transactions, AIME, Vol. 1957 (1944), Coal Division, pp. 281-305.
6. D. W. van Krevelen, "The Behaviour of Coal on Heating," Coal Science, Elsevier Publishing Company, New York, 1957, pp. 286-311.
7. N. Berkowitz, "On the Nature of Coking Coals and the Mechanism of Coke Formation," Blast Furnace, Coke Oven, and Raw Materials Proceedings, Vol. 9, AIME, 1960, pp. 95-111.
8. H. R. Brown, "The Decomposition of Coal in Relation to the Plastic Layer," Coke and Gas, October 1956, pp. 390-393.
9. N. Schapiro and R. J. Gray, "Petrographic Classification Applicable to Coals of All Ranks," Proceedings of the Illinois Mining Institute, 68th Year, 1960.

Table I  
Identification and Rank of Vitrinoids

<u>Rank of Original Coal</u>	<u>Seam</u>	<u>County</u>	<u>State</u>	<u>Concentration of Vitrinoids, %</u>	<u>Rank</u>	
					<u>Volatile Matter, % (dry basis)</u>	<u>Average Reflectance, R<sub>o</sub></u>
High-Volatile B	Illinois No. 6	Vermillion	Illinois	97.3	43.7	0.50
High-Volatile C	Herrin No. 6	Saline	Illinois	95.3	38.3	0.51
High-Volatile B	Sunnyside	Carbon	Utah - Colorado	86.2	37.4	0.71
High-Volatile B	Herrin No. 6	Saline	Illinois	94.6	34.1	0.77
High-Volatile A	High Splint	Harlan	Kentucky	91.2	33.6	0.93
Medium-Volatile	Sewell	Nicolas	West Virginia	83.8	29.4	1.15
Medium-Volatile	"A"	Pitkin	Colorado	94.8	22.6	1.39
Low-Volatile	Pocahontas No. 3	McDowell	West Virginia	90.4	21.5	1.39
Low-Volatile	"A"	Pitkin	Colorado	97.0	16.5	1.42

Table II

## Petrographic Entity Composition of Indicated Samples,\* Volume Percent\*\*

Coal	Reactive													Total		
	V4	V5	V6	V7	V8	V2	V10	V11	V12	V13	V14	V15	E		R	SF
Illinois No. 6	49.6	45.7	2.0										0.9	-	0.1	98.3
Herrin No. 6 "C"	40.0	55.3											0.5	-	0.2	96.0
Sunnyside			35.3	50.0	0.9								1.0	8.8	0.2	96.2
Herrin No. 6 "B"			6.6	60.6	27.4								1.6	-	0.2	96.4
High-Splint				2.7	21.0	62.9	4.6						1.2	0.5	0.2	93.1
Sewell						2.5	12.6	46.1	20.9	1.7			3.5	0.2	0.6	88.1
Colorado Medium										61.6	33.2		-	-	0.3	95.1
Pocahontas No. 3										62.4	28.0		-	-	0.2	90.6
Colorado Low										34.0	61.1	1.9	-	-	0.1	97.1

Coal	SF	M	F	Total
Illinois No. 6	0.2	1.2	0.3	1.7
Herrin No. 6 "C"	0.5	3.0	0.5	4.0
Sunnyside	0.5	1.7	1.6	3.8
Herrin No. 6 "B"	0.4	2.5	0.7	3.6
High-Splint	0.4	5.7	0.8	6.9
Sewell	1.2	7.8	2.9	11.9
Colorado Medium	1.0	2.8	1.1	4.9
Pocahontas No. 3	0.9	7.2	1.3	9.4
Colorado Low	0.6	1.4	0.9	2.9

\*Abbreviations for entities:

V4 = vitrinoid type 4, etc.

E = exinoids

R = resinoids

SF = semifusinoids

M = micrinoids

F = fusinoids

\*\*Pure-coal basis (excluding mineral matter).

Table III

Plastic Properties of Vitrinoids\*

<u>Sample</u>	<u>Maximum Fluidity</u>		<u>Temperature Range, C</u>	
	<u>ddpm** at</u>	<u>C</u>	<u>Softening</u>	<u>Solidification</u>
Sunnyside	1.3	412	373	451
High-Splint	100	433	355	472
Sewell	16,300	443	385	485
Colorado Medium-Volatile	330	459	390	498
Pocahontas No. 3	432	466	397	499
Colorado Low-Volatile	80	467	401	503

\*Stirrer broke loose on all Illinois coals.

\*\*Dial divisions per minute.

Table IV

Summary of Thermogravimetric Analyses

<u>Sample</u>	<u>Maximum Weight Rate Loss, % per minute</u>	<u>Temperature of Maximum Weight Rate Loss, C</u>
Illinois No. 6	0.54	463
Herrin No. 6 "C"	0.47	480
Sunnyside	0.67	475
Herrin No. 6 "B"	0.48	490
High-Splint	0.60	483
Sewell	0.64	510
Colorado Medium-Volatile	0.40	520
Pocahontas No. 3	0.40	520
Colorado Low-Volatile	0.37	530

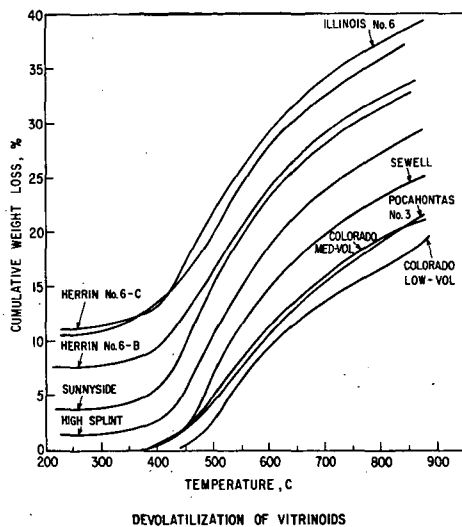


Figure 1

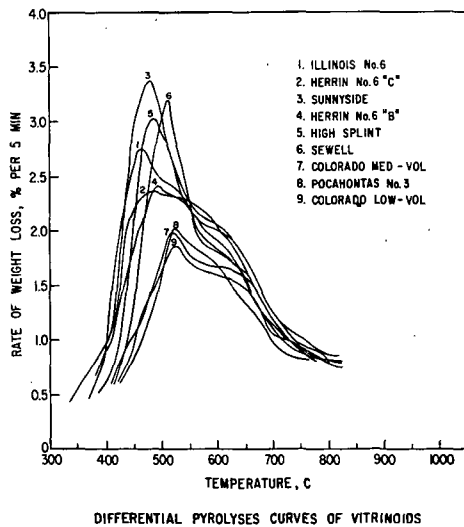


Figure 2

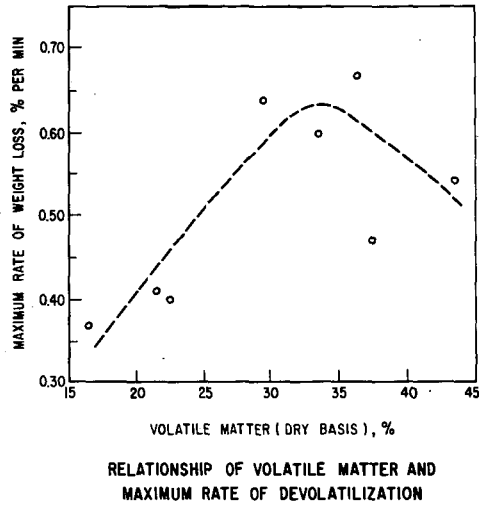


Figure 3

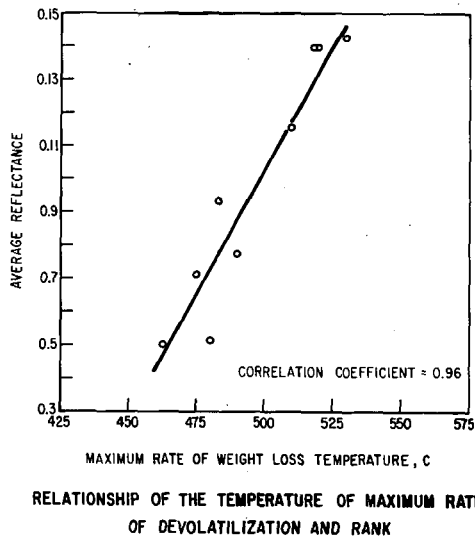
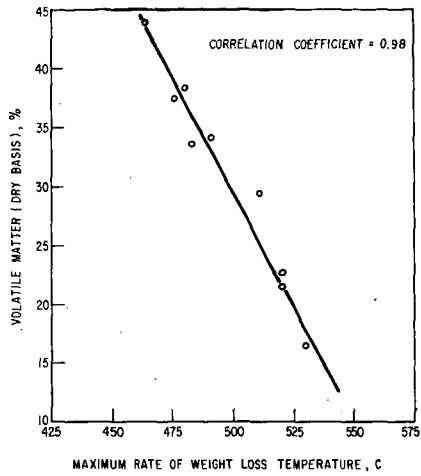
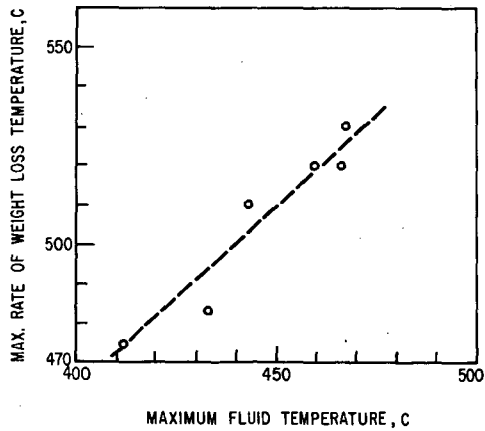


Figure 4



RELATIONSHIP OF THE TEMPERATURE OF MAXIMUM RATE  
OF DEVOLATILIZATION AND RANK

Figure 5



RELATIONSHIP OF MAXIMUM FLUIDITY AND  
MAXIMUM RATE LOSS TEMPERATURES

Figure 6